UNIVERSITAT DE BARCELONA

Multi-sensor remote sensing detection of biotic stress for crop phenotyping and management guidance

Yassine Hamdane

Multi-sensor remote sensing detection of biotic stress for crop phenotyping and management guidance

Yassine Hamdane

Doctoral Thesis

BARCELONA, 2023

UNIVERSITAT DE BARCELONA

"**Multi-sensor remote sensing detection of biotic stress for crop phenotyping and management guidance.**"

This work is part of the doctoral program in Ecology, Environmental Sciences, and Plant Physiology of the Department of Evolutionary Biology, Ecology and Environmental Sciences (BEECA) of the Faculty of Biology of the Universitat de Barcelona.

This work has been carried out in the Integrative Crop Ecophysiology Group research group, under the direction of Dr. Shawn C. Kefauver and Dr. Jose Luis Araus Ortega.

Memoir presented by **Yassine Hamdane** to opt for the doctoral degree at the Universitat de Barcelona.

Doctorant

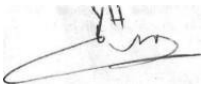

Yassine Hamdane

Director and tutor

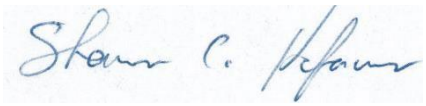

Dr. Shawn C. Kefauver

Co-Director

Dr. Jose Luis Araus Ortega

Barcelona, 2023

« Lorsque je tends vers un but, je me fais porter par l'espoir et oublie toute prudence; Je n'évite pas les chemins escarpés et n'appréhende pas la chute dans un feu brûlant. Qui n'aime pas gravir la montagne, vivra éternellement au fond des vallées ».

Abou El Kacem Chebbi

Dear God thank you for everything...

To my dear parents, Salah and Fatima. I appreciate your unwavering support, wise counsel, and affection. I appreciate everything you have done for me; I can never repay you, but I can make you happy and proud right now. To my brothers and Sister, Bassem, Hamdi, Sedik, Mohamed, Majdi, Zine, Sana, Najeh and Ibtissem, I appreciate you making me write your lovely names in the dedications. To my family (Hamdane family). Thank you is the least I can say to you.

Abstract

The main driving force behind crop research is to ensure food security. Climate change, which affects most crops and increases the risk of disease and famine, is addressed in this notion. The Food and Agriculture Organization (FAO) and the United Nations (UN) share the objective of providing food security for all people on Earth and ending hunger globally. Using strategies like reducing crop losses, maintaining sustainable production, and increasing the area under agricultural cultivation, this objective can be achieved. Food production is significantly impacted by climate change, which is directly to blame for numerous abiotic pressures such as temperature increases, droughts, and soil salinity. Invasive pests, disease, and other biotic stressors are all examples of the second type of stress. Specific tools can be used to identify the various forms of stress and provide guidance for their treatment. Remote sensing appears in this setting as a non-destructive technology capable of recognizing and pinpointing stress-prone areas. The first investigations involve the cultivation of the four horticultural crops listed below in soil that has been contaminated with the nematode *Meloidogyne incognita* throughout a five-year period between 2016 and 2020. Two treatments were used: plants grafted onto resistant rootstock and non-grafted plants. The second involved assessing 40 new bread wheat accessions for the presence of a fungus; some of them received fungicide application, while the remainder was left untreated. The trial sites were located across Northern Spain at Tordómar, Elorz, Briviesca, Sos del Rey Católico, and Ejea de los Caballeros.

From the straightforward to the complex, from the destructive to the non-destructive, from the high precision to the low precision, and from the ground to aerial perspectives, measurements are taken using a variety of scientific equipment. For the destructive measurement revealed by the stable isotope analysis, such as $\delta^{13}C$ and $\delta^{15}N$. The findings from stable isotopes showed interesting results in terms of the technique in explaining the plant status variation across the growing season. As, in the first study on nematodes, where the value of $\delta^{15}N$ ($\bar{x}$=4.02) in melon in 2016 and ($\bar{x}$=3.68, $p<0.05$) in pepper in non-grafted ones which means that grafted melon performed better than non-grafted ones and was characterized by better assimilation of nitrogen and low stress from the attack of nematode. In contrast, in the second study, the $\delta^{13}C$ value varied from ($\bar{x}$=-26.00) in Elorz to ($\bar{x}$=-27.08, $p<0.001$) in Ejea de los Caballeros, which indicated less water stress in the second location. The Dualex and SPAD (Soil Plant Analysis Development) leaf sensor instruments also produced significant results that allowed researchers to distinguish

between treatments, for example, where the value of flavonoids in the grafted plant was less than the non-grafted one or the value of Nitrogen Balance Index (NBI) in wheat treated by fungicide (Prosaro) ($\bar{x}$=35.69) exceed their untreated one ($\bar{x}$=34.56, $p<0.01$) in the Elorz site in the second study. In the first and second studies, canopy instruments like the GreenSeeker NDVI (Normalized Difference Vegetation Index) and RGB cameras were used to measure the whole canopy or plot. These instruments vegetation indicators or indexes produced good results that allowed for a comparison of the two different experimental treatments. For example, the Triangular Greenness Index (TGI) in the grafted plant ($\bar{x}$=2600, $p<0.001$) in melon 2016 whereas the non-grafted plant ($\bar{x}$ =1880). The second study demonstrated similar results, with treated wheat having a higher Green Area (GA) index than untreated wheat at least time in May and June in each location ($p<0.001$). Furthermore, aerial measurements were made using a standard RGB camera integrated into an Unmanned Aerial Vehicle (UAV) and showed similar outcomes for the RGB indices, as evidenced by the highest correlation between the vegetation indices at the ground and aerial levels in the case of TGI (r=0.817). This, however, was not the case for the experimental aerial NDVI modified camera, where the ground Greenseeker NDVI measurements made on Elorz 22 April (R^2=0.700, $p<0.001$) had a better correlation with grain yield than the aerial measurements where he registered the best value at 12 May Tordómar (R^2=0.231, $p<0.001$) made by the AgroCam GEO NDVI. In this sense, it is advisable to utilize a UAV for measuring RGB vegetation indices and the GreenSeeker for measuring the NDVI (or consider a better quality aerial NDVI sensor) due to the first's advantages of quickly covering a larger area and the latter's better results.

All of these tools, which operate at various levels, not only enable the identification of biotic stress but also demonstrate the importance of adopting smarter agricultural practices, such as grafting methods to safeguard horticultural crops from nematode aggression and the development of new varieties of fungal-resistant wheat or the careful application of fungicides. The use of intelligent crop production systems and management strategies is crucial for the sustainability of crop production as well as the security of food harvests.

Acknowledgements

I consider myself quite lucky to have completed my graduate studies at the University of Barcelona, which values collaboration. This is a special location with many wonderful individuals. And even though I'm only mentioning a few, many people have helped to make this journey successful and enjoyable.

My directors, **Dr. Shawn Carlisle Kefauver** and **Dr. Jose Luis Araus**, who made it possible for me to complete this thesis, have my sincere gratitude. Thank you, Dr. José, Luis Araus, for providing me with a place to call home in your lab and for your unwavering support throughout the years. The numerous possibilities you gave me and your invaluable advice made me very fortunate. Your knowledge, wisdom, and patience have caused me to view my research and work from angles I had not anticipated, and as a result, I gained fresh ideas. You were crucial to my professional and personal success as a scientist.

I would like to recognize my friend and colleagues in the Integrative Crop Ecophysiology Research Group (both the former and the recent ones).

You were always there for me when I needed you, **Adrian**, and **Fatima**.

You have such a heart of gold. Many thanks. How can I possibly thank **Adrian**, **Fatima**, **Luisa**, **Joel**, and **Rut** for everything. Thank you for being excellent coworkers and devoted friends.

Table of Contents

Table of Contents

Abbreviation **11**

Introduction **14**

Objectives **28**

Chapter 1: Comparison of proximal remote sensing devices of vegetable crops to determine the role of grafting in plant resistance to *Meloidogyne incognita*. **32**

Chapter 2: Using ground and UAV acquired vegetation indexes for the Assessment of fungal resistant bread wheat varieties. **61**

General Discussion **112**

Conclusions **120**

Summary of the thesis in Spanish **125**

References **129**

Abbreviations

Anth, Anthocyanin

CSI, Crop Senescence Index

Chl, Chlorophyll

CPRO, Protein Content

CT, Canopy temperature

Flav, Flavonoid

GA, Green Area

GGA, Greener Green Area

GY, Grain Yield

HTPP, High Throughput Phenotyping Platforms

LAI, Leaf Area Index

LCC, Leaf Chlorophyll Content

NBI, Nitrogen Balance Index

NDVI, Normalized Difference Vegetation Index

NGRDI, Normalized Green-Red Difference Index

PA, Precision Agriculture

PPNs, Phytoparasitic nematodes

RGB, Red-Green-Blue

RS, Remote Sensing

UAS, Unmanned Arial Sensors

UAV, Unmanned Arial vehicle

TGI, Triangular Greenness Index

VIs, Vegetation Indexes

$\delta^{13}C$, Stable Carbon Isotope Composition

$\delta^{15}N$, Stable Nitrogen Isotope Composition

Introduction

Introduction

Food systems that support food security are produced, processed, distributed, prepared, and consumed as a result of dynamic interactions between and within bio-geophysical and human contexts. To feed the world's population in the future, ensure nutritional security, take into account changing diets, and meet the rising demand for biological products from the energy and construction industries, global food production must increase by 70% (Galieni et al., 2021). Food systems can be directly affected by climate change in several ways, including crop yields. There are regional differences in the relative importance of climate change to food security (Gregory et al., 2005). As the frequency of extreme weather events, as well as significant changes in precipitation and temperature patterns, are anticipated to grow globally, climate change is exerting pressure (Cogato et al., 2019). As a result, abiotic (such as heat and drought) and/or biotic (such as diseases and pests) stresses and their combinations will likewise increase in frequency and, inthe absence of quick and efficient management responses (Nicol et al., 2011; Dresselhaus and Hückelhoven, 2018), result in declines in crop productivity (Gavender, 2009).

Crop protection experts need to address societal change and describe the key processes and influences of global change on agriculture to understand how to best control plant diseases to enhance food security in the context of climate change. Early detection of crop stress is therefore crucial to be able to respond with appropriate agrotechnical solutions and limit yield loss before permanent damage occurs. More specifically, improving food security is a critical task considering the increasing likelihood of extreme weather events (Figure 1).

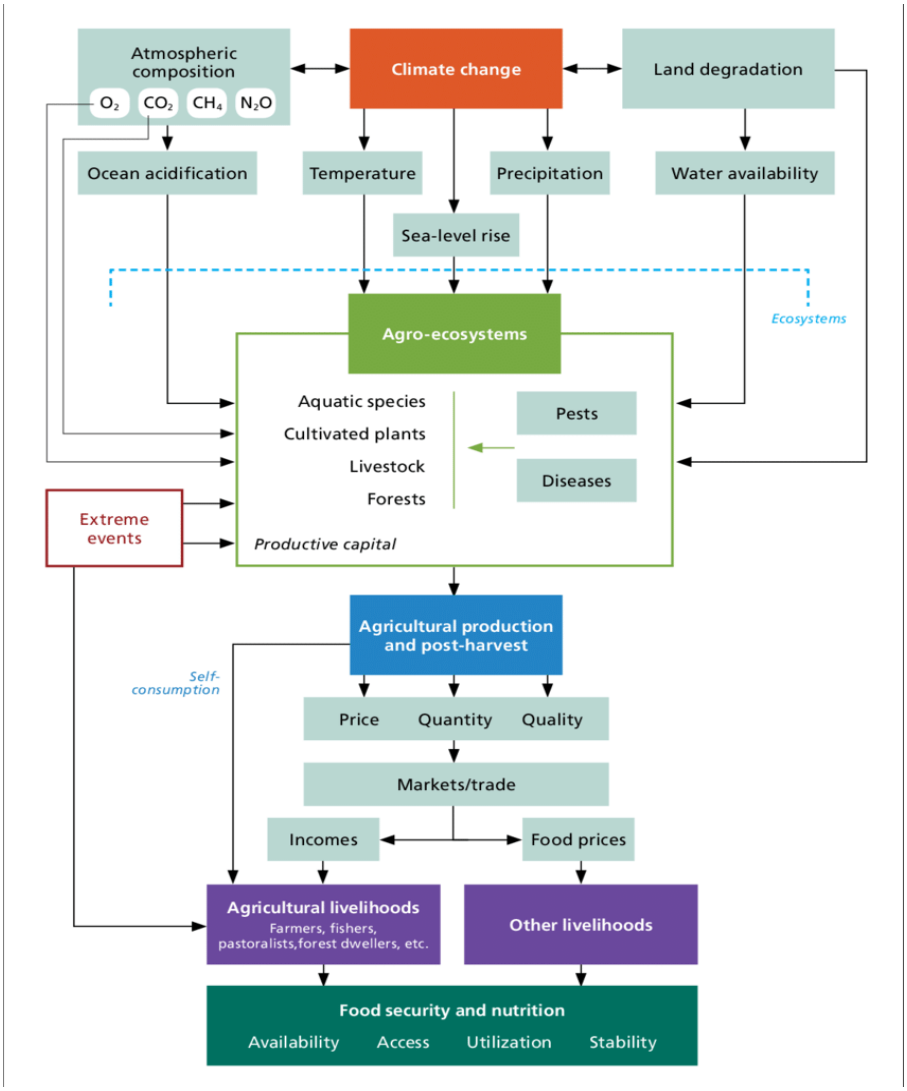

Figure 1. Cascading impacts of climate change from physical climate through to intermediate systems and then to people (SOFA, 2016).

The yield of a crop cultivar when cultivated in surroundings to which it is acclimated, with nutrients and water not being limited, and pests and diseases being adequately managed, is known as yield potential. For instance, the voluntary adoption of new crop varieties appears to have offsetthe detrimental effects of climate change on numerous crops throughout many nations in the world (Piao et al., 2010). Still, more crop productivity improvements will be required, including the creation of agricultural cultivars with increased yields and improved pest and disease resistance. Destructive and non-destructive approaches can be employed to identify and measure biotic and abiotic stressors. Regarding non-destructive quantitative techniques, at the leaf and canopy level, proximate sensors are employed to determine plant status. These instruments are frequently employed in smart

agriculture to monitor the state of the plant at various growth stages and can measure a range of different crop pigments or other properties like temperature and stomatal conductance.

Similarly, Remote Sensing (RS) technologies using light reflectance at the canopy level have been developed, including thermal, microwave, imaging spectroscopy, and fluorescence spectroscopy, all of which offer insights into how stress affects plants. In order to detect crop stress status and spatiotemporal changes across cultivated landscapes cost-effectively, RS can be implemented at greater spatial scales with high revisit frequency. Additionally, RS is appropriate for global coverage and may therefore help to improve food security in developing nations (see, for example, Rembold et al., 2013). Observations in various spectral domains are strongly advised in addition to the use of a single RS domain, as they may help to better understand the intricate relationships between stressors and crop attributes (Berger et al., 2022). Precision agriculture as well as plant breeding projects have both benefited from the identification of optical multi-sensor synergies for stress-related research in agriculture (Berger et al., 2022). Recent research suggests using multiscale UAV observations for effective early stress detection. The benefits of these platforms can be examined within such frameworks, such as the accessibility of data with improved temporal and spatial resolution (Alvarez-Vanhard et al., 2021). There are still logical holes in crop stress detection. The key shortcoming is that there is presently no concept that employs various spectral domains in an integrated manner to provide a comprehensive view of agricultural conditions to distinguish between different types of crop stress and to comprehend the intensity of the stress. Utilizing the full potential of the spectrum data offered by multi-domain RS data sources in a synergistic manner can help to address this deficiency. We thus intend to develop and put out a novel methodological idea for the evaluation of various plant stressors in agriculture using optical RS synergy.

1. Importance of horticultural crops for global nutrition security

Today, horticultural crops attract many impoverished farmers. Demand for cucumbers, melons, watermelons, squash, tomatoes, peppers, and other vegetables from the Solanaceae and Cucurbitaceae families has increased in recent years along with the consumption of fruits and vegetables. The high nutrient content of fruits and vegetables has helped to spread this trend (Lumpkin et al., 2005). For human nutrition, horticultural plants are an

important source of carbohydrates, proteins, organic acids, vitamins, and minerals. There is always a post-harvest component that results in losses when people use plants or plant components, whether they use for food or aesthetic reasons (Fallik, 2004). Fresh horticultural crops are distinguished by their content, general physiology, and morphological structure (roots, stems, leaves, flowers, fruits, etc. (Workneh and Osthoff, 2010).

Horticultural crops are important in developing countries both economically and socially to improve income and nutritional status. In addition, horticultural crops are considered by smallholder farmers as an alternative to staple crops, increasing income and improving employment prospects (Jaffee and Henson, 2004). To ensure a diet rich in vitamins and micronutrients, there is an opportunity to increase the production and consumption of vegetables and fruits (Davies and Bowman, 2014). Another factor is that a small-scale farmer can be economically successful in growing high-value horticultural crops if he or she has economies of scale.

2. Importance of wheat in world nutrition

It is necessary to improve food production and harvested area due to the world's growing population. where 10% of the world's population, particularly in Africa, was affected by hunger. The number of undernourished people will increase to 150 million between 2019 and 2022 (FAOSTAT, 2023).

Along with corn and rice, wheat is one of the world's most important crops, serving as a strategic staple for most of the world's population. With an estimated annual yield of 771 million tons, wheat is the second largest crop in the world after maize. About 219 million hectares are used for cultivation worldwide (FAOSTAT, 2019). Over 4.5 billion people in 94 developing countries obtain 20% of their protein needs and 21% of their food calories from wheat (Bock et al., 2010). Although bread wheat (*Triticum aestivum L.*) is the most important wheat species, durum wheat (*Triticum turgidum L. subsp. Durum (Desf) Husn*), even though it ranks ninth among the wheat species cultivated worldwide, is of great importance in the Mediterranean region as a crop and source of cultivation (FAOSTAT, 2019).

Global demand for wheat is increasing, and projections suggest that cereal production will need to increase by 2.4% annually to meet human needs in 2050. However, the current increase in global wheat productivity is only 0.9% per year, making it imperative to find

ways to increase wheat production (Ray et al., 2013). Between 2016 and 2021, the total area under bread wheat and durum wheat increased by only 6.8%, from 219 million ha to 221 million ha, while global production increased by 1%, from (with a global yield of 31.9 T/ha) to 33.5 (T/ha) (FAOSTAT, 2023). With a cultivated area of more than 220 million hectares and a production of 757 MT in 2017, Hexaploid bread wheat (*T. aestivum*) accounts for about 95% of global wheat production. According to FAO statistics, China, India, and Russia were the top three wheat producers, with a production of 134, 98.5, and 85.9 MT, respectively.

3. Different kinds of stress

From seed development to harvest, plants are regularly exposed to a variety of stressors at all stages of the life cycle. The two groups of these stressors are usually biotic and depending on the type of triggering component, abiotic stressors (Figure 2).

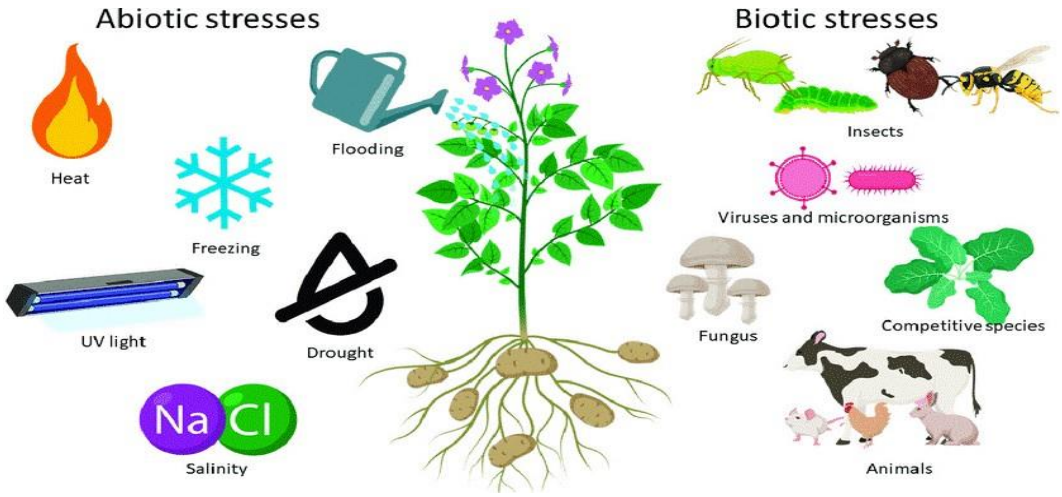

Figure 2. Different types of biotic and biotic stress can affect the plant (Paramo et al., 2020).

3.1. Biotic stress

Biotic stress is a problematic situation in which a plant is unable to maintain its regular growth because of interaction with harmful microbes (fungi, bacteria, viruses, viroid, phytoplasmas, and nematodes). These microorganisms develop primarily on or in plant tissues where they cause a variety of symptoms such as chlorosis, stunting, rotting, or the development of localized lesions (Balodi et al., 2017). Instead of infections caused by individual pathogens, infections caused by fungi, bacteria, and viruses together are common and result in severe disease symptoms (Pandey et al., 2017). Living organisms,

especially viruses, bacteria, fungi, nematodes, insects, arachnids, and weeds, cause biotic stress in plants that reduce plant vigor and, in severe cases, cause plant death. biotic stress in agriculture is a major factor in pre- and post-harvest losses. Infectious diseases that manifest in harvested fruits, usually caused by bacteria, fungi, or yeasts, cause biotic stress, also known as rot. Plants have a defense mechanism by which they respond to biotic stress (Atkinson and Urwin, 2012).

As viral, fungal, and bacterial infections affect leaves, photosynthesis is reduced in all major crops, significantly reducing productivity. About 28.2%, 37.4%, 31.2%, 40.3%, 26.3%, and 28.8% of yield losses in wheat, rice, corn, potato, soybean, and cotton, respectively, are attributed to biotic stressors, according to Sharma et al. (2017). Unlike vertebrates, plants do not have an adaptive immune system, i.e., the ability to adapt to new pathogens and remember previous infections. Despite the lack of an adaptive immune system, plants have evolved a wide range of complex defenses against biotic stressors. The plant genetic code contains the genetic basis for various defense mechanisms. Numerous genes for biotic stress tolerance are encoded in the plant genome. The defense mechanism falls under the category of an inherent and systemic response. During infection, plants increase cell lignification in response to pathogen attacks. This process prevents parasite invasion and reduces host susceptibility (Atkinson and Urwin, 2012).

Biotic stress is resisted by morphological and structural barriers, chemical substances, proteins, and enzymes. These provide strength and rigidity to products, as well as protection that gives them tolerance or resistance to biotic stressors. Many signal transduction pathways are used by plants to protect themselves against biotic stressors. The most important hormone involved in sensing numerous abiotic stressors is abscisic acid (ABA) (Cramer et al., 2011). On the other hand, ABA increases biotic stress resistance. Under biotic and abiotic stress, ABA and ethylene interact negatively and make the plant more susceptible to disease attack. However, ABA increases in response to abiotic stress and causes stomatal closure. As a result, biotic attackers cannot enter through the stomata. Consequently, under these circumstances, the plant is protected from biotic and abiotic stresses (Rejeb et al., 2014).

3.2. Abiotic stress

Abiotic stressors have a significant impact on plant development, growth, and quality; stress at the most sensitive phenological stages of plants can seriously affect the later

harvest. Perhaps the most important production limiting factor in agricultural systems is environmental stress. Production losses due to abiotic stressors such as adverse environmental conditions can increase significantly and range from 50% to 70% (Boyer, 1982). One of the top current and future difficulties facing the agricultural sector is climate change, which is often referred to as the leading cause of hunger globally. It is believed that the increase in temperature is the main cause of the decrease in water quality and quantity. The availability of this natural resource affects both agricultural productivity and human life. Abiotic stress conditions cause significant losses in agricultural production worldwide (Boyer, 1982).

Individual stress conditions such as drought, salinity, or heat are the subject of intensive research (Cushman and Bohnert, 2000). In practice, however, crops and other plants are routinely exposed to a combination of different abiotic stresses (Jiang and Huang, 2001). In drought areas, for example, many crops are exposed to a combination of drought and other stress factors such as heat or salinity. In addition, plant stress tolerance must be increased through genetic improvement, which requires long breeding programs and different production conditions to validate plant performance.

Abiotic stressors such as drought, salinity, unfavorable temperatures, and poor soil fertility are found almost everywhere in the world. Drought and nutrient deficiencies are two of them. Boyer estimated in 1982 that yield losses from adverse conditions can be as high as 70% (La Peña and Hughes, 2007), and Farooq and others (Farooq et al., 2009) showed that drought reduces yield between 13% and 94%, depending on the crop. This depends on depends on the duration and intensity of the stress. Subsequently, Cramer et al. 2011 calculated the impact in terms of the proportion of global land area affected by abiotic stresses affecting agricultural productivity, taking into account FAO reports from 2000 to 2007. Additionally, the host range of infections will extend due to climate change, increasing the likelihood that virulent strains may emerge (Garrett et al., 2006). Therefore, it is expected that mixed biotic and abiotic stress will occur more frequently in the future. According to the evidence at hand, depending on the stress and pathogen under study, the simultaneous occurrence of biotic and abiotic stresses can have a negative (i.e., susceptibility) or a positive (i.e., tolerance) effect on plants (Tippmann et al., 2006). According to reports on coupled pathogens and high-temperature stress, plants are more susceptible to disease at high temperatures.

4. Stable isotopic analyses for integrative assessments of crop stress

Many analyses can detect biotic or abiotic stresses that threaten crops and impacts their performance, with the stable isotope composition $\delta^{13}C$ (‰) and $\delta^{15}N$ (‰) being one of the most exact and comprehensive. While the analysis of $\delta^{13}C$ can provide information about the plant's water state, $\delta^{15}N$ informs about the plant's nitrogen uptake, sources, and root health. The analysis of $\delta^{13}C$ and $\delta^{15}N$ can provide information about biotic stress caused by organisms such as nematode attacks in horticultural crops indirectly through inference based on the impacts affecting root water and nutrient uptake, where especially the value of $\delta^{13}C$ can be heavily influenced by the crop species and the degree of resistance of the rootstock used in the crop, when grafting is applied (Hamdane et al., 2019). The isotope composition analysis of $\delta^{13}C$ and $\delta^{15}N$ has also been used to detect wheat abiotic stress (temperature, drought) in the durum wheat, where the analysis showed different results depending on the plant water regime and the temperature of the site (Rezzouk et al., 2020). Even stable isotope compositions of $\delta^{13}C$ and $\delta^{15}N$ in combination have been proven effective for studying the genotypic responses of durum wheat under diverse combinations of stress (drought, salinity) of particular interest in Mediterranean climates (Yousfi et al., 2012).

5. Leaf sensors for assessing crop stress

The SPAD (The Soil Plant Analysis Development) sensor is a leaf sensor tool that measures chlorophyll, giving information about the plant nutrient status and the efficiency of photosynthetic processes. The SPAD utilizes two LEDs with peak emission wavelengths of 650 nm and 940 nm to measure the leaf absorbance in the red and near-infrared areas to calculate the relative chlorophyll content. Newer, more advanced tools as the Dualex (Force-A, Orsay, France, Tremblay et al., 2012), which gives us a basic concept of the chlorophyll, flavonoid, anthocyanin, and Nitrogen Balance Index (NBI), can be used to determine plant pigment concentration. Some of its pigments, known as flavonoids, where the rise in flavonoid production serves as a plant stress signal, indicate that the plant was under stress, are a potent tool to study plant stress and learn about its state (Cerovic, 2015). The measurement of the pigment produces quick results and a general idea of the status of the plant, making it considered a non-destructive ground tool for researching how a plant reacts to different states. The selection of performance types is made possible by the much information this gadget sends. These tools enable one to follow the functioning of the plant, which directly influences the performance and final production (Gracia-Romero et

al., 2019). Other proximal tools, which are useful as non-destructive tools in the phenotyping process, include the GreenSeeker, which measures the NDVI index and other image-based approaches using different types of imaging sensors, which gather data that require additional know how for processing and the calculation of different vegetation indexes.

6. Proximal remote sensing tools to detect plant stress

Many tools of proximal remote sensing were used to detect the biotic and abiotic stress. One of the (RGB) cameras is made to resemble by detecting light in the visible spectrum derived from 400 to 700 nm. The reflectance in this range is mostly controlled by plant colors and thus pigments related to different plant biophysical properties, such as chlorophyll (Mahlein, 2016). This enables the process of computing various vegetation indices (VIs) using the blue, green, and red-light specific band's electromagnetic spectrum reflectivity (Jelínek et al., 2019). Healthy plants have green vegetation as the green light is reflected more due to the photosynthetic absorption of incident light relatively very low red reflectance of incident light is because chlorophyll absorbs red light. High chlorophyll content causes a combination of high green reflectance and low red reflectance, as opposed to unhealthy, stressed plants, where chlorophyll pigment is diminished, resulting in a smaller difference between green and red reflectance (generating a yellow or even brown color). Thus, RGB picture analysis can be used to identify physiological changes in plants that result in pigment changes, including those caused by pathogen infections (Simko et al., 2016).

On the other hand, Thermal Infrared (TIR) sensors, record point measurements (active “thermos gun” sensors) or images (passive imaging sensors) with information about surface energy emissions in the TIR electromagnetic spectrum, such as a canopy or leaf temperature of plants. Plant pathogens infections that cause high values for plant temperature denote places where stomata are closed (Chaerle et al., 2007), and this may have an impact on water stress in plants whose stomata control growth (Fang and Ramasamy, 2015). Thus, it may be possible to use thermography to detect early plant infection before symptoms appear as losses in pigments.

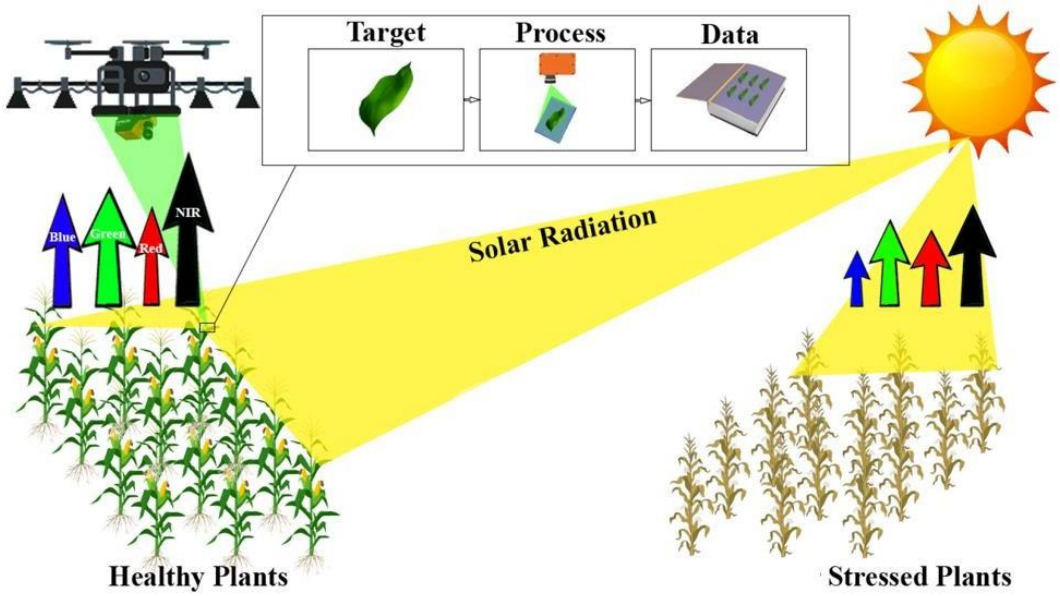

Figure 3. Detection of plant stress using remote sensing (Ahmad et al., 2021).

One of the most popular tools for monitoring crop growth and nutrients is the Trimble GreenSeeker for measuring the Normalized Difference Vegetation Index (NDVI, Trimble Navigation Limited, Sunnyvale, CA, USA). GreenSeeker NDVI was used (Zhang et al., 2019) to evaluate spring wheat growth and N status. A substantial correlation has been found between NDVI and grain production, biomass, nitrogen concentration, and plant absorption. Several vegetation indices have been used to improve crop production capacity, including the NDVI. NDVI has long been used to comprehend remote sensing data and has been widely used as remote sensing means in land use cover, vegetation cover density evaluation, crop identification, and growth monitoring (Tucker, 1979). Among various vegetation indices, NDVI has been proposed and used for decades and was most widely used in monitoring plant chlorophyll, N content, and disease (Xue and Sue, 2017) (Figure 3).

7. Phenotyping using high-throughput phenotyping (HTP) tools

Crop monitoring and breeding technologies must be highly effective, widely applicable, and reasonably priced, especially (but not exclusively) when small farmers from developing nations, national agricultural systems, or seed businesses are the target audiences. Additionally, breeding needs to be improved to get beyond the bottleneck caused by field phenotyping, which prevents breeding and PA (Precision Agriculture) advancements (Araus et al., 2008; Araus and Cairns, 2014). Different scales of observation (high vs. low-resolution sensors) and complexities (high and low throughput) can be used for phenotyping (Cobb, 2013). In general, high-throughput approaches result in whole plant examination at

medium to low resolution. This is the case with field phenotyping methods used for resource management and agricultural monitoring, such as nutrient and water allocation, weed infestation, and epidemiology, which allow automated systems to non-destructively examine hundreds of plants daily (Cobb, 2013). High throughput phenotyping (HTP) platforms can measure plant architecture, development, and environmental conditions using a wide range of image analysis and data processing tools. Remote sensing techniques are a powerful tool for plant breeding using HTP (Deery Sankaran and colleagues (2015), decision-making (Gago et al., 2020), PA, and crop yield forecasting. Their value depends on the fact that they are rapid, inexpensive, non-invasive, non-destructive, and well-linked to critical physiological plant traits. Thus, the use of HTPs for remote monitoring is becoming increasingly popular among scientists, especially in breeding and germplasm analysis (Fiorani and Schurr, 2013). Among the ground-based phenotyping devices are modified vehicles with deployed proximal sensing sensors. The term "proximal sensing" describes measurements made up close with tractors and portable sensors, which don't always involve seeing reflected light. Proximal, or close-range, sensing is expected to provide data collection with a range of view angles, lighting control, and a known distance between the plants and the sensors, as well as to offer a higher resolution for phenotyping studies. The scale at which these ground-based platforms can be used, their portability, and the length of time required to take the measurements in various field locations are only a few of their limitations (White et al., 2012).

Aerial-based phenotyping platforms, which are a supplement to ground-based platforms, allow for the quick characterization of multiple plots, eliminating one of the drawbacks of ground-based phenotyping platforms. An increasing body of research demonstrates how automated high-throughput field-based phenotyping techniques are improved by these approaches in remote and proximal sensing. Unmanned Aerial Systems (UAS), which have seen a surprising amount of development recently and are now potent sensor-bearing platforms for diverse agricultural and environmental applications, are one of the developing technologies in aerial-based platforms. UAS can quickly survey a whole experiment, providing a thorough evaluation of all the plots while reducing the impact of rapidly changing environmental factors such as wind speed, cloud cover, and solar radiation (Araus and Cairns., 2014). Airborne HTP systems have recently attracted more interest, especially for use in breeding and germplasm evaluation activities. Since UASs allow for finer resolutions of the same sensor technologies used on airplanes and satellites, remote sensing has finally been applied to crop breeding and phenotyping.

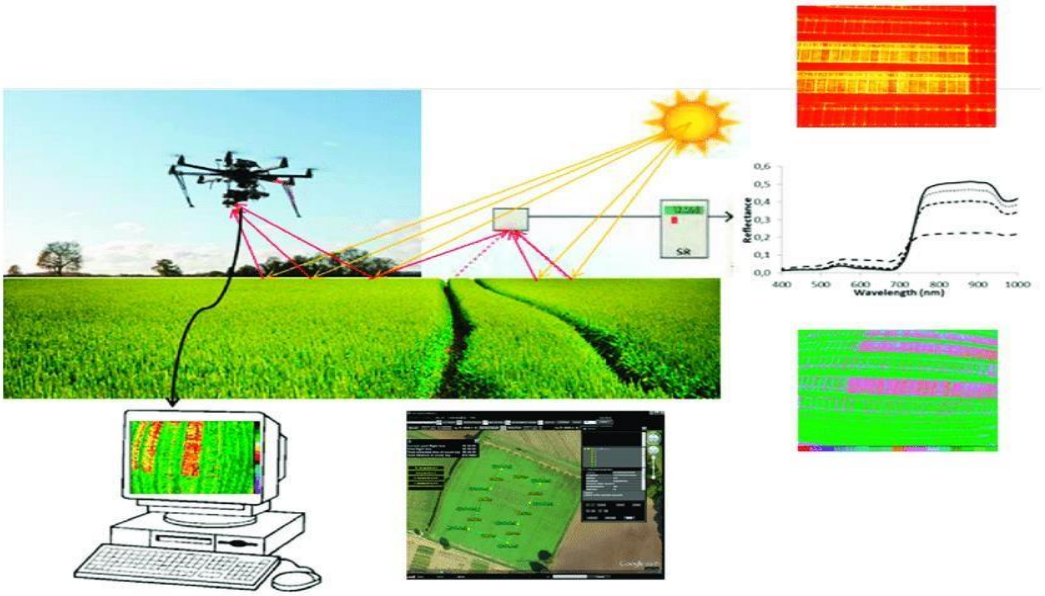

Figure 4. High throughput phenotyping using remote sensing (Morales et al., 2020).

The speed and affordability of UAS imaging allow for various measurements during different crop growth stages from emergence until senescence (Figure 4). There are several metrics to assess the best growth stage for measurements, as the likelihood that the ideal recording stage will change with crop type and experiments (Bowman et al., 2015). The effective use of such technology depends on the UAS attributes, such as stability, safety, control, reliability, steadiness, independence, sensor mount, control, sensor characteristics, image processing, and data analysis (Sankaran et al., 2015). The effectiveness of aircraft remote sensing methods depends on using direct plant data for training and evaluation (Liebisch et al., 2015). Numerous studies addressed the possibility of using image data generated by sensors on UASs and additional types of remotely piloted or manned platforms for aerial crop management (Rutkoski et al., 2016).

The use of remote sensing enables the assessment of plant characteristics at a scale and with an accuracy that is not possible as quickly using conventional methods. Numerous experiments using either RGB, TIR, or fluorescence tools to determine morphological traits, biomass, plant development, plant production, water status, canopy temperature, or disease signs in many crop and breeding programs (Yang et al., 2017). Apart from plant growth rate and plant height variation, spatial mapping was discovered in wheat at both individual and field levels. The RGB images can be taken at two levels at the ground using an RGB camera or at the aerial level with a camera mounted on a UAS (Holman et al., 2016).

Recently platforms with high throughput phenotyping sensors (as HTPs) that predominantly use ground-based and/or UASs offer tremendous opportunities for precise measurement of proxy characteristics (Peteinatos et al., 2016) across thousands of plots. In this context, increasing airborne and ground-based technologies are given special consideration. Such high-throughput phenotyping is enabled by HTPs (Madec et al., 2017). One potential drawback of the much longer duration method is ground-based phenotyping platforms. Due to the time required to conduct measurements compared to remote sensing using drones, which allows phenotyping over a larger space in a shorter time, large-scale experiments will always fail (Tuberosa, 2012). However, ground-based platforms may be more advantageous due to the greater data resolution provided by the closer proximity of sensors and the target plant.

In addition to visible and infrared images, the reflected spectra of crops can provide details about their structure and overall health, making them useful for evaluating plant growth characteristics. On UAS platforms, various imaging systems are being used for crop remote sensing. RGB, multispectral, hyperspectral, thermal, and inexpensive consumer-grade cameras that have been modified to capture near-infrared (NIR) are a few of the cameras employed. Due to their low price, light weight design, low power consumption, and ability to store thousands of images, consumer-grade digital cameras are frequently used as the sensor of choice (Liebisch et al., 2015).

Objectives

Objectives

The main objective of this work is to identify biotic stress in horticultural and cereal crops. The first study will highlight the effects of biotic stress and the role of grafting in protecting horticultural crops against nematode attacks in greenhouse environments. In addition, for the second study, we try to select the wheat variety that is resistant to fungal attack using some more advanced methods, such as spatial remote sensing using UAS imagery. We furthermore try to align the importance of fungicide treatment in the protection of bread wheat crops across different study sites and crop growth stages.

The Ph.D. thesis study was divided into two sections, the first of which was based on a collection of field data from five horticultural crops planted under a greenhouse (pepper, tomato, eggplant,and melon) grown over five years from 2016 to 2020. The middle parts of each culture are planted on their proper roots, and the remaining parts are grafted onto disease-resistant stocks. In the soil where the root-knot nematode (*Meloidogyne incognita*) occurs, each plant is exposed to identical growth conditions. The plants were monitored until harvest.

For the second part of the study, 40 new lines of bread wheat were grown at five experimental sites across Spain operated by Limagrain (Tordómar, Briviesca, Elorz, Sos del Rey Católico, and Ejea de Los Caballeros). There were four replicate plots at each site, each containing the same panel of new lines fixed produced by the Limagrain company. Three of the plots received a fungicide treatment (Prosaro) while the fourth remained untreated.

The following specific objectives relate to these general objectives:

To highlight the role of the platform of sensors used in the detection of the difference between the treatment (grafting in the first study, treatment by fungicide in the second study)

To determine the impact of biotic stress (nematode for the horticultural crops and fungal (septoria, brown rust, and stripe rust) attack for the bread wheat crop.

To protect horticultural crops from attack by the specific nematode (*Meloidogyne incognita*), it is important to emphasize the importance of grafting techniques.

Emphasize the importance of fungicide (Prosaro) treatments in protecting wheat crops

from fungal attack and their impact on crop performance.

In the first study, emphasize the significance of RGB images and pigment tools in the early detection of nematode assault.

In the second study, establish the significance of the RGB and NDVI indices from ground and aerial levels in the early identification of wheat illness (fungal disease).

Emphasizing the importance of new methods for examining the health and phenotyping of assets,such as unmanned UASs and direct remote sensing.

Two chapters, developed as information instances for publication as scholarly articles in internationally indexed and high impact factor journals, make up this doctoral thesis report.

Chapter 1 of the dissertation on the use of sensors for horticultural crops has already been published in the journal Agronomy as “Comparison of Proximal Remote Sensing Devices of Vegetable Crops to Determine the Role of Grafting in Plant Resistance to *Meloidogyne incognita.*”

Chapter 2 of the dissertation on the use of sensors and UAV remote sensing, “Using ground and UAV vegetation indexes for the assessment of fungal resistant bread wheat varieties” has been accepted for publication in the journal Drones.

Chapter 1

Comparison of Proximal Remote Sensing Devices of Vegetable Crops to Determine the Role of Grafting in Plant Resistance to *Meloidogyne incognita*

Abstract: Proximal remote sensing devices are novel tools that enable the study of plant health status through the measurement of specific characteristics, including the color or spectrum of light reflected or transmitted by the leaves or the canopy. The aim of this study is to compare the RGB and multispectral data collected during five years (2016–2020) of four fruiting vegetables (melon, tomato, eggplant, and peppers) with trial treatments of non-grafted and grafted onto resistant rootstocks cultivated in a *Meloidogyne incognita* (a root-knot nematode) infested soil in a greenhouse. The proximal remote sensing of plant health status data collected was divided into three levels. Firstly, leaf level pigments were measured using two different handheld sensors (SPAD and Dualex). Secondly, canopy vigor and biomass were assessed using vegetation indices derived from RGB images and the Normalized Difference Vegetation Index (NDVI) measured with a portable spectroradiometer (Greenseeker). Third, we assessed plant level water stress, as a consequence of the root damage by nematodes, using stomatal conductance measured with a porometer and indirectly using plant temperature with an infrared thermometer, and also the stable carbon isotope composition of leaf dry matter. It was found that the interaction between treatments and crops (ANOVA) was statistically different for only four of seventeen parameters: flavonoid ($p<0.05$), NBI ($p<0.05$), NDVI ($p<0.05$) and the RGB CSI (Crop Senescence Index) ($p<0.05$). Concerning the effect of treatments across all crops, differences existed only in two parameters, which were flavonoid ($p<0.05$) and CSI ($p<0.001$). Grafted plants contained fewer flavonoids ($\bar{x}=1.37$) and showed lower CSI ($\bar{x}=11.65$) than non-grafted plants ($\bar{x}=1.98$ and $\bar{x}=17.28$, respectively, $p<0.05$ and $p<0.05$) when combining all five years and four crops. We conclude that the grafted plants were less stressed and more protected against nematode attack. Leaf flavonoids content and the CSI index were robust indicators of root-knot nematode impacts across multiple crop types.

Keywords: proximal remote sensing; root-knot nematode; RGB images; rootstock; melon; pepper; eggplant; tomato; grafted plants; non-grafted plants

Introduction

Phytoparasitic nematodes (PPNs) are responsible for significant economic losses to a wide variety of crops worldwide [1]. PPNs cause a reduction in crop yield by the direct destruction of root cells or indirectly, by propagating viruses, or by facilitating the invasion of fungi and bacteria through lesions caused during their penetration into the roots. The total losses caused by PPNs are estimated at more than 100 billion dollars per year worldwide, correlatively to reductions in yields of the order of 10–20% for cash crops [2]. These losses are generally greater in tropical regions, where the reproduction rate of nematodes is higher than in temperate zones [2]. In addition, the reduction in yields caused by PPNs could be intensified due to restrictions imposed on the use of chemical fumigants [3] and the voluntary withdrawal of certain nematicides from the market. The environmental complexities facing world agriculture today challenge conventional methods of production. Agronomic research is therefore moving toward alternatives aimed at reducing or even eliminating synthetic nematicides [4]. Meloidogyne is mandatory sedentary endoparasite nematodes (Table 1). They complete their cycle in the root, the only free stage in the soil being the second stage juvenile (J2). They induce significant root transformations leading to the formation of galls typically by infection of the conductive tissues of the plant, which may wither and die, reducing yield and losses in fruit quality. They are characteristically polyphagous, with more than 5500 species of host plants [5].

Table 1. General characteristics of Meloidogyne.

Size and Description	Microscopic Soil Worm Measuring 0.3 mm Long (2nd Grade Juvenile Free Stage in the Soil) at 0.7 mm (Female Obese Pear Shaped in the Root). Oral Perforator Stylus [6].
Reproduction	Sexual or asexual (parthenogenesis) [1].
Life cycle	3 weeks to 3 months (depending on temperature). Mandatory endoparasite (inside the root). Eggs/juveniles/adults: 4 successive molts –evolution, Female [1].
Multiplication	Lays 300 to 1000 eggs per cycle, Several possible cycles per year = 300 to 200,000 eggs per year [1].
Conservation	In the form of eggs in the soil, between 5 and 30 cm deep [1].
Survival	Juveniles live at least up to 15 days, depending on environmental conditions (pH, temperature, soil moisture, presence or not of plants). Eggs > 1 year, under certain conditions. Dispersion can be by humans (shoes, tools, machines) and by water at stage J2 [6]
Wales	Damage to roots (gall index from 0 to 10). Wilting, withering or even death of plants [1].
Main hosts	Vegetables: asparagus, eggplant, vegetable beet, carrot, celery, chicory, cucumber, melon, pumpkin, zucchini, spinach, beans, lettuce, onion, pepper, tomato, potato, leek; rapeseed; cereals; fruit trees; flower crops; weeds including *Rumex* spp., amaranth, nightshade [6].
Protection	Prophylaxis: cleaning, disinfection of tools, no spreading potentially by waste or sludge. Physical protection: solarization, steam disinfection, soil flood. Biological protection: organic matter, bacteria, mushrooms, mycorrhizae. Chemical protection: pre- and post-planting, treatment seeds, plant extract Crop protection: rotation, trap plant, green manure "nematicide", black fallow, bio-fumigation, anaerobic bio-disinfection Varietal protection: resistance, grafting [6].

New techniques have been brought to agriculture by advancements in precision agriculture and plant phenotyping that allow for rapid and non-destructive assessments of crop health [7]. In order to better study the crop physiological status and nutrient or other management requirements, we propose the use of advanced tools such as leaf sensors and proximal remote sensing instruments. For instance, the leaf level chlorophyll (measured for example with a portable device), may be considered a reflection of the reduced capacity of nematode infested roots to capture nutrients. Additionally, measuring the NDVI (Normalized Difference Vegetation Index, an index of above ground biomass and plant vigor combined) is useful for assessing whole plant level vigor and may be understood as a combination of root damage effects on nutrient and water uptake capacity, plus plant reallocation of resources to root growth from shoot growth. Then, the combined used of RGB (red, green, and blue) and multispectral (visible and near infrared reflectance combinations) cameras allows for the calculation of NDVI and other different image indexes informing on Leaf Area Index (LAI), Leaf Chlorophyll Content (LCC), crop biomass and vigor [8]. At the single leaf level, sensors such as the Dualex, assess different pigment contents (chlorophyll, flavonol, anthocyanin) together with the nitrogen balance index (NBI).

All of these indices can give a general idea about the modification in the production of the pigment and then the reaction of the plant against the attack of the pest. The use of natural abundance stable isotopes such as carbon and nitrogen isotope composition may allow monitoring the response of plants to different growing conditions because stable isotope data can quickly give information on the condition of the plant [9]. Carbon isotope composition ($\delta^{13}C‰$) in its natural abundance in plant dry matter has been used for decades as a tool for screening water use efficiency (WUE) and thus indirectly water plant status during in C3 plants [9]. The use of natural variation on the stable nitrogen isotope composition ($\delta^{15}N‰$) has been used as a proxy to study nitrogen plant dynamics and as a tracer of then nitrogen sources used by the plant [10–13]. In this study, field sensors and rapid assessment techniques including non-destructive, proximal, and remote sensing, together with carbon and nitrogen stable signatures and total elemental contents were used to assess the interaction between nematode presence and grafting on physiological status of different horticultural crops growing in a greenhouse. To highlight the need for rapidly assessing nematode damage to crop growth, comparisons were made between the growth and physiological status of different crops grafted to rootstock resistant to root-knot nematodes (RKNs) and those without grafting (non-grafted). In this work, we first summarize some important aspects concerning the

different trials and data collected regarding nematodes and horticultural crops, and then we follow with combined analyses, which include the comparison and synthesis of five seasons of field data collected of different crops grown sequentially in the same greenhouse with a strong nematode presence for five years from 2016–2020.

2. Materials and Methods

2.1. Study site

This research was carried out between 28 September and 8 October over five successive years from 2016 to 2020 in a plastic greenhouse located at the experimental station of Agròpolis (41°17′18.1″ N 2°02′38.5″ E+18 m above the sea level, approx.) of the Barcelona School of Agri-food and Biosystems Engineering of the Universitat Politècnica de Catalunya (EEABB-UPC), in the municipality of Viladecans (Barcelona, Spain) (Figure 1). The inside of the greenhouse during the 2019 trial is shown in Figure 2.

Figure 1. Satellite image of the experimental station of Agròpolis (The red box indicates the specific location of the research greenhouse).

Figure 2. The greenhouse at Agròpolis, place of realization of the experiments, showing rows of pepper plants (*Capsicum annuum cv. Tinsena*) from year 2019. Drip irrigation was used, and plastic mats were deployed between rows to limit weed growth.

2.2. Experimental Trial Designs

In the year 2016, we used 40 plots total of melon (*Cucumis melo var. reticulatus)* cv. Paloma, of which each block contained five plants and there were two treatment variables, the first non-grafted or grafted onto the rootstock *Cucumis metuliferus* and the second consisting of three levels of nematode infection. So, in total, we have two crop treatments (grafted or non-grafted) and (control, low, high infection) for 6 total treatments. Each treatment has repetitions with an increase to 10 plots for grafted and non-grafted control.

Regarding the experiment of the year 2017, during which melon (*Cucumis melo var. reticulatus*) and tomato plants (*Solanum lycopersicum cv. Durinta*) were cultivated, the total number of sample plots was 80, which are distributed as 40 melon plots and 40 tomato plots. For the 40 plots of each species, they were divided into six treatments melon grafted onto *Cucumis metuliferus* or non-grafted and tomato grafted onto the rootstock 'Alligator' or non-grafted and (control, low, high infection by nematode). The number of plot repetitions per treatment was five for control, 10 for grafted and 10 for non-grafted.

Moving on to 2018, during which we studied solely eggplant (*Solanum melongena cv. Cristal*), the total number of 20 sample plots were divided into four blocks containing five plants in each block. At the block level, non-grafted eggplants were placed in front and

grafted eggplants onto *Solanum torvum* ‘Brutus’ in back for both crop lines for 10 non-grafted and 10 grafted eggplants total.

Pepper plants (*Capsicum annuum cv. Tinsena*) were studied in 2019 with 40 sample plots divided into four lines, with each line containing one treatment. The number of repetitions per treatment per line was ten, so each treatment had 20 repetitions. The treatments were non-grafted and grafted pepper plants onto pepper rootstock ‘Oscos’. Ending with 2020, 40 sample plots were divided into four lines of tomato (*Solanum lycopersicum*). Then, two lines were cultivated with tomato cv. Durinta and the rest with the resistant tomato cv. Caramba. In total, we registered 20 susceptible and 20 resistant tomato plots each in order to show its effects on the plant performance.

The experiments were conducted in the same plots from 2016 to 2020: from March to July (spring crop) and July to November (summer crop). In 2017, only the spring crop was carried out. Grafted and non-grafted melon and tomato were cultivated from April to August and from April to September, respectively. Individual plots consisted of a row 2.5 m long and 1.5 m wide containing 4 plants spaced 0.55 m between them. Plots were spaced 0.9 m within a row and 1.5 m between rows. The soil of each plot was prepared separately to avoid cross-contamination. The soil was loamy sand textured, with 1.8 % organic matter (w/w) and 0.5 dS m^{-1} electric conductivity. Plants were irrigated and fertilized by a drip irrigation system with a solution of NPK (15–5-30) at 31 kg ha^{-1}, and iron chelate and micronutrients at 0.9 kg ha^{-1}. The fruits were collected and weighed when they reached approximately the United Nations Economic Commission for Europe (UNECE) commercial standards for fresh fruit and vegetables (https://unece.org/trade/wp7/FFV-Standards accessed on 20 April 2022 [14]), and the relative crop yield was calculated as the crop yield in a RKN infested plot in relation to the mean crop yield in non-infested plots.

2.3. Sensors and Measurements

All sensors were used during the fruit development phase (varies by crop) in a modified fall season of the open-air greenhouse at the Agròpolis between the last week of September and the first week of October. All the sensors were used at the same time of day for each year in one single data collection activity between 15:30 h and 18:30 h CET.

2.3.1. Determination of Leaf Level Pigments

SPAD

The Konika Minolta SPAD-502 Plus (Spectrum Technologies Inc., Plainfield, IL, USA; [15]) determines the relative chlorophyll concentration by measuring the leaf absorbance in red

and near-infrared regions [16] from light emitted by two LEDs with peak wavelengths at 650 nm and 940 nm. With these absorbance values, the SPAD (Soil Plant Analysis Development) calculates a company defined SPAD value by division of light transmission intensities at 650 nm (red) by 942 nm (infrared) to estimate chlorophyll content [15]. For each plant we placed the third mature leaf of each plant in each plot between the two measuring heads and waited for a few seconds to read the SPAD index value of chlorophyll.

Dualex

Leaf pigment contents were measured using a leaf-clip portable sensor Dualex Force-A (Force-A, Orsay, France) that measures chlorophyll, flavonoids and anthocyanins non-destructively, as actual estimations of leaf pigment concentrations [17]. In addition, the Dualex calculates the proprietary Nitrogen Balance Index (NBI), which is the chlorophyll/flavonoids ratio related to the nitrogen and carbon allocation [18]. The Dualex operates with a UV excitation beam at 357 nm, corresponding to the maximum absorption for flavonoids; another LED operates in the green band for anthocyanins; a red reference beam at 650 nm, corresponding to the absorption for chlorophyll; and two other reference bands operate in the near-infrared. For each plot, the measurements were done at the adaxial leaf side closing the two terminals of the device on the sheet chosen in the plant.

2.3.2. Determination of Plant Health and Vigor

Trimble GreenSeeker NDVI

The NDVI was determined at ground level for each plot using a portable active sensor, the Greenseeker handheld crop sensor (Trimble, Sunnyvale, CA, USA) by passing the sensor over the middle of each plot at a constant height of 0.5 m above a perpendicular to the canopy [19]. The sensor emits brief bursts of red and infrared light (656 nm and 774 nm), and then measures the amount of each type of light that is reflected from the plant. It continues to sample the scanned area for as long as the trigger remains engaged. Then, the average measured value in terms of an NDVI index reading (ranging from 0.00 to 0.99) is displayed on its LCD display screen.

Red, Green, Blue (RGB) Images

Vegetation indexes derived from RGB images (Table 2) were evaluated for each plot, from the ground. At ground level, one picture was taken per plot, holding the camera at 80 cm above the plant canopy in a zenithal plane and focusing near the center of each

plot. RGB images were obtained using a 16-megapixel Panasonic Lumix DMC GX7 (Panasonic, Osaka, Japan). The images were subsequently analyzed using the Cereal Scanner plugin (https://gitlab.com/sckefauver/cerealscanner accessed on 12 March 2019 [20]). This software includes a JAVA8 version of Breedpix 2.0 (https://bio-protocol.org/e1488 accessed on 14 March 2019, IRTA, Lleida, Spain), which calculates RGB vegetation indices using RGB and different color properties, such as Hue, Saturation, and Intensity (HSI) to measure plant properties of interest, such as foliar surface area, a close proxy to plant biomass or Leaf Area Index (LAI). In addition, the portion of pixels with hue classified as green was determined with the green area (GA) and greener area (GGA) indexes. GA is the percentage of pixels in the image with a hue range from 60 to 180, including yellow to bluish-green color values. Meanwhile, GGA is more restrictive, because it reduces the range from 80 to 180, thus excluding the yellowish-green tones. Both indexes are also used for the formulation of the CSI [21], which provides a scaled ratio between yellow and green pixels to assess the percentage of senescent vegetation. Besides the Breedpix indexes mentioned, two other indexes were measured with digital values of the red, green, and blue bands derived from the RGB color model. The Normalized Green Red Difference Index (NGRDI) is similar to the NDVI but uses green instead of near infrared (NIR) bands [22]. The Triangular Greenness Index (TGI) estimates chlorophyll content based on the area of a triangle with the three points corresponding to the red, green, and blue bands [23]. Details of the RGB index calculations are provided in Table 2.

Table 2. Indexes derived from the RGB cameras.

Target Group	Index	Formula
Vegetation Cover	Green Area (GA)	60 < Hue < 180 [20]
	Greener Area (GGA)	80 < Hue <180 [20]
Greenness	Crop Senescence Index (CSI)	(GA-GGA)/GA [24]
	Normalized Green-Red Difference Index (NGRDI)	(R550-R670)/(R550 + R670) [25]
	Triangular Greenness Index (TGI)	$-0.5[190(R670 - R550) - 120(R670 - R480)$ [26]

2.3.2. Water Stress and Root Health

Porometer

Measurement of leaf stomatal conductance (mmol m^{-2} s^{-1}) is critical for numerous aspects of viticulture research. Stomatal conductance regulates many plant processes (carbon dioxide assimilation, respiration, transpiration) and may be used to determine water status, response to climatic factors, stomatal conductance (g_s) was measured with a Decagon Leaf Porometer SC-1 (Decagon Device Inc., Pullman, WA, USA). One flag leaf was measured for each plot [27].

Canopy Temperature

Canopy temperature (CT) was measured by the infrared thermometer Photo Temp TM MXSTM TD infrared thermometer (Raytek, Santa Cruz, CA, USA), pointing towards the canopy at approximately 1 m and in the opposite direction to the sun [28]. A few measurements were taken per plant, for plot and leaf temperature. The results are presented in degrees Celsius (°C). The temperature of the plant was further adjusted by the ambient temperature to provide an estimate of crop water stress as the plant actively cools through transpiration; this is called the canopy temperature deficit, which may increase as a sign of nematode damage to the crop root system [29].

Determination of Stable Isotopes: ^{13}C and ^{15}N of the Soluble Fraction

The determination of stable isotopes was conducted to further validate whether the plants suffered from water stress over the whole of the crop season, which can be seen as an integral measurement that is complementary to the instantaneous water stress assessments provided by the leaf and air temperature measurements. The leaves (obtained from the determination of the dry weight) were dried, weighed and crushed following the soluble fraction extraction protocol as follows. Samples of 50 mg were added to 1 mL of MiliQ (Ultra-pure) and mixed well while on ice and centrifuged for 5 min at 5 °C at 12,000 rpm. The supernatant was recovered and incubated for 5 min at 100 °C and then again put in ice for 6 min. A second centrifugation was carried out for 5 min at 5 °C and rpm to separate the proteins from the soluble fraction. Then, a 50 µL aliquot of protein-free supernatant was transferred and dried for two hours at 70 °C. The stable carbon isotope composition ($\delta^{13}C$) together with the total carbon and nitrogen concentrations of the control and resistant plant leaves were determined using an elemental analyzer (EA; Flash 1112 EA, Thermo Fisher Scientific, Bremen, Germany) coupled with an isotope ratio-mass

spectrometer (IRMS; Delta C with CONFLO III interface, Thermo Fisher Scientific, Bremen, Germany) operating in continuous-flow mode in order to determine the stable carbon ($^{13}C/^{12}C$) isotope ratios of the same samples. Samples of approximately 50 µL were placed into tin capsules, weighted, sealed, and then loaded into an automatic sampler (Thermo Fisher Scientific, Bremen, Germany) before EA-IRMS analysis. The $^{13}C/^{12}C$ ratios of the plant material were expressed in δ notation: $\delta^{13}C$ (‰) = ($^{13}C/^{12}C$) sample/($^{13}C/^{12}C$) standard 1, where "sample" refers to plant material and "standard" to international secondary standards of known $^{13}C/^{12}C$ ratios (International Atomic Energy Agency (IAEA) CH7 polyethylene foil, IAEA CH6 Sucrose, and the United States Geological Survey, USGS) 40 l-glutamic acid) calibrated against Vienna Pee Dee Belemnite calcium carbonate with an analytical precision (SD) of 0.10‰. The ($^{15}N/^{14}N$) ratios of plant material were expressed in δ notation (Coplen, 2008): $\delta^{15}N$ = ($^{15}N/^{14}N$) sample/($^{15}N/^{14}N$) standard 1, where "sample" refers to plant material and "standard" N^2 in air. Total carbon and nitrogen contents were expressed as a percentage of the dry matter (%). Measurements were carried out at the Scientific Facilities of the University of Barcelona [30,31].

2.4. Statistical Processing

Statistical treatment was done using Statgraphics Centurion XVI (Developed by Stat-point Technologies, Warrenton, VA, USA) for basic data analyses like mean and standard error and ANOVA. The calculation of correlation values was completed in MS Office Excel 2007 (developed by Microsoft, Redmond, WA, USA). Finally, the graphics were obtained using Sigma Plot 12.5 (Systat software, Chicago, IL, USA).

3. Results

3.1. Physiological Parameters

The general trial data presented in Table 3 is further complemented by the data listed in the supplemental tables (Tables S1, S3, S4, S6, S7, S9 and S11), where for most parameters, we can observe that the values of grafted plants exceeded those of non-grafted plants. We can classify the parameters depending on the higher values recorded in all the crops. We note for melon (Chl, Flav, Anth, NDVI, TGI, CSI), tomato (GGA, NRGDI, Porometer, $\delta^{13}C$, Percent N), eggplant (GA, Percent C), and pepper (SPAD, Temperature, $\delta^{13}C$, $\delta^{15}N$). We should say for eggplant and pepper that porometer was not measured in contrast to the other species. Data analyses for individual years and different combinations of repeated crops are presented as Supplemental Tables S1–S11. SPAD (Soil Plant Analysis Development), Chl (chlorophyll), Flav (flavonoid), Anth

(anthocyanin), NBI (Nitrogen Balance Index), GA (Green area), GGA (Greener Green Area), TGI (Triangular Greenness Index), NGRDI (Normalized Green Red Difference Index), CSI (Crop Senescence Index), $\delta^{13}C$ (isotopic composition of carbon 13), percent C (percentage of carbon), $\delta^{15}N$ (isotopic composition of nitrogen 15), and percent N (percentage of nitrogen).

Table 3. Mean and standard error of each crop combining values of repeated years of crops for three classes of parameters (leaf level pigments, canopy vigor and biomass, water stress and root health), n=152.

	Parameters	Mean Melon 2016 + 2017 n = 36 (20 + 16)	Mean Tomato 2017 + 2020 n = 56 (16 + 40)	Mean Eggplant 2018 n = 20	Mean pepper 2019 n = 40
Leaf level pigments (SPAD, Dualex)	SPAD	39.42 ± 1.16	44.58 ± 0.93	40.16 ± 1.56	55.03 ± 1.10
	Chl	33.20 ± 0.67	24.20 ± 0.54	24.04 ± 0.90	24.76 ± 0.64
	Flav	1.82 ± 0.04	0.69 ± 0.05	0.65 ± 0.04	0.66 ± 0.03
	Anth	0.17 ± 0.01	0.05 ± 0.02	0.02 ± 0.04	0.02 ± 0.02
	NBI	18.79 ± 0.83	36.31 ± 0.67	38.09 ± 1.12	38.17 ± 0.79
Canopy vigor, biomass (GA and GGA up to RGB)	NDVI	0.41 ± 0.02	0.39 ± 0.04	0.64 ± 0.03	0.39 ± 0.02
	GA	0.43 ± 0.03	0.37 ± 0.02	0.68 ± 0.04	0.07 ± 0.03
	GGA	0.22 ± 0.03	0.49 ± 0.02	0.48 ± 0.03	0.06 ± 0.02
	NGRDI	−0.60 ± 0.36	1.46 ± 0.29	0.05 ± 0.48	−0.13 ± 0.35
	TGI	6300.72 ± 603.65	4525.35 ± 484	3601.41 ± 809.89	895.58 ± 588.37
	CSI	50.09 ± 2.58	17.45 ± 2.07	31.63 ± 3.46	19.29 ± 2.45
Water stress and root health	Porometer	102.60 ± 5.89	123.21 ± 4.72		
	Temp	25.18 ± 0.27	24.36 ± 0.22	25.53 ± 0.36	26.67 ± 0.26
	$\delta^{13}C$	14.16 ± 1.13	−30.57 ± 0.89	−30.19 ± 1.54	−29.58 ± 1.06
	Percent C	21.12 ± 1.35	36.81 ± 1.07	37.94 ± 1.84	26.63 ± 1.26
	$\delta^{15}N$	4.02 ± 0.30	4.63 ± 0.24	6.05 ± 0.41	7.12 ± 0.28
	Percent N	1.16 ± 0.13	3.31 ± 0.10	2.96 ± 0.18	1.96 ± 0.12

Table 4. ANOVA of three classes of parameters (leaf level pigments, canopy vigor and biomass, water stress and root health) achieved for four crops (melon, tomato, eggplant, pepper) with two treatments (grafted, non-grafted) n=152 for an experience during five years (2016–2020) under greenhouse in soil infected by root-knot nematode in order to show the role of grafting in the protection of plant and reduce the effect of this pest. We also show the effect separately of crop, treatments, and the interaction of both. SPAD (Soil Plant Analysis Development), Chl (chlorophyll), Flav (flavonoid), Anth (anthocyanin), NBI (Nitrogen Balance Index), GA (Green area), GGA (Greener Green Area), TGI (Triangular Greenness Index), NGRDI (Normalized Green Red Difference Index), CSI (Crop Senescence Index), $\delta^{13}C$ (isotopic composition of carbon 13), percent C (percentage of carbon), $\delta^{15}N$ (isotopic composition of nitrogen 15), and percent N (percentage of nitrogen), *: Interaction between variables.

	Parameters	*p* Value Treatments (Grafted, Non-Grafted)	*p* Value Interaction (Crop * Treatments)
Leaf level pigments (SPAD and Dualex)	SPAD	0.110	0.380
	Chl	0.140	0.066
	Flav	0.003	0.002
	Anth	0.607	0.565
	NBI	0.060	0.044
Canopy vigor, biomass (GA and GGA up to RGB)	NDVI	0.768	0.004
	GA	0.725	0.606
	GGA	0.102	0.810
	NGRDI	0.474	0.889
	TGI	0.322	0.810
	CSI	0.001	0.002
Water stress and root health	Porometer	0.724	0.267
	Temperature	0.178	0.654
	$\delta^{13}C$	0.819	0.984
	Percent C	0.702	0.925
	$\delta^{15}N$	0.335	0.121
	Percent N	0.793	0.210

The trial sensor data from Table 4 are complemented by supplemental data tables in the Supplemental (Tables S2, S5, S8 and S10), where we may furthermore note that for treatments, two factors were statically significant, Flav and CSI. For the interaction crop * treatment, two other parameters were statically significant, NBI and NDVI. The significant difference of parameters measured is important in considering that each species has physiological and biological responses to pest attacks that may affect the measured parameter values. Data analyses for individual years and different combinations of repeated crops are presented as Supplemental Tables S1–S11.

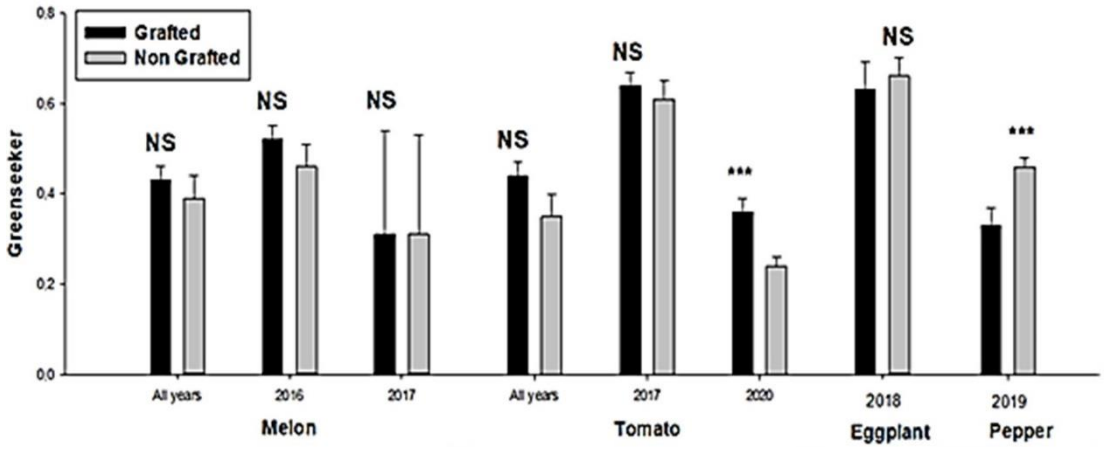
Grafted
Non Grafted
Greenseeker
0.0
0.2
0.4
0.6
0.8
NS
NS
NS
NS
NS
NS
***
***
All years
2016
2017
All years
2017
2020
2018
2019
Melon
Tomato
Eggplant
Pepper

(a)

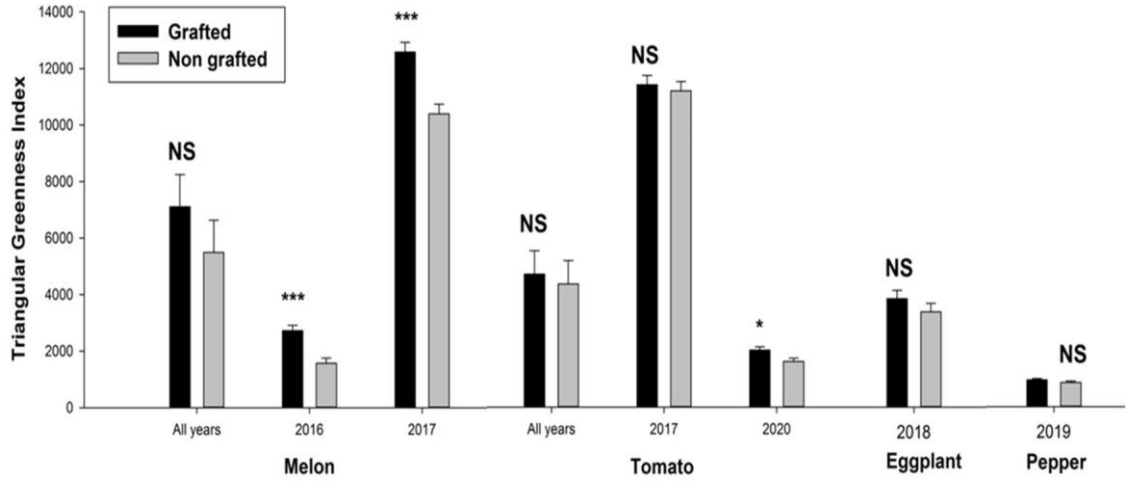
Grafted
Non grafted
Triangular Greenness Index
0
2000
4000
6000
8000
10000
12000
14000
NS
***
***
NS
NS
*
NS
NS
All years
2016
2017
All years
2017
2020
2018
2019
Melon
Tomato
Eggplant
Pepper

(b)

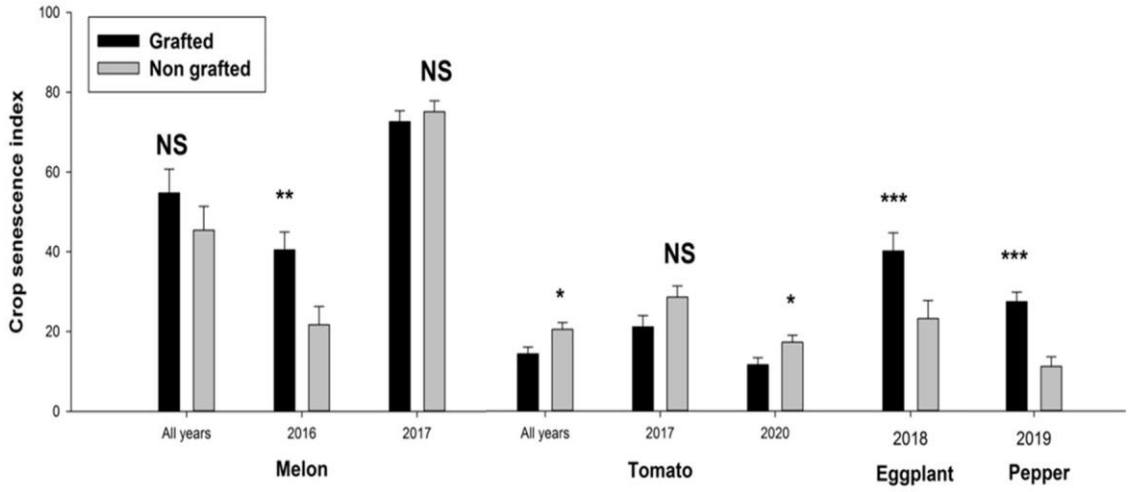
Grafted
Non grafted
Crop senescence index
0
20
40
60
80
100
NS
**
NS
*
NS
*
***
***
All years
2016
2017
All years
2017
2020
2018
2019
Melon
Tomato
Eggplant
Pepper

(c)

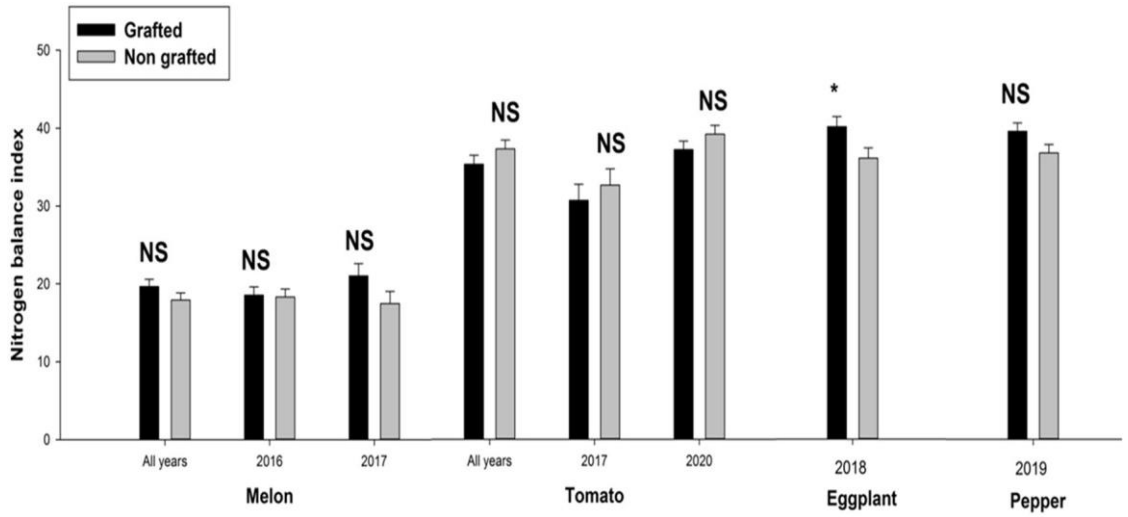

(d)

Figure 3. Cont.

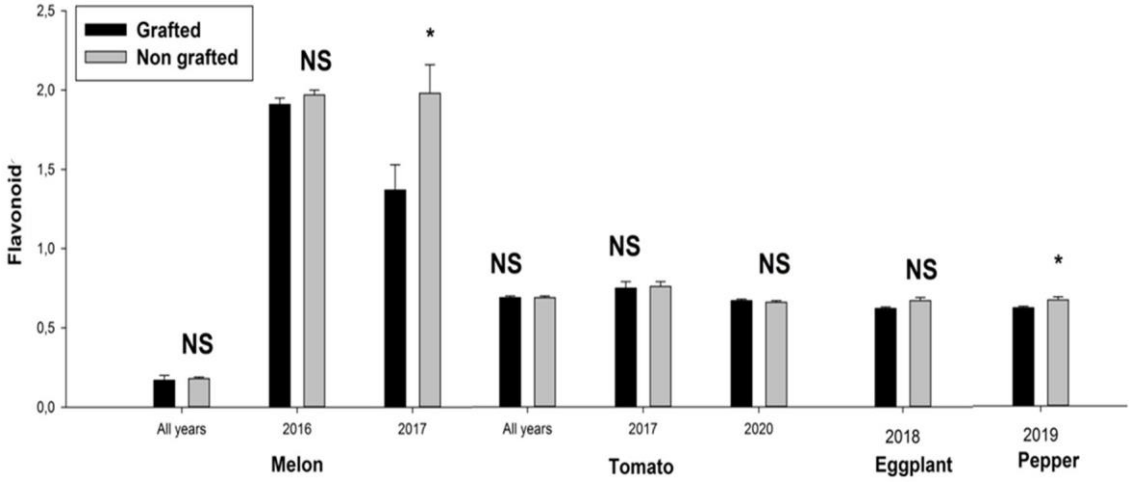

(e)

Figure 3. Variation of (a) Greenseeker (NDVI), (b) RGB-based Triangular Greenness Index (TGI), (c) RGB-based Crop Senescence Index (CSI), (d) Nitrogen Balance Index (NBI), and (e) Flavonoid (Flav) values between two treatments (grafted, non-grafted) for four crops (melon, tomato, eggplant, pepper) during five years of experience (2016–2020). For melon, we present both the combined and separate analyses for 2016 and 2017. Concerning the tomato crop combined years and 2017 and 2020 are shown. The eggplant crop was studied for just one year (2018) as well as pepper (2019). NS: non-significant ($p>0.05$), *: weakly significant ($p<0.05$), **: significant ($p<0.01$), ***: highly significant ($p<0.001$).

Figure 3a shows the variation of values for the NDVI, an indicator about the general vigor and biomass of each plant. We note that for melon and eggplant no significant differences were observed between grafted and non-grafted plants. In contrast, for tomato and melon during 2020, we observed significant differences for NDVI. Where, the grafted tomato exceeds the non-grafted. However, the opposite is seen for pepper of 2019, where the NDVI values were significantly higher for non-grafted plants.

Figure 3b informs on the variation the RGB image based TGI values as an indicator of the photosynthetically active chlorophyll content of the crop. Significant differences between the two treatments were recorded in melon and tomato, where the grafted treatment was favored. According to previous results presented in Table 4 and Figure 3, we understand that some pigments such as Flav, NBI and other parameters like CSI were the most efficient indicators for plant reaction to *Meloidogyne* root-knot nematode attacks. TGI, NBI and NDVI were higher in grafted plants, as indicators of crop vigor. In contrast, Flav and CSI recorded higher values in the non-grafted plants, as an indication of the level of stress. In contrast to the treatments (grafted, non-grafted), crop comparisons were not considered, as each species had physiological and biological characteristics that would greatly affect the measurement, especially the canopy proximal remote sensing approaches that are impacted by canopy features, like the RGB indexes TGI and CSI and also the NDVI.

Figure 3c gives a general idea about the variation of the RGB-based CSI. This index is an indicator of senescence level in the plant, which can be accelerated by many factors and may also be impacted by the view of the RGB cameras. The existence of differences in CSI can be observed between the two treatments in the different crops, but this difference was altogether absent in 2017. The most highly significant differences in CSI were detected for eggplant and pepper, where the value of grafted plant exceeded that of non-grafted plants, although, for combined years and in 2020 in tomato crop, the opposite was recorded. The attack of nematode can accelerate the senescence of plant, but other factors can also affect this index like the measurement stage, picture angles, and climatic conditions.

Figure 3d illustrates the variation of NBI values from the Dualex leaf level sensor. From this figure, we observe only one significant difference, that grafted exceeded non-grafted eggplant values. The level of nitrogen balance in the plant may provide information about rate of nitrogen absorption by the plant, thus indirectly providing information about the crop root health and assimilation capacity.

Figure 3e indicates the difference between the treatments in Flav level as measured using

the Force-A Dualex leaf sensor. In pepper, we found that non-grafted plant Flav values exceeded that of grafted plants and the same for melon in 2017. Flav is one of the most important indicators of stress state of plants, with Flav production increased with increasing stress.

3.2. Crop Yield

As we see from Table 5, there is a significant difference between grafted and non-grafted plants. It is seen that grafted plants consistently produced more than non-grafted plants with exception of the tomato 2020 rotation, where the susceptible tomato cultivar yielded more than the resistant one due to different performance of the cultivars used that year.

Table 5. Variation of crop yield between grafted and non-grafted plants for the different species cultivated during the different years, *: ANOVA test significance $p \leq 0.05$.

		Crop Yield (kg/plant)	
Year	Crop	Grafted	Non-grafted
2016	Melon	0.8 ± 0.2	0.1 ± 0.1 *
2017	Melon	3.1 ± 0.3	0.3 ± 0.1 *
	Tomato	2.9 ± 0.2	2.0 ± 0.2 *
2018	Eggplant	4.0 ± 0.4	1.9 ± 0.2 *
2019	Pepper	0.4 ± 0.002	0.2 ± 0.05
2020	Tomato	Resistant cv. Caramba	Susceptible cv. Durinta
		1.6 ± 0.01	2.2 ± 0.2 *

4. Discussion

Grafting onto resistant-tolerant rootstocks is a promising non-chemical technique to suppress RKN populations and to reduce yield losses of the most susceptible cucurbit crops. Similar results as those presented here in this study have been previously discussed by several authors, which have touched on the topic in relation to similar species and the impact of nematodes on crop health. Plant resistance has been noted as an effective and profitable control method to reduce the RKN reproduction rate and equilibrium density [4,32]. The grafting technique was demonstrated to enable an increase in uptake of water and nutrients, resulting from the larger root systems and increased disease tolerance [33].

The different parameters extracted from RGB images like GA, TGI, and CSI and other direct sensor measurements such as the NDVI can provide a means to evaluate overall plant health and growth and, inversely, delayed onset of crop senescence [21,24,34]. These techniques are non-destructive tools that rapidly provide highly relevant information on plant physiological state and effectively quantify how grafted plants benefit in multiple ways from the resistant rootstocks and show fewer symptoms related to nutrition or water stress as a sign of an overall improvement in root system function, as reflected in both vegetative vigor and total yields at the end of life crop cycle [35,36].

Nutrition is essential for plant growth and production. Crop root capacity for uptake of nitrogen and other essential macronutrients that support the production of chlorophyll and other vital processes of plant is essential. The highest values of NBI from the Dualex sensor was consistently recorded in grafted plants when compared over multiple years. NBI is an indicator of the balance of leaf N with other essential macro-nutrients, and thus its ability to positively contribute to plant processes, specifically photosynthesis. Greater NBI thus supported estimations of improved yield when compared over multiple years and crop types, contrary to the analysis made by Silva-Sanchez and others [28] on just one year of the same data, where their results supported the use of whole canopy measurements over leaf sensor measurements such as the Dualex NBI. Thus, another indicator of plant state nutrition, TGI from RGB images, serves as an indicator of leaf chlorophyll content [23]. The highest value of this indicator was observed in grafted plants, indicating that an increased photosynthetic capacity is supported by grafting, and these plants were protected from different stressors that reduce chlorophyll content-improvements in plant nutrition related to healthy roots absorption function [37].

Likewise, leaf senescence, considered as the last stage in leaf development, can serve as an indicator for the acceleration of plant biological life cycle processes. Longer crop cycles often result in a longer reproductive phase and increased yields [38]. Highly regulated changes at the molecular, cellular, biochemical, and physiological levels can cause leaves to senesce, all of which can be advanced by biotic or abiotic factors like pathogen attack (here considering nematodes). The highest values of CSI were observed in the non-grafted tomato crop as a result of increased *Meloidogyne* impacts due to its susceptibility; crop stress due to the RKN accelerated the process of senescence and subsequently shortened the life cycle of the plants, which usually results in a reduction in the crop production and quality [4,39–41].

Another unique parameter derived by the Dualex leaf sensor is flavanoid concentration. Flavanoid biosynthesis pathways in the plant can be induced by a broad pathogenesis

response through jasmonic acid, salicylic acid, ethylene, auxin, and ROS cross-talks, likely triggered when the PPNs cause mechanical damage and wounding during feeding and penetration [42]. The higher concentration of Flav recorded in non-grafted plants is related stress signaling and indicative of a reduction in vital processes; the consequences of which may be reduced by grafting because it may limit the RKNs infection.

The stable isotopes of C and N and the percentage of carbon and nitrogen by biomass are general indicators for plant water conditions and nutrient status. Firstly, stable carbon ($^{13}C/^{12}C$) isotope ratios directly indicate the water state of plant that for ($^{13}C/^{12}C$) less negative values indicate a poorer hydric state for the plant, while the stable nitrogen isotope ratios ($\delta^{15}N$) are more indicative of nutrient status and specific nutrient uptake. Although, the concentration of C and N in plant leaf indicate directly plant nutrition. The best ratio of ($^{13}C/^{12}C$) and ($\delta^{15}N$) recorded in grafted plant means that this plant benefited from a good water state. Therefore, a good functioning of root. In addition, the same conclusion is founded for C and N concentration in this plant show the good absorption of nutrient by the root [43].

Grafting is also an effective tool for controlling other soil borne pathogens such as bacterial wilt (caused by *Ralstonia solanacearum*) and fusarium wilt (caused by *Fusarium oxysporum* fs. lycopersici) [44]. However, resistance to RKN has been found in wild Cucumis spp., including accessions of *C. africanus, C. anguria, C. ficifolius, C. metuliferus, C. myriocarpus,C. postulatus, C. subsericeus* [45]. One method to solve the problem of nematode infections in melon is to graft susceptible scions onto nematode resistant rootstocks [41,46–48]. Another consequence for grafting was that a higher fruit yield was obtained when plants of melon were grafted onto different Cucurbita rootstocks [30]. This may have resulted from different factors such as an increase in uptake of water and nutrients, resulting from the larger root systems and increased diseases tolerance. Other previous studies [48,49] show that the grafting of melon (*Cucumis melo*), and watermelon (*Citrullus lanatus*) has been reported to increase crop vigor and yield of melon and may be useful for low-input sustainable horticulture.

Furthermore, yield data, pooled by crop and treatment, indicate that grafting did not affect fruit quality, but that it was decisive in minimizing crop yield losses in RKN infected soil conditions [41]. In our study, the tolerance to *Meloidogyne* for grafted plants was a crucial factor that determined the crop yield per plant, similar as previously reported by Giné et al. [40]. In relation to melon, Expósito and others [41] found that the yield of non-grafted and grafted melon onto *C. metuliferus* cultivated in non-nematode infested soil did not differ irrespective of the cropping season, however; another study led by the same

authors showed that maximum yield losses did differ at 98% yield losses for non-grafted compared to 38% yield losses for grafted melon. Reports on grafted melon tolerance to RKN and yield losses are scarce. Grafting onto tolerant rootstocks has been used widely to overcome the damage to different abiotic stresses, including high temperatures [50]. Consequently, screening for resistant RKN and tolerance to abiotic stress will increase the availability of scion rootstock combinations for agriculture production to overcome RKN and suboptimal growing conditions.

Concerning the tomato cultivars studied in the 2020 experiment, we have shown that resistant plants registered higher vigor (NDVI), greenness (TGI) and lower senescence (CSI) as shown in Figure 3a–c, yet yielded slightly less than the susceptible variety (Table 5). This suggests that the crop health was improved by RKN resistance and that the differences in yield were related to cultivar normal expected yields. Similarly, Giné et al. [40] showed that in normal conditions and in a soil deprived of RKNs, the susceptible cv. Durinta registered a yield (2.6±0.3 Kg m^{-2}), while the resistant Monika (2.3±0.4 Kg m^{-2}). The soil where both susceptible and resistant cultivars were planted was not sufficiently infected by RKNs to make a difference in yield though other differences were observed in crop physiological status.

5. Conclusions

According to all the results obtained over the five successive years, we note that the grafting techniques constitute a means of protection against attack by root nematodes. This is seen in most cases studied by the value of physiological parameters (NDVI, NBI, Flavonoid, CSI, and TGI) of grafted plants, which indicated better crop health compared to the non-grafted plants. These limited sensor results indicate good functioning of the plant physiological defense processes in the grafted plants inversely to that of the non-grafted, which suffered from the intensity of attacks by nematodes that overcame plant defense mechanisms. In addition, the combination of resistant rootstocks grafted to commercial crop varieties consistently improved crop yields by ensuring good resistance and adaptation to soil containing nematode pests.

This grafting technique has been previously observed to be more effective on other crops and is potentially linked to the compatibility between the rootstock, scion (cultivar) and quality of benefits obtained from the rootstock. Some of these are more efficient than others and bring more qualities to the plant, which affects the growth and the final production in addition to the resistance to RKN. Then, the grafted plants yielded more than non-grafted, improving economic benefits. Considering climate change impacts on

aboveground crop performance as well as soil characteristics, both of which may be improved by effective grafting techniques to provide resistance to RKNs and also to changing environmental conditions [51]. These additional desirable traits may be obtained through new techniques such as genetic engineering, which can provide certain characteristics of rootstocks, favoring their adaptation to global change. Despite the important role of grafting in the resistance against this plant-pathogen and the reduction of its impact on the plant growth and production, it alone remains insufficient to fight against nematodes, which necessitates an integrated control strategy combining different techniques, namely biological control by useful microorganisms and physical protection by solarization [52,53]. We also highlighted the potential of more cost-effective RGB images as a non-destructive technique that can ensure a detailed diagnosis of plant health status [7]. Proximal imaging is promising in the agricultural field, on the one hand, to save time, but in addition to directly address the needs of crops and to ensure the best possible condition for development and subsequently optimize production. The use of proximal remote sensing would require training, but not be overly costly for even smallholder farmers and potentially support the management of their farms by providing effective monitoring of biotic and abiotic factors affecting crop production.

Supplementary Materials: The following supporting information can be downloaded at: https: //www.mdpi.com/article/10.3390/agronomy12051098/s1, Table S1: Mean and standard error of two treatments (grafted, non-grafted) of three classes of parameters (leaf level pigments, canopy vigor and biomass, water stress and root health) combination of the values of the four crops (melon, tomato, eggplant, pepper) n=152 for 5 years (2016–2020); Table S2: ANOVA of melon crops of two years combined (2016, 2017) n=20+16, including value of separate years of three classes of parameters (leaf level pigments, canopy vigor and biomass, water stress and root health); Table S3: Mean and standard error of two treatments (grafted, non-grafted) of combined two years (2016, 2017) n=20+16 of melon crops grown in a greenhouse in soil infected by root knot nematode of three classes of parameters (leaf level pigments, canopy vigor and biomass, water stress and root health); Table S4: Mean and standard error of two treatments (grafted, non-grafted) of separate years (2016, 2017) n=20+16 of melon crops grown in a greenhouse in soil infected by root knot nematode of three classes of parameters (leaf level pigments, canopy vigor and biomass, water stress and root health); Table S5: ANOVA of tomato crop of two years combined (2017, 2020) n=16+20, and melon separate years of three classes of parameters (leaf level pigments, canopy vigor and biomass, water stress and root health); Table S6: Mean and standard error of two treatments (grafted, non-grafted) of separate years (2017, 2020) n=17+20 of tomato crop grown in a greenhouse in soil infected by root knot

nematode of three classes of parameters (leaf level pigments, canopy vigor and biomass, after stress and root health); Table S7: Mean and standard error of two treatments (grafted, non-grafted) of combined two years (2017 and 2020), with n=16+40 of tomato crop grown in a greenhouse in soil infected by root knot nematode of three classes of parameters (leaf level pigments, canopy vigor and biomass, water stress and root health); Table S8: ANOVA of eggplant crop of 2018 with n=20 of three classes of parameters (leaf level pigments, canopy vigor and biomass, water stress and root health); Table S9: Mean and standard error of two treatments (grafted, non-grafted) of 2018 with n=20 of eggplant crop grown in a greenhouse in soil infected by root knot nematode; Table S10: ANOVA of Pepper crop of 2019 with n=40 of three classes of parameters (leaf level pigments, canopy vigor and biomass, water stress and root health); Table S11: Mean and standard error of two treatments (grafted, non-grafted) of 2019 with n=40 of pepper crop grown in a greenhouse in soil infected by root knot nematode of three classes of parameters (leaf level pigments, canopy vigor and biomass, water stress and root health).

References

1-Koenning, S.R.; Overstreet, C.; Noling, J.W.; Donald, P.A.; Becker, J.O.; Fortnum, B.A. Survey of crop losses in response to phytoparasitic nematodes in the United States for 1994. *J. Nematol*. **1999**, *31*, 587.

2-Kashaija, I.; Kizito, F.; McIntyre, B.; Sali, H. Spatial distribution of roots, nematode populations and root necrosis in highland banana in Uganda. *Nematology*. **2004**, *6*, 7–12.

3-Djian Caporalino, C. Root knot nematodes (*Meloidogyne spp*.), a growing problem in French vegetable crops. *EPPO Bull*. **2012**, *42*,127–137.

4-Sorribas, F.J.; Ornat, C.; Verdejo-Lucas, S.; Galeano, M.; Valero, J. Effectiveness and profitability of the Mi-resistant tomatoes to control root-knot nematodes. *Eur. J. Plant Pathol*. **2005**, *111*, 29–38.

5-Blok, V.C.; Jones, J.T.; Phillips, M.S.; Trudgill, D.L. Parasitism genes and host range

disparities in biotrophic nematodes: The conundrum of polyphag versus specialisation. *Bioessays* **2008**, *30*, 249–259.

6-Davila, M.; Dickson, D.W. Base temperature and heat unit requirements for development of *Meloidogyne arenaria* and *Meloidogyne javanica*. *J. Nematol*, **2004**, *36*, 314.

7-Araus, J.L.; Kefauver, S.C. Breeding to adapt agriculture to climate change: Affordable phenotyping solutions. *Curr. Opin. PlantBiol*. **2018**, *45*, 237–247.

8-Araus, J.L.; Cairns, J.E. Field high-throughput phenotyping: The new crop breeding frontier. *Trends Plant Sci*. **2014**, *19*, 52–61.

9-Condon, A.G.; Richards, R.A.; Rebetzke, G.J.; Farquhar, G.D. Breeding for high water use efficiency. *J. Exp. Bot*. **2004**, *55*,2447–2460.

10-Evans, R.D. Physiological mechanisms influencing plant nitrogen isotope composition. *Trends Plant Sci*. **2001**, *6*, 121–126.

11-Rossato, L. Nitrogen storage and remobilization in *Brassicanapus L*. during the growth cycle: Effects of methyl jasmonate on nitrate uptake, senescence, growth, and VSP accumulation. *J. Exp. Bot*. **2002**, *53*, 1131–1141.

12-Malagoli, P.; Laine, P.; Rossato, L.; Ourry, A. Dynamics of nitrogen uptake and mobilization in field-grown winter oil seed rape (*Brassicanapus*) from stem extension to harvest: I. Global N flows between vegetative and reproductive tissues in relation to leaf fall and their residual N. *Ann. Bot*. **2005**, *95*, 853–861.

13-Peterson, B.J.; Fry, B. Stable isotopes in ecosystem studies. *Annu. Rev. Ecol. Syst*. **1987**, *18*, 293–320.

14-United Nations Economic Commission for Europe (UNECE) Fresh Fruit and Vegetables-Standards. Available online: https://unece.org/trade/wp7/FFV-Standards (accessed on 20 April 2022).

15-Konica, M.O. Chlorophyll Meter SPAD-502 Plus-A Lightweight Handheld Meter for Measuring the Chlorophyll Content of Leaves without Causing Damage to Plants. **2012**. Availableonline:http://www.konikcaminolta.com/instrments/download/catalog/color/pdf/spad502plus_e1.pdf (accessed on 12 March 2019).

16-Kaufmann, H.; Segl, K.; Itzerott, S.; Bach, H.; Wagner, A.; Hill, J.; Müller, A. *Hyperspectral Algorithms: Report in the Frame of EnMAP Preparation Activities*; Potsdam: Darst, Germany, **2010**.

17-Cerovic, Z.G.; Masdoumier, G.; Ghozlen, N.B.; Latouche, G. A new optical leaf-clip meter for simultaneous non-destructive assessment of leaf chlorophyll and epidermal flavonoids. *Physiol. Plant*. **2012**, *146*, 251–260.

18-Cerovic, Z.G.; Ghozlen, N.B.; Milhade, C.; Obert, M.; Debuisson, S.; Le Moigne, M. Nondestructive Diagnostic Test for Nitrogen Nutrition of Grapevine (*Vitis vinifera L.*) Based on Dualex Leaf-Clip Measurements in the Field. *J. Agric. Food Chem*. **2015**, *3*, 3669–3680.

19-Gracia-Romero, A.; Kefauver, S.C.; Fernandez-Gallego, J.A.; Vergara-Díaz, O.; Nieto-Taladriz, M.T.; Araus, J.L. UAV and ground image-based phenotyping: A proof of concept with Durum wheat. *Remote Sens*. **2019**, *11*, 1244.

20-Kefauver, S.; Kerfal, S.; Fernandez Gallego, J.A.; El-Haddad, G. CerealScanner

Gitlab. Available online: https://gitlab.com/ sckefauver/cerealscanner (accessed on 14 March 2019).

21-Zaman-Allah, M.; Vergara, O.; Araus, J.L.; Tarekegne, A.; Magorokosho, C.; Zarco-Tejada, P.J.; Hornero, A.; Albà, A.H.; Das, B.; Craufurd, P.; et al. Unmanned aerial platform-based multi-spectral imaging for field phenotyping of maize. *Plant Methods.* **2015**,*11*, 35.

22-Hunt, E.R.; Cavigelli, M.; Daughtry, C.S.; Mcmurtrey, J.E.; Walthall, C.L. Evaluation of digital photography from model aircraft for remote sensing of crop biomass and nitrogen status. *Precis. Agric.* **2005**, *6*, 359–378.

23-Hunt, E.R.; Doraiswamy, P.C.; Mcmurtrey, J.E.; Daughtry, C.S.T.; Perry, E.M.; Akhmedov, B. A visible band index for remote sensing leaf chlorophyll content at the canopy scale. *Int. J. Appl. Earth Obser. Geoinf.* **2013**, *21*, 103–112.

24-Vergara-Díaz, O.; Zaman-Allah, M.A.; Masuka, B.; Hornero, A.; Zarco-Tejada, P.; Prasanna, B.M.; Araus, J.L. A novel remote sensing approach for prediction of maize yield under different conditions of nitrogen fertilization. *Front. Plant Sci*. **2016**, 7, 666.

25-Stern, A.; Doraiswamy, P.C.; Hunt Jr, E.R. Changes of crop rotation in Iowa determined from the United States Department of Agriculture, National Agricultural Statistics Service cropland data layer product. *J. Appl. Remote Sens.* **2012**, *6*, 063590.

26-Hunt, E.R.; Daughtry, C.S.T.; Eitel, J.U.; Long, D.S. Remote sensing leaf chlorophyll content using a visible band index. *Agron. J.* **2011**, *103*, 1090–1099.

27-Montague, T.; Hellman, E.; Krawitzky, M. Comparison of greenhouse grown,

containerized grapevine stomatal conductance measurements using two differing porometers. In Proceedings of the 2nd Annual National Viticulture Research Conference, Davis, CA, USA, 9–11 July **2008**; 58–61.

28-Silva-Sánchez, A.; Buil-Salafranca, J.; Cabral, A.C.; Uriz-Ezcaray, N.; García-Mendívil, H.A.; Sorribas, F.J.; Gracia-Romero, A. Comparison of proximal remote sensing devices for estimating physiological responses of eggplants to root-knot nematodes. *Proceedings*. **2019**, *18*, 9.

29-Duncan, G.A.; Gates, R.; Montross, M.D. Measuring Relative Humidity in Agricultural Environments; Agricultural Engineering Extension Publications-Uknowledge: Lexington, KY, USA, **2005**.

30-Cabrera-Bosquet, L.; Albrizio, R.; Nogues, S.; Araus, J.L. Dual Delta ^{13}C/delta ^{18}O response to water and nitrogen availability and its relationship with yield in field-grown durum wheat. *Plant Cell Environ*. **2011**, *34*, 418–433.

31-Yousfi, S.; Serret, M.D.; Araus, J.L. Comparative response of d^{13}C, d^{18}O and d^{15}N in durum wheat exposed to salinity at the vegetative and reproductive stages. *Plant Cell Environ*. **2013**, *36*, 1214–1227.

32-Fernandez-Gallego, J.A.; Kefauver, S.C.; Gutiérrez, N.A.; Nieto-Taladriz, M.T.; Araus, J.L. Wheat ear counting in-field conditions: High throughput and low-cost approach using RGB images. *Plant Methods*. **2018**, *14*, 1–12.

33-Miguel, A.; Maroto, J.V.; San Bautista, A.; Baixauli, C.; Cebolla, V.; Pascual, B.; Guardiola, J.L. The grafting of triploid watermelon is an advantageous alternative to soil fumigation by methyl bromide for control of *Fusarium wilt*. *Sci. Hortic*. **2004**, *103*, 9–17.

34-Casadesus, J.; Kaya, Y.; Bort, J.; Nachit, M.M.; Araus, J.L.; Amor, S.; Ferrazzano, G.; Maalouf, F. Using vegetation indices derived from conventional digital cameras as selection criteria for wheat breeding in water-limited environments. *Ann. Appl. Biol*. **2007**, *150*, 227–236.

35-De Guiran, G. Protection des Cultures Maraîchères et Fruitières Face Aux Capacités D'adaptation des Nématodes Meloidogyne; Comptes Rendus de l'Académie d'agriculture: Paris, France, **1983**.

36-Feng, X.; Zhan, Y.; Wang, Q.; Yang, X.; Yu, C.; Wang, H.; He, Y. Hyperspectral imaging combined with machine learning as a tool to obtain high-throughput plant salt-stress phenotyping. *Plant J*. **2020**, *101*, 1448–1461.

37-Yang, M.D.; Tseng, H.H.; Hsu, Y.C.; Tsai, H.P. Semantic segmentation using deep learning with vegetation indices for rice lodging identification in multi-date UAV visible images. *Remote Sens*. **2020**, *12*, 633.

38-Sinclair, T.R.; Rufty, T.W. Nitrogen and water resources commonly limit crop yield increases, not necessarily plant genetics. *Glob.Food Secur*. **2012**, *1*, 94–98.

39-Munné-Bosch, S.; Queval, G.; Foyer, C.H. The impact of global change factors on redox signaling underpinning stress tolerance. *Plant Physiol*. **2013**, *161*, 5–19.

40-Giné, A.; González, C.; Serrano, L.; Sorribas, F.J. Population dynamics of Meloidogyne incognita on cucumber grafted onto the Cucurbita hybrid RS841 or non-grafted and yield losses under protected cultivation. Eur. J. *Plant Pathol*. **2017**, *148*, 795–805.

41-Expósito, A.; Pujolà, M.; Achaerandio, I.; Giné, A.; Escudero, N.; Fullana, A.M.; Cunquero, M.; Loza-Alvarez, P.; Sorribas, F.J. Tomato and melon Meloidogyne resistant rootstocks improve crop yield but melon fruit quality is influenced by the cropping season. *Front. Plant Sci*. **2020**, 1742.

42-Goverse, A.; Smant, G. The activation and suppression of plant innate immunity by parasitic nematodes. *Ann Rev Phytopath*. **2014**, *52*, 243–265.

43-Haverkort, A.J.; Valkenburg, G.W. The influence of cyst nematodes and drought on potato growth. 3. Effects on carbon isotope fractionation. *Neth.* J. *Plant Pathol*. **1992**, *98*, 12–20.

44-Rivard, C.L.; Louws, F.J. Grafting to manage soilborne diseases in heirloom tomato production. *Hort Sci*. **2008**, *43*, 2104–2111.

45-Guan, W.; Zhao, X.; Dickson, D.W.; Mendes, M.L.; Thies, J. Root-knot nematode resistance, yield, and fruit quality of specialty melons grafted onto *Cucumis metulifer. Hort Sci*. **2014**, *49*, 1046–1051.

46-Sigüenza, C.; Schochow, M.; Turini, T.; Ploeg, A. Use of *Cucumis metuliferus* as a rootstock for melon to manage *Meloidogyne incognita*. *J. Nematol.* **2005**, *37*, 276.

47-Expósito, A.; Munera, M.; Giné, A.; López-Gómez, M.; Cáceres, A.; Picó, B.; Gisbert, C.; Medina, V.; Sorribas, F.J. *Cucumis metuliferus* is resistant to root-knot nematode Mi1.2 gene (a)virulent isolates and a promising melon rootstock. *Plant Pathol*. **2018**,*67*, 1161–1167.

48-Expósito, A.; García, S.; Giné, A.; Escudero, N.; Sorribas, F.J. Cucumis metuliferus reduces Meloidogyne incognita virulence against the Mi1.2 resistance gene in a tomato–melon rotation sequence. *Pest Manag. Sci*. **2019**, *75*, 1902–1910.

49-Bletsos, F.A. Use of grafting and calcium cyanamide as alternatives to methyl bromide soil fumigation and their effects on growth, yield, quality, and fusarium wilt control in melon. *J. Phytopathol*. **2005**, *153*, 155–161.

50-Tao, M.Q.; Jahan, M.S.; Hou, K.; Shu, S.; Wang, Y.; Sun, J.; Guo, S.-R. Bitter Melon (*Momordica charantia L.*) Rootstock Improves the Heat Tolerance of Cucumber by Regulating Photosynthetic and Antioxidant Defense Pathways. *Plants*. **2020**, *9*, 692.

51-Abd-Elgawad, M.M. Biological control agents in the integrated nematode management of potato in Egypt. Egypt. *J. Biol. Pest Control*. **2020**, *30*, 1–13.

52-Gassmann, A.J.; Stock, S.P.; Sisterson, M.S.; Carrière, Y.; Tabashnik, B.E. Synergism between entomopathogenic nematodes and *Bacillus thuringiensis* crops: Integrating biological control and resistance management. *J. Appl. Ecol*. **2008**, *45*, 957–966.

53-Nisha, M.S.; Sheela, M.S. Bio-Management of Meloidogyne incognita on Coleus, Solenostemon rotundifolius by Integrating Solarization, *Paecilomyces lilacinus*, *Bacillus macerans* and Neemcake. *Indian J. Nematol*. **2006**, *36*, 136–138.

Chapter 2

Using ground and UAV vegetation indexes for the assessment of fungal resistant bread wheat varieties

Abstract:

The productivity of wheat in the Mediterranean region is under threat due to climate change-related environmental factors, including fungal diseases that can negatively impact wheat yield and quality. Wheat phenotyping tools utilizing affordable high throughput plant phenotyping (HTPP) techniques, such as aerial and ground RGB images and quick canopy and leaf sensors, can aid in assessing crop status and selecting tolerant wheat varieties. This study focused on the impact of fungal diseases on wheat productivity in the Mediterranean region, considering the need for a precise selection of tolerant wheat varieties. The research examined the use of affordable HTPP methods, including imaging and active multispectral sensors, to aid in crop management for improved wheat health and to support commercial field phenotyping programs. The study evaluated 40 advanced lines of bread wheat (*Triticum aestivum L.)* at five locations across northern Spain, comparing fungicide treated and untreated blocks under fungal disease pressure (Septoria, brown rust and stripe rust observed). Measurements of leaf level pigments and canopy vegetation indexes were taken using portable sensors, field cameras, and imaging sensors mounted on unmanned aerial vehicles (UAVs). Significant differences were observed in Dualex flavonoids and nitrogen balance index (NBI) between treated and untreated treatments in some locations ($p<0.001$ between Elorz and Ejea). Measurements of canopy vigor and color at the plot level showed significant differences between treatments at all sites, highlighting indexes like the Green Area (GA), Crop Senescence Index (CSI), and Triangular Greenness Index (TGI) in assessing the effects of fungicide treatments on different wheat cultivars. RGB vegetation indexes from the ground and UAV were highly correlated ($r=0.817$ and $r=0.810$ for TGI and NGRDI). However, the Greenseeker NDVI sensor was found to be more effective in estimating grain yield and protein content ($R^2=0.61$-0.7 and $R^2=0.45$-0.55, respectively) compared to the aerial AgroCam GEO NDVI ($R^2=0.25$-0.35 and $R^2=0.12$-0.21, respectively). We suggest as a practical consideration the use of the GreenSeeker NDVI as more user friendly and less affected by external environmental factors. The study emphasized the throughput benefits of RGB UAV HTPPs with the high similarity between ground and aerial result and highlighted the potential for HTPPs in supporting the selection of fungal disease resistant bread wheat varieties.

Keywords: Generation F8; bread wheat; fungicide; treated; untreated; cereal crop; breeding; phenotyping; UAV; NDVI; RGB; stable isotope composition.

Introduction

Crop productivity can be significantly impacted by climate change, reducing food production in many parts of the world. Climate change impacts are not limited to the effect of abiotic stresses but also the outbreaks of biotic stresses. The projected rapid pace of climatic change without mitigation will have increasingly serious implications for the world economy and food security [1]. Crop scientists are faced with the dual challenge of increasing production while also maintaining long-term sustainability and food security by reducing the negative impacts of biotic and abiotic stressors, among others. As in many other Mediterranean countries, wheat is mostly grown under rainfed conditions in Spain. This is especially true in the north of Spain, where yields can be unpredictable due to erratic rainfall patterns, characterized by cold winters and moderate precipitation throughout the year [2-4]. The main abiotic variables limiting bread wheat (*Triticum aestivum L.*) productivity in this region are thus drought and heat stress; however, fungal outbreaks (stem rust, Fusarium head blight, powdery mildew, etc.) are frequent, predicted to accompany climate change and can have a significant effect on grain productivity and quality [5-7]. Fungal pathogens can spread quickly when temperature and humidity are favorable for disease development. In fact, temperature and relative humidity control the most crucial stages of the pathogen life cycle, including spore germination, infection, latent period, sporulation, spore survival, and host resistance, all of which influence epidemic onset [8]. Fungal pathogens reduce grain yield and quality by different mechanisms, including limiting root growth, reducing water and nutrient uptake, and inducing chlorosis and necrosis of photosynthetic tissues, which affects photosynthesis, and causes widespread foliar senescence and poor grain filling [9-11].

The most economical and environmentally beneficial technique of disease management is the development of resistant cultivars. However, the creation of new cultivars that are more productive and offer greater yield stability across a range of environmental situations and disease pressures, requires tremendous effort through breeding programs and phenolic selection [12]. To that end it is necessary to explore the available genetic variability for developing modern high yielding varieties that are disease-resistant and flexible to changing environmental conditions [13]. Furthermore, it will be imperative to find cost effective and high throughput technologies in order to better support and speed up these advancements in crop breeding [14].

The use of high throughput phenotyping platforms (HTPPs), such as unmanned aerial vehicles (UAVs) equipped with high-resolution cameras, permits the rapid and non-destructive screening of crops to distinguish between abiotic and disease-related symptoms, such as vigor or crop color characteristics, at the crop canopy level [15]. In order to identify plant diseases in wheat and track their progression, a variety of imaging and spectroscopic approaches have been investigated. These techniques vary in their complexity and data requirements (e.g.; [16-18]). For instance, at an early point in the development of winter stem rust, changes in spectral reflectance using in-field spectral images between healthy and diseased wheat plants allowed for the identification of infected plants [16].

Also, vegetation indexes derived from conventional RGB (red, green, and blue) cameras have been demonstrated as robust indicators of biotic stress in wheat [19,20]. In fact, genotypic variability in the susceptibility to fungal diseases has been observed at the field level using conventional red, RGB images. Where, based on the combination of RGB spectral bands, wheat affected by leaf rust and stripe rust were identified [15]. The findings of Heidarian and colleagues [15] further mentioned that two foliar fungal illnesses (stem rust, Fusarium head blight) altered the reflectance of wheat leaves between the green and red spectral channels. Other researchers have focused on the extraction of color parameters and the use of alternative color spaces for quantifying fungal infections [20]. An additional advantage of RGB indexes is their affordability and quality color calibration [19].

Among multispectral indexes, the normalized difference vegetation index (NDVI) has been to date one of the most commonly used multispectral near infrared indexes when phenotyping resistance to fungal diseases [21-23], though other indexes have been found to have similar performance. Still, RGB sensors offer increased image resolution compared to other spectral sensors, which may be important to detect early symptoms of fungal stress [18,20,24], and often equal or surpass the capacity of NDVI for assessing fungal infection and estimating grain yield losses [20]. Besides the spectral nature of the sensors (RGB cameras versus multispectral field sensors and imagers), spatial resolution and the distance between camera and subject are relevant issues. This means that ground-based cameras and sensors placed, on a UAV, are both approaches amenable to high throughput wheat phenotyping in multi-environment setups where several trials differing in growing conditions are assessed, through each may offer some advantages over the other [25].

Our study enters this context by comparing the effectiveness of RGB indexes acquired at both the ground level and from a UAV aerial platform. We compared their relative performance

against a baseline consisting in measurements using an active NDVI canopy sensor at the ground level and final yield and protein content. We compared a large set of advanced (F8) lines of bread wheat growing in five different locations varying in water availability and temperature, which may strongly affect the impact yield and fungal disease pressure. Moreover, we also compared the value of assessing photosynthetic and protective pigments at the leaf level using an advanced portable leaf clip sensor. For each location we compared the same set of genotypes in trials untreated and treated with fungicide. Further, the genotypic differences in grain yield and susceptibly to fungal attacks were assessed by comparing relative differences between treated and untreated plots to vegetation indexes and yield and protein content at harvest.

2. Materials and Methods

2.1. Study sites

The research was carried out, during the 2020-2021 growing season, in five experimental field trials located across Central-NE Spain that the Limagrain seed Company uses for its annual evaluation of accessions: Tordómar in the municipality of Tordómar 42º 2' 9.76" N (Burgos, Spain), Quintanilla de San Garcia in the municipality of Briviesca 42º 33' 51.39" N (Burgos, Spain), Elorz in the municipality of Noain 42º 43' 8.12" N (Navarra, Spain), Sos del Rey Católico in the municipality of Sos del Rey Católico 42º 32' 39.66" N (Zaragoza, Spain) and Ejea de los Caballeros in the same municipality at 42º 6' 53.67" N (Zaragoza, Spain). The geographic location and province of each field site are shown in Figure 1.

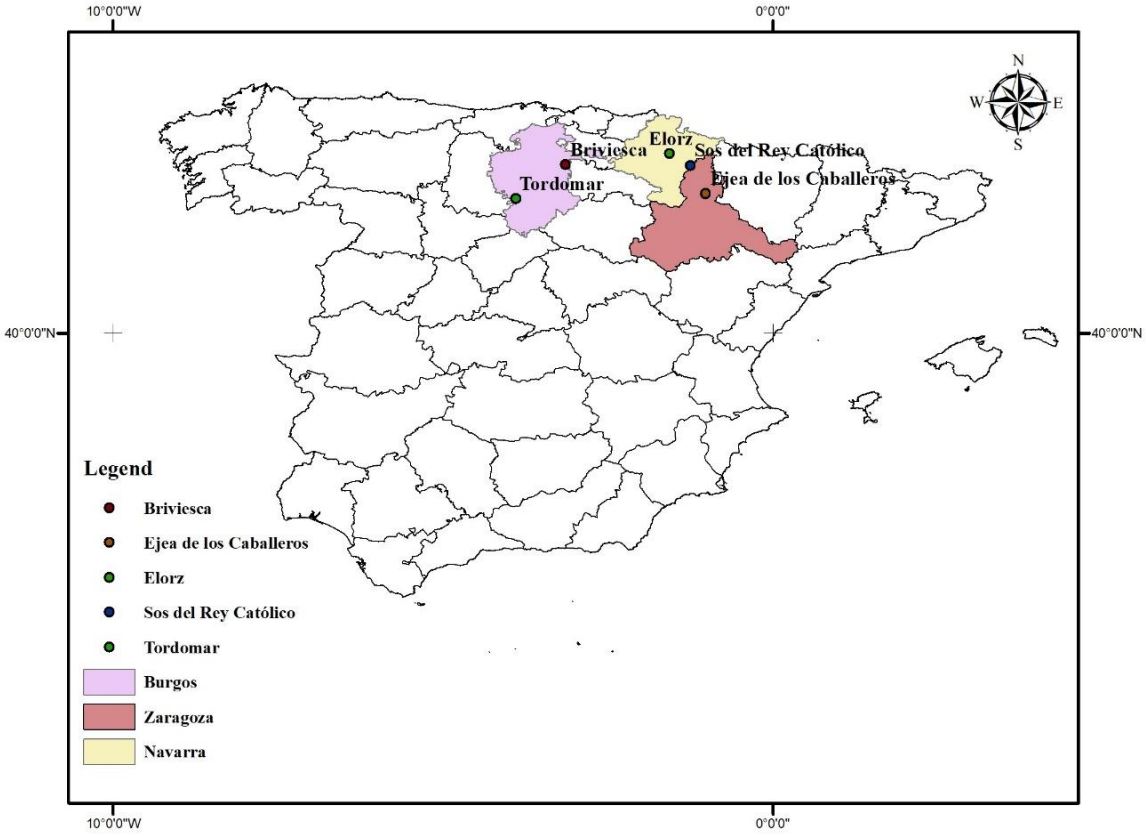

Figure 1. Map showing the locations of experimental sites across Northern Spain. The experiment was conducted in five locations located in three provinces (Zaragoza, Navarra, and Burgos).

2.2. Climate conditions of experimental sites

The five experimental sites were characterized by generally continental Mediterranean climate conditions, with large variability in ranges of temperature and precipitation. Climatic data from 2021 was recorded through the Spanish platform SIAR Servicio de Informacion Agroclimática para el Regadio, www.siar.es (accessed on 12 September 2022) from meteorological stations close to the field sites. All the five field sites exhibited a strong trend from wet, cool to dry, warmer, moving from the more Western (especially Tordómar, Briviesca and Elorz) to the Eastern (Sos del Rey Católico and Ejea de los Caballeros) study sites. The data of climate condition variation for temperature and precipitation during the field season in 2021 at the five experimental sites is presented in Figure 2 and Supplemental Table S1.

2.2.1. Tordómar

In Tordómar, the wintertime precipitation is noticeably heavier than the summertime precipitation though summer precipitation events can be frequent. Rainfall during field season 2021 was 437 mm. April was the wettest month of the year after February in 2021, while March was relatively less wet. Less than 2 mm of precipitation was recorded as the least amount in July with minimal precipitation in August as well.

2.2.2. Briviesca

The Briviesca site (near the town of Quintanilla de San Garcia) generally receives a considerable amount of rain all year long. The average rainfall during the field season is 768 mm. Even in the driest months, there can still appear a sizable amount of rainfall. Only the two driest months, July, and August, recorded less than 6 mm of precipitation each. In 2021, precipitation increased from March until June but dropped off sharply in July.

2.2.3. Elorz

It can rain heavily during most of the year in Noáin (Elorz), with 714 mm of rainfall on average each year. July and August were the driest months of the year in the field season 2021, as usual; however, March and May saw relatively low precipitation, while June experienced some heavy rains.

2.2.4. Sos del Rey Católico

The average rainfall of the field season in Sos del Rey Católico was 532 mm. The driest months are July and August, with less than 2 mm of precipitation. Rainfall in Sos del Rey Católico was moderate for March, May, and June in 2021.

2.2.5. Ejea de los Caballeros

Low rainfall is a year-round occurrence in Ejea de los Caballeros with a total of 350 mm of rainfall on average during the field season. These three months were the driest in 2021: May, June, and July. The smallest amount of precipitation, less than 1 mm, was recorded in July.

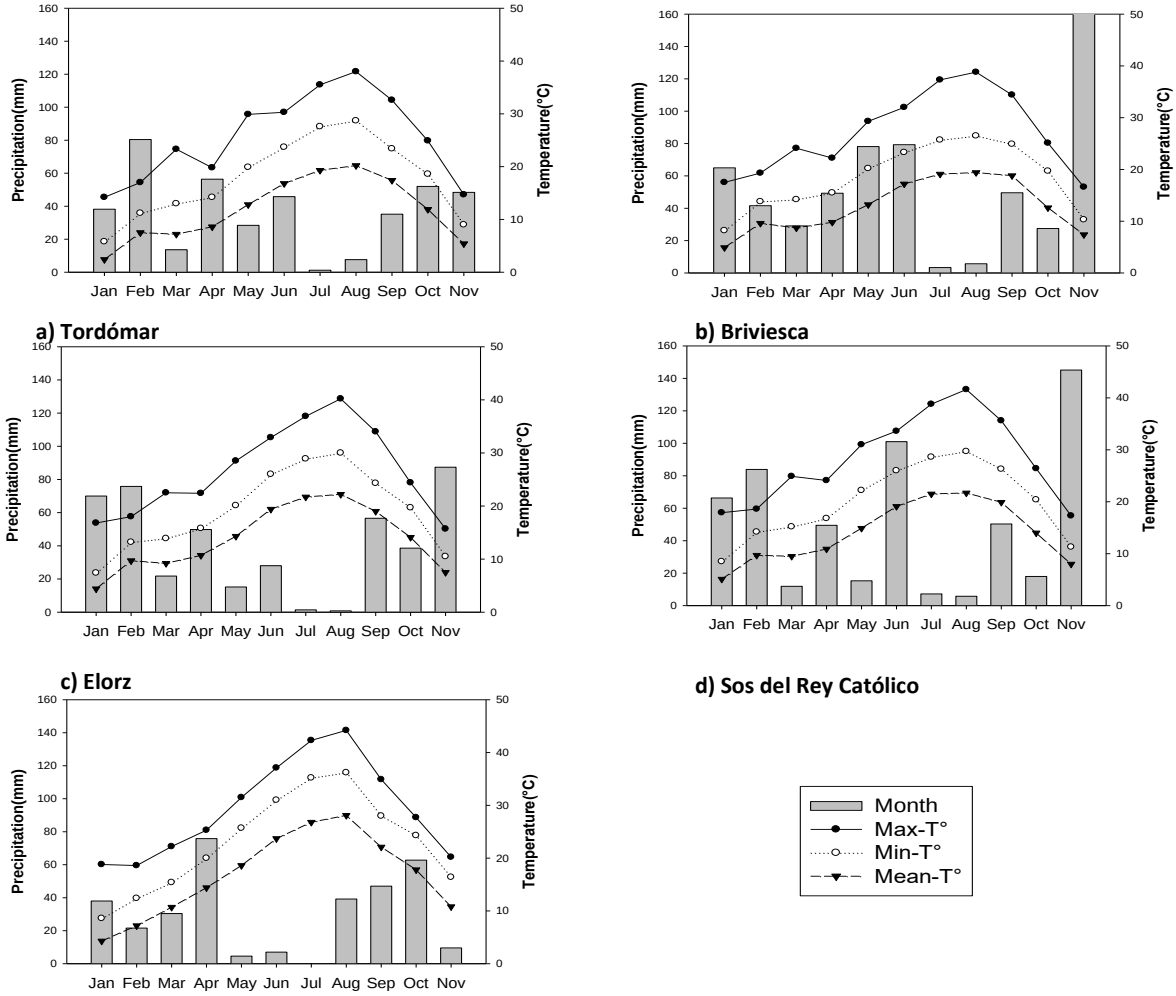

Figure 2. Variation of monthly temperature (Max, Min, Mean) defined by lines and points and precipitation defined by bars during 2021 in the five experimental sites by order of most Western (Tordómar) to Eastern (Ejea de los Caballeros), showing the Mediterranean pattern of seasonality.

2.3. Experimental trial designs

Forty (40) advanced (F8) winter wheat (*Triticum aestivum*. L.) accessions were assessed at the five experimental sites. A randomized complete block design with three untreated replicates and one treated replicate of plots made up the experimental setup for a total of 160 separate 8.5 m2 plots at each site. Due to their geographical and climatological differences, different sowing dates were followed for each site as detailed at top of Figure 3. The control trial that did not receive any anti-fungal treatments, to determine varietal susceptibility to fungal attack, and the treated trials received fungicide applications by spraying (Prosaro®, prothioconazole and tebuconazole, Bayer Crop Science, Germany) three times at tillering, flag leaf emergence, and heading/flowering. Fungal diseases identified as present at the trials during 2021 field season included Septoria (*Mycosphaerella graminicola* and *Stagonospora*

nodorum), brown rust (*Puccinia triticina*), and stripe rust (*Puccinia striiformis*). The insecticide Decis (Bayer Crop Science, Luverkusen, Germany) was applied to all trial sites and blocks at the same time as the fungicide applications. Ejea de los Caballeros additionally received 3 supplemental irrigations by inundation, each 40-50 mm, and Sos del Rey Católico received sprinkler supple-mental irrigation 5 times, each 18 mm. Meanwhile, the other three sites at Tordómar, Briviesca and Elorz were rainfed only.

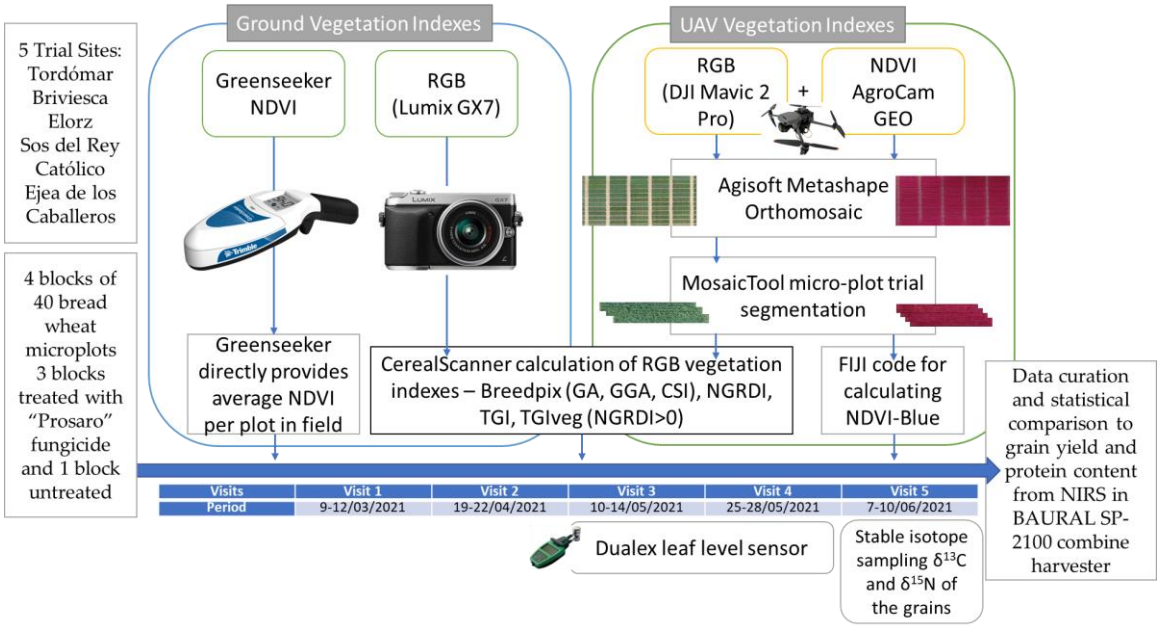

Figure 3. Flow chart describing the experimental design of the various trials from sites across Northern Spain. The experiment was conducted in five locations located in Tordómar, Briviesca, Elorz, Sos del Rey Católico and Ejea de los Caballeros. Sowing date was staggered between the sites as indicated at the top. At each location 160 plots were divided into 4 blocks with 3 treated and 1 untreated with fungicide. Ground and UAV RGB and NVDI data were captured during 5 visits to each site. Dualex was measured on visits 3 and 5 and stable isotope samples were collected of the grains during the last visit 5. Final yield and protein content were assessed in situ using a combine harvester with an integrated NIRS (near infrared spectrometer).

During the five field samplings, the following physiological stages match approximately the research visit timing: 1. March (stem elongation), 2. April (anthesis), 3. mid-May (heading), 4. late-May (grain filling), and 5. June (maturity) as detailed in Figure 3. The warmer sites, Ejea de los Caballeros, followed by Sos del Rey Católico and Elorz developed faster than Tordómar and Briviesca, due to their higher temperatures. As shown in the summary flow chart in Figure 3.; the portable NDVI Greenseeker, RGB ground camera and the UAV RGB and NDVI cameras were employed during all five visits. Dualex leaf sensor measurements

were conducted twice, during the third and fourth visits and the isotope analysis grain samples were gathered during the fifth field visit.

2.4. Imaging and sensor field measurements

2.4.1. Dualex

The Dualex is an optical portable leaf clip sensor (Force-A, Orsay, France) for deter-mining flavonoids, anthocyanins, and chlorophyll levels in leaves that was used for the additional assessment of leaf chlorophyll (Chl), epidermal flavonoids (Flav), and nitrogen balance of the study sites during the 3rd and 4th visits (Figure 3). The Dualex offers the advantages of high throughput, non-destructive and real-time measurements to be made of these relevant physiological crop components and is factory calibrated to provide leaf Chl content in µg cm^{-2} units with a linear response function and a documented error of 2.4 and 3.4% compared to chemical composition analyses and for Chl and Flav, respectively [26]. Furthermore, the Dualex determines the Nitrogen Balance Index (NBI) was determined, which is the chlorophyll/flavonoids ratio which and informs on the nitrogen and carbon allocation [27].

The Dualex manages high precision and linear response functions using a unique combination of a UV excitation beam at 357 nm, which corresponds to the maxi-mum absorption for flavonoids, as well as a green LED for anthocyanins, a red reference beam at 650 nm, which corresponds to chlorophyll absorption, and two other near-infrared reference wavelengths (710 nm and 850 nm) [28, 29]. The Dualex displayed high accuracy in Chl content assessment when specifically tested on wheat in a study that assessed fluorescence techniques for estimations of phenolic compounds positively [28]. As a field device, it adjusts the level of fluorescence caused by a reference red light to the level of fluorescence caused by UV light to quickly provide measurements from attached leaves in field conditions, is water resistant, stores data digitally, and has an integrated GPS sensor for both location and accurate time stamping. It has furthermore been used to estimate soil nitrogen wheat productivity estimations [30].

The measurements with the Dualex sensor were performed on the leaf adaxial side and repeated five times for each plot, in order to sample a representative measurement of the various pigments on both sides of the plot. In each case the last fully expanded leaf was measured.

2.4.2. Trimble GreenSeeker

The Trimble Greenseeker (Greenseeker, Trimble, Sunnyvale, CA, USA) uses an active light source to measure the Normalized Difference Vegetation Index (NDVI) at the canopy level,

which is an indicator of crop vigor, understood as a combination of photosynthetic capacity and biomass. NDVI measures the difference between near-infrared (which vegetation biomass strongly reflects) and red light to quantify vegetation (which photosynthetic vegetation absorbs). Measurements were performed with the portable crop canopy sensor measured at ground level, with the sensor placed over the middle of each wheat plot at a constant height of 0.5 m above the canopy [19]. The sensor sends out brief bursts of red and infrared light (656 nm and 774 nm, respectively) and then quantifies light is reflectance for by the plant for each wavelength. For as long as the trigger is pressed, it continues to sample the scanned area to provide the average value measured in terms of an NDVI index reading (normalized index between 0 and 1) for the whole plot.

2.4.3. RGB images and derived vegetation indices

A selection of different vegetation indexes was extracted from the RGB photos acquired during each of the visits. The ground images were taken in the middle of each plot, with the camera placed zenithally above the canopy at a height of 80 cm. The camera utilized in this operation was a Panasonic Lumix DMC GX7 with 16 MP (Panasonic, Osaka, Japan). The CerealScanner plugin (https://gitlab.com/sckefauver/cerealscanner, accessed on 25 September 2022) [31] was then used to analyze the images implementing Breedpix 2.0 (https://bio-protocol.org/e1488, accessed on 25 September 2022, IRTA, Lleida, Spain), which creates RGB vegetation indexes using RGB and alternative color space attributes, such as Hue, Saturation, and Intensity (HSI) to quantify plant properties of interest, which is included in this package. The percentage of pixels classed as green or very green were used to calculate indexes like GA (Green Area) and GGA (Greener Green Area). The percentage of pixels in photos with a Hue range of 60 to 180, including yellow to bluish green, was used to determine GA. GGA, on the other hand, has a narrower range, ranging from 80 to 180, which means it excludes yellowish-green tones. The Crop Senescence Index (CSI) was created by combining the two earlier indexes [32], which use a scaled ratio of yellow and green pixels to determine the number of senescent plants.

Other indexes with calculated with the digital values of the red, green, and blue bands obtained from the RGB images directly. Thus, the Triangular Greenness Index (TGI) is an index that estimates chlorophyll content based on the area of a triangle with three points corresponding to the red, green, and blue bands following Table 1.

The Normalized Green Red Difference Index (NGRDI) is similar to the NDVI, but instead of red and near-infrared (NIR) bands, it employs green and red [33]. Meanwhile, two vegetation

index adaptations like the NGRDIveg and the TGIveg were filtered for vegetation pixels only (the selection of vegetated pixels was NGRDI>0) to create a vegetation mask, thus removing the effects of the soil back-ground). As a result, they recorded values higher than the whole plot level calculations that included some soil background effects [34].

Table 1. Select vegetation **i**ndexes derived from the RGB cameras.

Index	**Formula**
Green Area (GA)	60<Hue<180 [35]
Greener Area (GGA)	80<Hue <180 [35]
Crop Senescence Index (CSI)	(GA−GGA) /GA [36]
Normalized Green-Red Difference Index (NGRDI)	(R550−R670) / (R550 + R670) [37]
Triangular Greenness Index (TGI)	−0.5[190(R670 – R550) −120(R670−R480) [38]

2.4.4. Aerial images

A DJI Mavic Pro 2 UAV, (DJI, Shenzhen, China) was used to capture aerial photographs. The Mavic 2 Pro UAV weighs 907 grams and, features an integrated gimbal-stabilized, Hasselblad optics, 20 MP camera with a high-quality adjustable aperture f/2.8-f/11 lens (28 mm full-frame equivalent). The UAV was programmed to take pictures every 2 from a height of 50 m for an overlap of 80% along and between flight paths guided by its internal GPS system. A separate GPS receiver was mounted on top of the UAV and connected to the AgroCam GEO NDVI (AgroCam, Debrecen, Hungary) camera mounted below the UAV. The AgroCam is a modified RGB camera with the near infrared (NIR) removed and replaced with a special “NDVI 7” filter that allows the camera to capture NIR-Red-Blue, and thus enabling it to calculate the NDVI-blue variant of NDVI ((NIR−blue)/(NIR+blue)). The AgroCam is furthermore equipped with a special signal sensor that triggers its image capture function whenever the Mavic 2 Pro camera captures an image, thus effectively providing separately georeferenced yet simultaneous image captures. Agisoft Metashape Professional software (Agisoft, St. Petersburg, Russia) was used to produce the orthomosaic images from each camera for the flights at each site for each visit (2x5x5 total flights). Then, using the MosaicTool plugin [39], regions of interest corresponding to each variety micro-plot image were segmented and exported using the image analysis platform FIJI (Fiji is Just ImageJ; http://fiji.sc/Fiji (accessed on 25 September 2021). The MosaicTool also includes integrated

processing tools for calculating the different RGB vegetation indexes in the same way as the field RGB im-ages. The AgroCam NDVI-blue was calculated using a custom code implemented in FIJI. An overview of the process is also detailed in Figure 3.

3. 5. Additional analyses

2.5.1. Determination of stable isotopes: $\delta^{13}C$ and $\delta^{15}N$ of the grains

The determination of stable isotopes was conducted to further validate whether the plants suffered from water stress over the whole of the crop season, these traits can be seen as an integral measurement of water stress. From each plot, mature grains were collected at harvest from the two sites Ejea de los Caballeros and Elorz. were dried at 60 °C for a minimum of 48 h and pulverized to a fine powder, from which 1 mg was enclosed in tin capsules, and analyzed using an elemental analyzer (Flash 1112 EA; Thermo Finnigan, Schwerte, Germany) coupled with an isotope ratio mass spectrometer (Delta C IRMS, Thermo Finnigan), operating in continuous flow mode at the Scientific and Technical facilities of the University of Barcelona. Different secondary standards were utilized. for carbon (IAEA CH7, IAEA CH6 and IAEA-600, and USGS 40) and nitrogen (IAEA-600, N1, N2, NO3, urea, and acetanilide) isotope studies. Nitrogen content in grains was expressed in percentages (%), and the corresponding isotope compositions in parts per thousand (‰), with an analytical precision (standard deviation) of 0.2‰ for $\delta^{13}C$ and 0.2‰ for $\delta^{15}N$ and following:

$$\delta^{13}C\ (‰)/\delta^{15}N\ (‰) = [(R_{sample}/R_{standard}) - 1] \times 1000, \quad (1)$$

where R standard is the molar abundance ratio of the secondary standard calibrated against the primary standard, Pee Dee Belemnite in the case of carbon ($\delta^{13}C$) and N^2 from air in the case of nitrogen ($\delta^{15}N$) [40].

2.5.2. Grain yield and Protein content (CPRO)

At maturity, each plot was mechanically harvested, and the grain yield was obtained. After that, the grain yield (GY, T ha^{-1}) was determined considering the final total surface area of each plot. Furthermore, total protein content was also determined by the Limagrain company. For experimental purposes. A NIRS (Near Infrared Spectrometer) integrated into the combine harvester (BAURAL SP-2100, Blois, France) was used for the determination of protein content in situ during harvest, which, being incorporated into the same harvesting process, and therefore provides, increased efficiency for large trials [41].

2.6. Statistical processing

To determine which indexes exhibited the best correlation and assess the best

complementarity between sensors, a comparison of aerial and ground data was conducted as part our study in addition to comparisons to yield and protein as our principal metrics of varietal performance. Statgraphics Centurion XVI (Statpoint Technologies, Warrenton (Virginia), USA) software was used to perform ANOVA analyses. For simple data analysis such as mean and correlations between different indexes, we used Stat-graphics Centurion XVI (Statpoint Technologies, Warrenton (Virginia), USA). Finally, the graphics were created by Sigmaplot (Systat Software Inc, Chicago, USA).

3. Results

3.1. Isotopic composition of sites with contrasting water condition

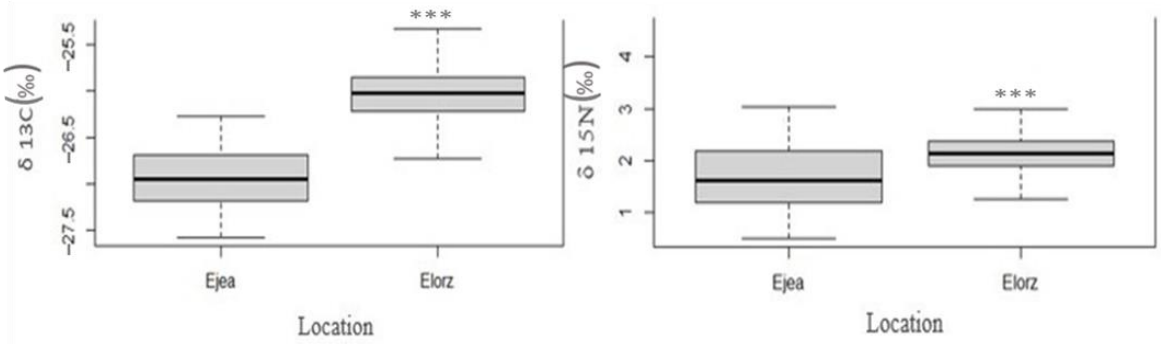

Figure 4. Comparison of $\delta^{13}C$ (left) and $\delta^{15}N$ (right) of grains collected at two locations, Ejea de los Caballeros and Elorz. Values are means and ± standard error of 35 samples are shown for each site as well as the upper and lower quartiles of the distribution. To investigate the impact of the site on the isotopic composition, an ANOVA analysis was conducted. *, $p < 0.05$, **, $p < 0.01$, ***, $p < 0.001$.

Figure 4 shows that both $\delta^{13}C$ and $\delta^{15}N$ revealed a highly significant difference between the two sites ($p<0.001$), with Elorz having nitrogen composition values compared to Ejea de los Caballeros and less negative value of carbon composition. This may be a general assessment of the difference in site condition between the two most different sites in terms of water and nutrient status.

3.2. Comparison of leaf pigments between treated and untreated plants.

Differences between treated and untreated plants were only significant for two leaf traits (Flavonoids (Flav) and the Nitrogen Balance Index, NBI, the ratio between chlorophyll (Chl) and flavonoids) at two sites (Elorz and Ejea de los Caballeros). In addition, differences in Chl content were also evidenced at Ejea (Table 4). The untreated plots reported values of Flav that were higher than the treated ones at Elorz ($\bar{x}$=1.510 Treated vs $\bar{x}$=1.592 Untreated,

p<0.01) and Ejea de los Caballeros ($\bar{x}$=1.58 Treated vs $\bar{x}$=1.62 Untreated, p<0.05), whereas for the NBI the treated wheat plots had significantly higher values than the untreated plots at both sites (p<0.01 for Elorz and p<0.001 for Ejea de los Caballeros). In the case of Ejea de los Caballeros, Chl was significantly higher in the treated than the untreated genotypes. No significant differences were found for the 4th visit later that same month. Due to differences in site location and planting times, no comparisons were made directly between sites, only between treated and untreated blocks at each site.

Table 2. ANOVA analyses comparing the effects of the two treatments (Treated, T and Untreated, U) for all sites during the 3rd visit on the 10-14 of May 2021.

	Tordómar		**Briviesca**		**Elorz**		**Sos**		**Ejea**	
	Mean	p-value	Mean	p-value	Mean	p-value	Mean	p-value	Mean	p-value
Chl	T=48.69	0.81	T=35.90	0.08	T=1.50	0.5	T=34.92	0.97	T=48.00	0.011*
	U=48.69		U=35.20		U=1.54		U=34.94		U=45.78	
Flav	T=1.54	0.83	T=1.553	0.19	T=1.510	0.002**	T=1.46	0.2	T=1.58	0.005*
	U= 1.55		U=1.552		U=1.592		U=1.44		U=1.62	
Anth	T=0.056	0.94	T=0.049	0.8	T=0.023	0.28	T=0.026	0.93	T=0.023	0.088
	U=0.054		U=0.047		U=0.021		U=0.026		U=0.021	
NBI	T=31.65	0.75	T=23.38	0.14	T=35.69	0.006**	T=24.29	0.65	T=30.4	0.000***
	U=31.85		U=22.82		U=34.56		U=24.64		U=28.08	

*, p<0.05, **, p<0.01, ***, p<0.001. Chl, chlorophyll leaf content, Flav, flavonoids leaf content, anthocyanins leaf content, NBI, Nitrogen Balance Index.

3.3. Comparison of treated and untreated trials using different RGB ground vegetation indexes for all experimental sites and visits.

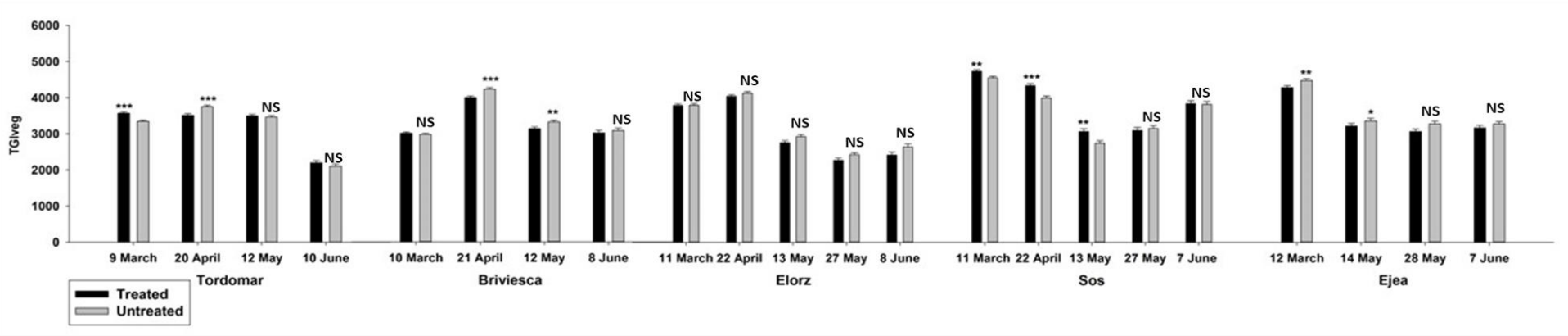

Figure 5. Variation of Triangular Greenness Index (TGIveg) measured at the ground level for the five different sites and five different dates. NS, no significant; *, p<0.05, **, p<0.01, ***, p<0.001.

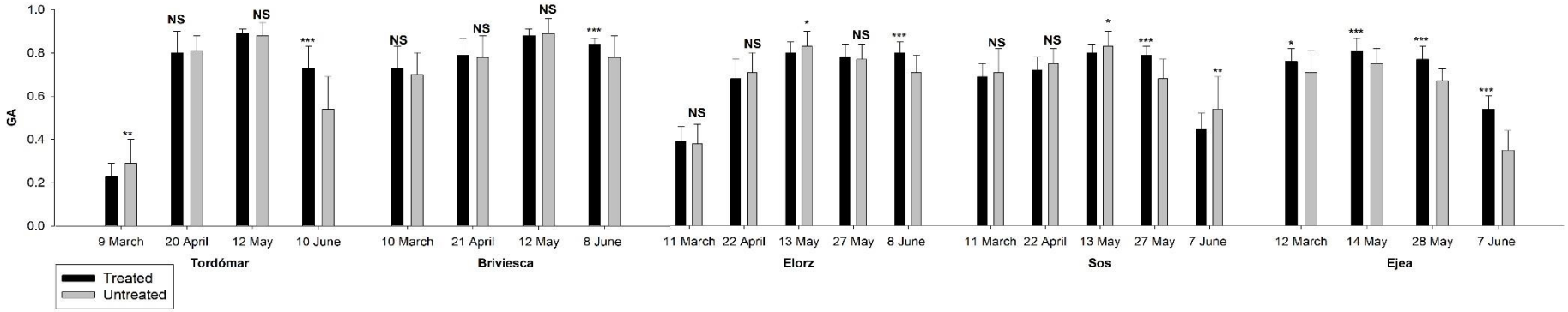

Figure 6. Variation of Green Area (GA) measured at ground level for the five different sites and five different dates. NS, no significant; *, p<0.05, **, p<0.01, ***, p<0.001.

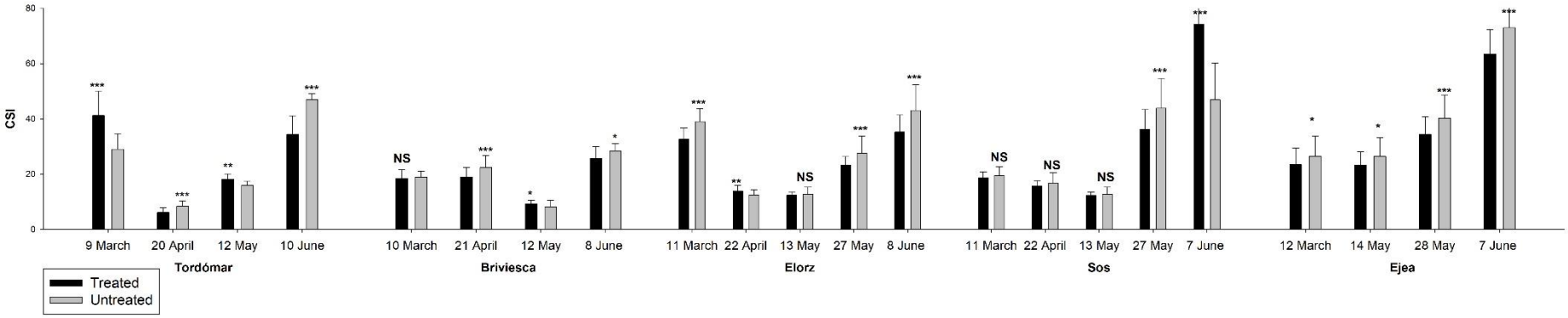

Figure 7. Variation of Crop Senescence Index (CSI) measured at the ground level for the five different sites and five different dates. NS, no significant; *, $p<0.05$, **, $p<0.01$, ***, $p<0.001$.

The evolution of the vegetation indexes TGIveg, GA and CSI for each of the treatments across the different visits is shown in Figures 5, 6 and 7, respectively. Differences in vegetation indexes at early stages may inform about differences in emergence and fractional vegetation cover, while after anthesis vegetation indexes might be saturated by high biomass at higher quality sites, and at grain filling and onward the indexes might indicate water stress or early onset of senescence (whether due to fungal infection or not). In the case of TGIveg (Figure 5), the differences in Tordómar were only observed for the two first visits (March 9 and April 20, $p<0.001$), and the same occurred for Ejea de los Caballeros, (March 12, stem elongation and May 14, heading, $p<0.05$). Meanwhile, there are no differences between treatments for Elorz at any of the visits. On April 21 and May 12, ($p<0.001$) in Briviesca, a significant difference was discovered between untreated and treated plants. In the case of Sos del Rey Católico, TGIveg values of treated were significantly higher than those of untreated on March 11, April 22, and May 13 ($p<0.05$).

Figure 6 shows that differences in GA between treatments existed within each site for at least for one of the visits (e.g., Briviesca), while for the other two sites differences were recorded for two visits (e.g., Tordómar and Elorz), and at one site (Sos del Rey Católico) differences were recorded for three visits; finally, at Ejea de los Caballeros differences were recorded for four separate visits. In almost all cases GA was significantly higher in treated versus the untreated plants and for all the sites differences were significant during the last visit ($p<0.001$).

CSI (Figure 7) was the index that performed the best, with Tordómar, Briviesca and Ejea de los Caballeros showing significant differences for all the visits, Elorz in four of the five visits, and Sos del Rey Católico in two of the five ($p<0.001$). For all the sites, the two last visits show significant differences. In most cases treated plants exhibited lower values than untreated ones. The three vegetation indexes detailed above (TGIveg, GA, and CSI) in Figures 5-7 exhibited the greatest number of significant differences between treated and untreated wheat considering all of the sites and field visit dates of the study.

3.4. Relationships between ground vegetation indexes with grain yield and protein.

To see how the different vegetation indexes can be used to estimate yield, the relationship across treated and untreated genotypes between NDVI and both grain yield (Fig. 8a, upper part) and grain protein content (Figure 8b, lower part) were assessed. There was variability in the strength of the relationship among different sites and across the various dates inside

the same site. Treated trials exhibited higher correlations with grain yield and protein content than untreated ones, while Ejea de los Caballeros and Tordómar exhibited the highest correlations, and Briviesca had the lowest correlation (Figure 8b, lower part).

Subsequently, Figure 9 shows the relationships between the ground-level RGB index NGRDI against grain yield (Figure 9a, upper part) and protein (Figure 9b, lower part) within sites and across visits. The best correlations with grain yield and protein were found in Ejea de los Caballeros, while the lowest correlations were found in Briviesca. Moreover, the correlations increased during the consecutive visits (from tillering to booting and anthesis, while correlations declined during the last visit, coinciding with grain filling, and the onset of crop senescence. Among the vegetation indexes, NDVI and NGRDI are featured here for the most consistently high correlations with grain yield across sites and dates.

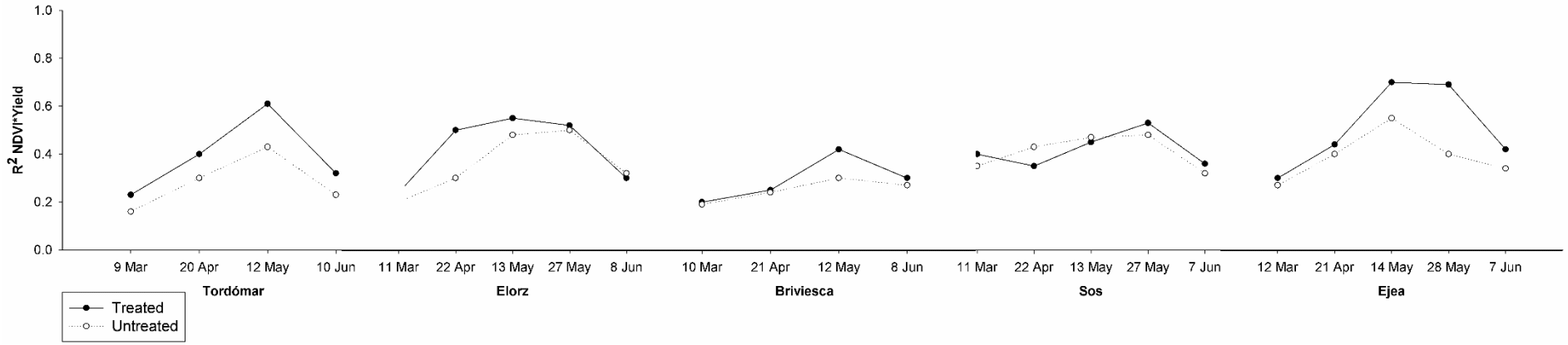

(a)

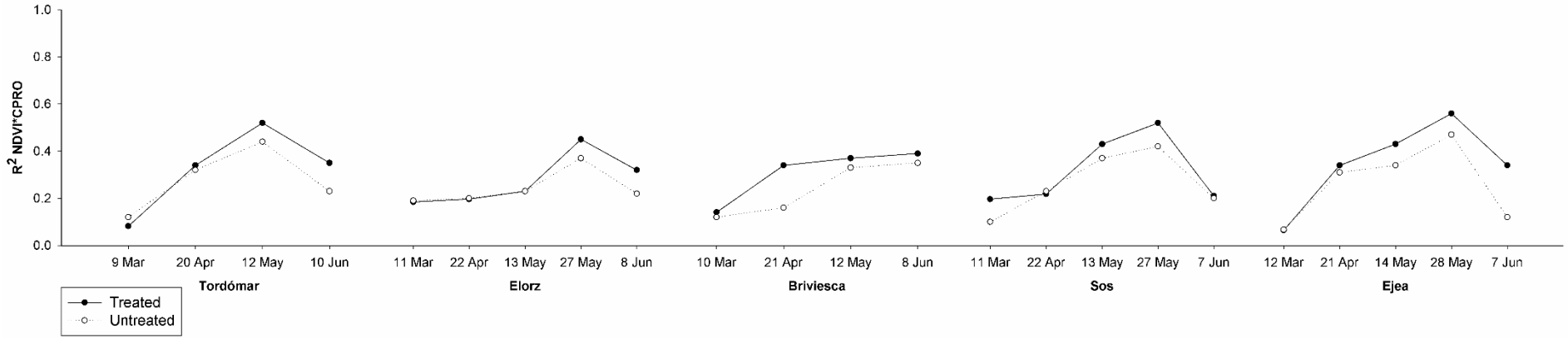

(b)

Figure 8. Regression coefficient) (R^2) between the Greenseeker Normalized Difference Vegetation Index (NDVI) and (upper) grain yield and (lower) protein content (CPRO) around the different sites for the different dates of visit.

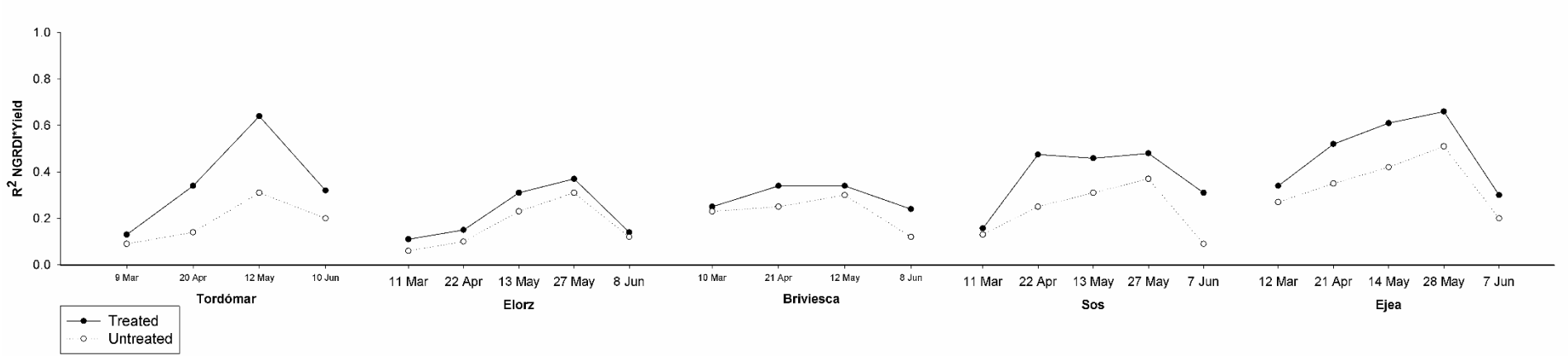

(a)

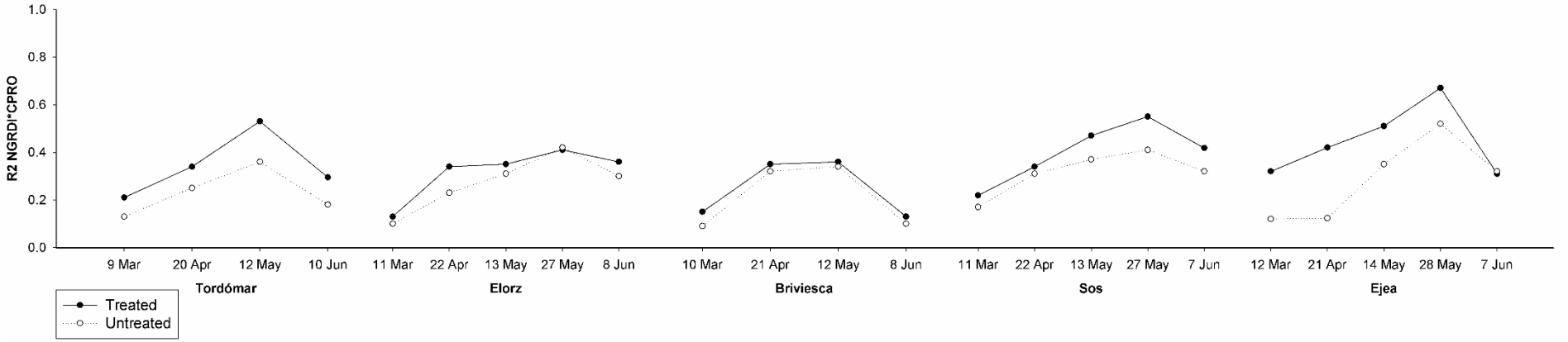

(b)

Figure 9. Regression coefficient(R^2) Determination between the Normalized Green Red Difference Index (NGRDI) from ground images and (upper) grain yield and (lower) the CPRO (protein content) of the different sites for the different dates of visit.

3.5. Comparisons of aerial and ground RGB images and analysis of aerial images for the assessment of treated and untreated trials at the five different study sites

According to Table 3, most of the sites observing the link between ground and aerial level had the highest level of compatibility with NGRDI indexes, where Briviesca registered the highest correlation (r) of this value (r=0.810). Incorporating the mask (i.e.; NGRDIveg, including plot values only where NGRDI>0) only weakened the relationship. In the same context, TGI also performed strongly, with a strong correlation registered at all five locations, with Ejea de los Caballeros exhibiting the highest aerial-ground correlation (r=0.817). These results further indicate the promise of some of the RGB indexes, and, in particular, TGI and NGRDI (r=0.817, r=0.800) for their use from the aerial platform, where higher throughput can be managed for large trials.

Table 3. Comparison between vegetation indexes extracted at the ground level, using RGB images taken by camera Panasonic Lumix GX7, and from the aerial level, using the UAV DJI Mavic 2 Pro during the last visit (June) to the different sites of Limagrain company: Ejea de los Caballeros June 7, Sos del Rey Católico June 7, Briviesca June 8, Elorz June 8, and Tordómar June 10.

Aerial / Ground	GA	GGA	CSI	NGRDI	NGRDI veg	TGI	TGIveg
Tordómar	0.599	0.508	0.329	0.793	0.639	0.741	0.627
Briviesca	0.568	0.543	0.355	0.810	0.699	0.677	0.583
Elorz	0.048	0.578	0.552	0.646	0.706	0.619	0.639
Sos	-0.077	0.313	0.250	0.773	0.546	0.800	0.349
Ejea	0.247	0.139	0.041	0.559	0.167	0.817	0.256

This is in addition to the strong performance of these band math RGB vegetation indexes in separating treatments, as shown for TGI at Figure 5, while the high correlations between NGRDI and grain yield and protein were demonstrated in Figure 9. By contrast, GA and CSI only exhibited strong ground-aerial correlations at some sites, being potentially more susceptible to the related changes in spatial resolution when capturing the image from further away.

In Figure 10, based on the best performing vegetation indexes during each field visit, we present the utility of different UAV-acquired RGB and NDVI vegetation indexes for separating treated and untreated plots captured using the DJI Mavic 2 Pro Hasselblad 20 MP RGB camera and the AgroCam NDVI 12 MP modified camera, showing NDVI-Blue. TGI showed significant differences between treatments for Briviesca and Elorz in April

(p<0.001 and p<0.05, respectively), while the TGIveg detected significant differences between treated and untreated only for Tordómar (p<0.001). The CSI demonstrated differences between treatments in May for all sites except for Tordómar, one of the coldest sites, which also had the lowest levels of senescence. GA detected differences for all sites in June (p<0.001). Meanwhile, the AgroCam NDVI-blue only detected differences in Sos del Rey Católico and Ejea de los Caballeros in May (p<0.05).

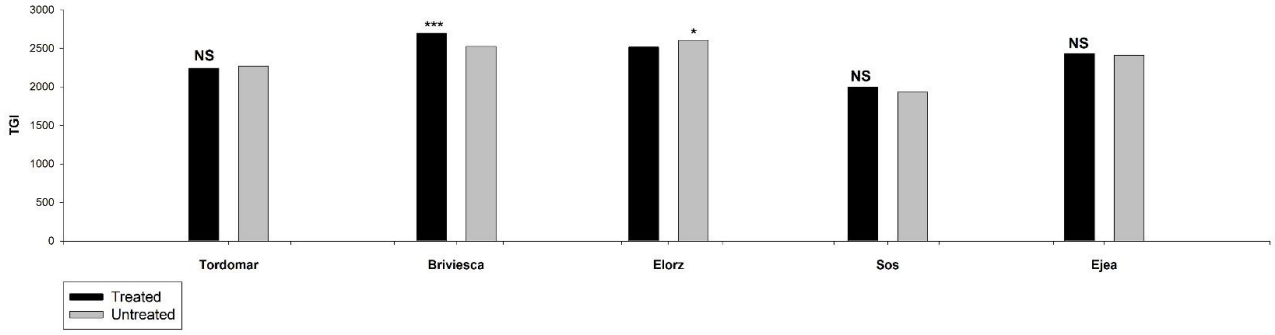

(a)

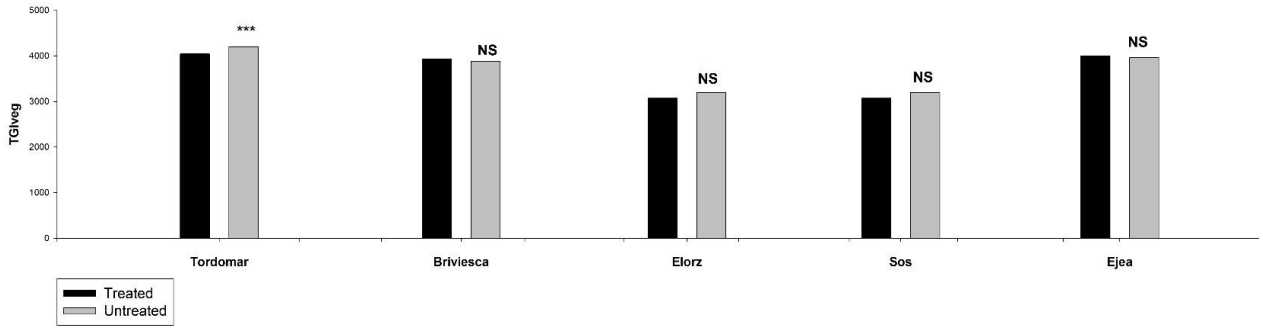

(b)

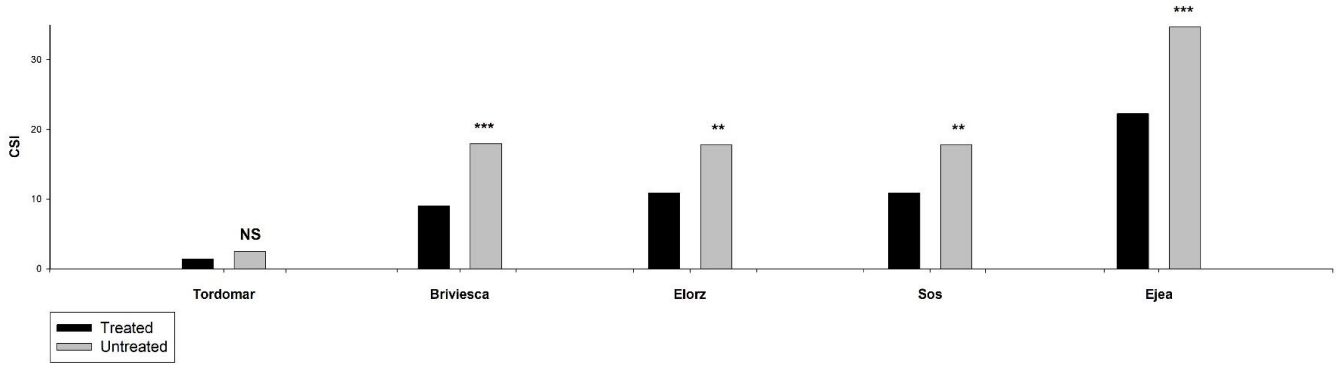

(c)

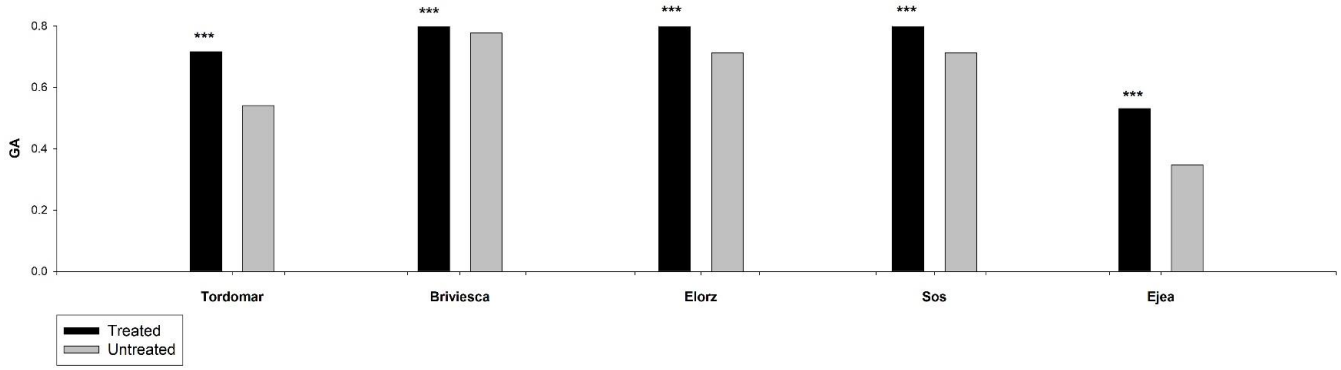

(d)

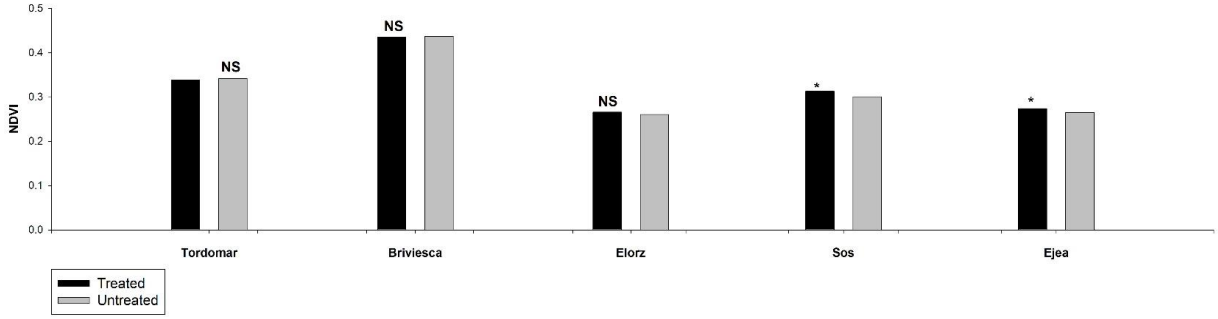

(e)

Figure 10. ANOVA comparisons of mean values for treated and untreated UAV acquired RGB vegetation indexes across the five different sites and measurement following: (a) and (b) show the separability of treated and untreated plots for April 19-22, 2021, using the TGI, Triangular Greenness Index and TGIveg, the Triangular Greenness Index with a mask for vegetation pixels only. (c) shows the CSI, Crop Senescence Index, for May 12-14, 2021; and (d) shows the best performing GA, Green Area index for June 7-10, 2021. For the NDVI AgroCam sensor in e, the highest difference between the treatment and best forming data was identified on May 12-14, 2021. The data shown in Figure 10 are all vegetation indexes that were retrieved at the aerial level. NS, no significant; *, $p<0.05$, **, $p<0.01$, ***, $p<0.001$.

3.6. Evaluation of ground and aerial-acquired vegetation indexes assessing genotypic variability in the response to disease treatments.

We compared the relationships across genotypes through regressions between the ratios of treated versus untreated vegetation indexes (VIs), NDVI and NGRDI at the ground and aerial levels, (RVI=treated/untreated VI values) against the ratios of treated versus untreated grain yield (RGY=GY treated/GY untreated).

When NDVI was assessed at ground level (i.e.; with the GreenSeeker), most of the correlations shown against GY (Supplemental Table S2) were significant. Nevertheless, we can observe a variation in the value of correlation across genotypes between the ratio of treated versus un-treated Greenseeker NDVI (R NDVI ground) and the Ratio of treated/untreated Grain Yield (RGY=GY treated/GY untreated). Elorz registered the highest value during the visits on April 22 (R^2=0.700, p<0.001). These results have demonstrated a strong correlation between the relative sensibility of the lines in terms of leaf color and the calculated sensitivity to grain yield. In the Supplemental Table S3, we have detailed that the correlation value across genotypes recorded at the majority of the sites was low for the ratio of treated to untreated aerial NDVI (R NDVI aerial) and the ratio of treated to un-treated grain yield (RGY=GY treated/GY untreated), which contrasts with results at the ground level. The highest value of determination coefficient between aerial NDVI and grain yield recorded at Tordómar on May 12 (R^2=0.231, p<0.001). Meanwhile, the coefficient is higher in the NDVI at ground level, As Example Elorz on April 22 (R^2=0.700, p<0.001).

Furthermore, as detailed in the Supplemental Table S4, the link between the ground NGRDI ratio (R NDVI ground) and the grain yield ratio (R GY=GY treated/GY untreated) varied across the visits, but except for Sos del Rey Católico, the highest correlation was achieved in the last visits. The greatest value was achieved on March 11 in Elorz (R^2 =0.956, p<0.001). The association between the ratios of NGRDI at the aerial level (R NGRDI aerial) and grain yield ratio (R GY=GY treated/GY untreated) was quite good and comparable (or even somewhat better) than the correlations observed between the two ratios at the ground level. In this case, Elorz on May 27 exhibited the highest determination coefficient value (R^2=0.94, p<0.05), further detailed in the Supplemental Table S5.

3.7. Combinations of NDVI, grain yield and treatments for guiding the selection of genotypes.

Some of the relationships at the five sites between the ratios of treated versus untreated NDVI at ground level and the ratio of treated versus untreated grain yield was depicted in Figure 11. The strongest correlation seen in Figure 11 was on April 21 at Briviesca (R^2=0.65, p<0.001), demonstrating the strength of the correlation between the ratio of NDVI from the ground and the ratio of grain yield. This makes it clear that the treatment played a part in determining the index value. Yet, the ratio of the treatments for the same index (NDVI and grain yield) were well correlated.

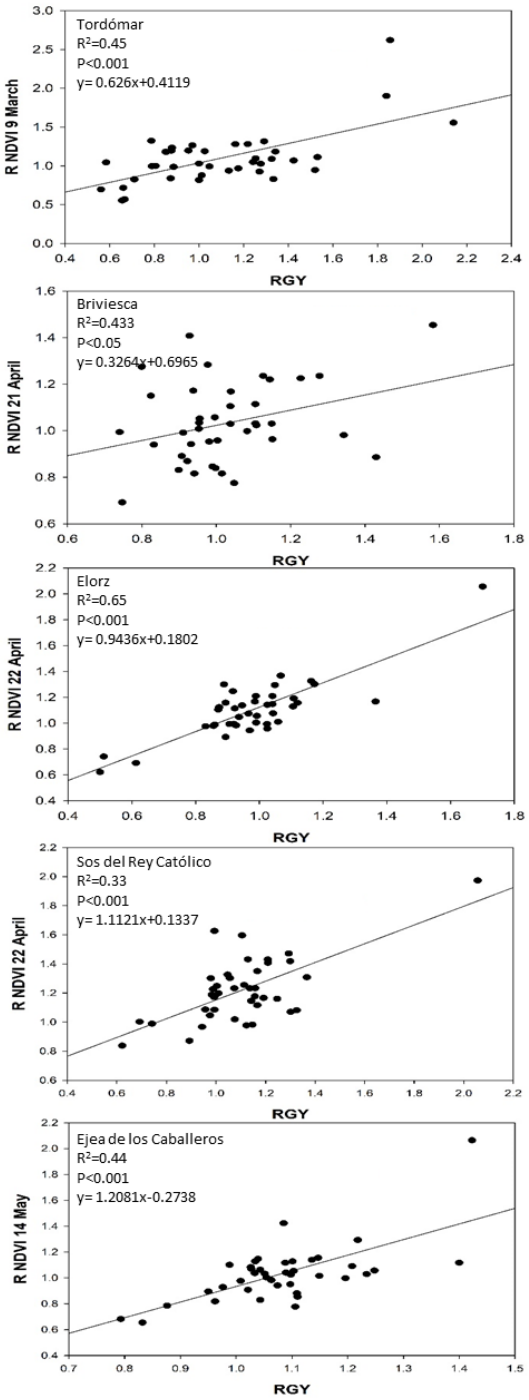

Figure 11. Regressions for the highest correlation values registered between the Ratio of Grain Yield (R GY=Treated/Untreated grain yield values for each variety) and Ratio of NDVI (R NDVI = Treated/Untreated NDVI values at the ground level for each variety) for specific dates and sites as follows: R^2= 0.45 for Tordómar on March 9, R^2=0.433 for Briviesca on April 21, R^2=0.65 for Elorz on April 22, R^2=0.33 for Sos del Rey Católico on April 22, and R^2=0.44 for Ejea de los Caballeros for May 14. R NDVI (ratio treated/untreated wheat NDVI), R GY (ratio treated/untreated grain yield).

4. Discussion

Bread wheat is central to the nourishment of the world population and is under threat from a number of sources, including biotic or abiotic stress [3,4]. Our study investigated the dynamics of crop growth and fungal resistance in advanced (F8) bread lines growing at five different sites across northern Spain with a range of different local climates. We showed the differences in temperature and precipitation patterns across the geographic distribution of the selected sites in Figures 1 and 2. Sowing dates also varies between sites (Figure 3), and site visits were adjust slightly accordingly (Figure 3); we furthermore detailed other relevant differences with the $\delta^{13}C$ and $\delta^{15}N$ stable isotope comparison between two of the most extreme sites, Elorz and Ejea de los Caballeros in Figure 4, showing significant differences in site water and nutrient conditions. In addition, the vegetation indexes showed by Figures 5-7 can help to identify the effect of the treatment. Our main objective was to better comprehend fungal resistance, across different environmental conditions, and which cost-effective affordable remote sensing phenotyping tools work best in different growing conditions and crop growth stages. The evaluation of fungicide treatment efficacy and varietal resistance in protecting bread wheat was compared using ground and aerial level remote sensing tools. Further insights were explored regarding how to best leverage this information for optimizing varietal selection. To better structure the different times, locations, and scales of observation, we have organized our discussion around four specific questions related to the stated objectives:

1. What were the differences in crop status between the different sites on dates of visit?

2. Are RGB and NDVI vegetation indexes able to detect the treatments and fungal tolerance?

3. When is the best phenological time to assess vegetation indexes in order to screen for fungal resistance?

4. Can proximal imaging or aerial imaging be used accurately to select cultivars with a greater fungal resistance?

4.1. What were the differences in crop status between the different sites on dates of visit?

At the leaf level, some pigments, such as flavonoids, chlorophyll, anthocyanins and the NBI ratio detected significant differences between the two treatments (treated/untreated) at various sites. Particularly, the differences in Elorz and Ejea de los Caballeros are obvious

derived from the various leaf level pigment measurements. Both flavonoid and NBI serve as plant stress signals, showing the importance of fungicide treatment in the protection of wheat against the fungal stressors. In treated wheat, the Dualex sensor recorded higher NBI values in treated than untreated wheats in both Elorz ($p<0.01$) and Ejea de los Caballeros ($p<0.001$). NBI is a measure of how well-balanced leaf N is with other crucial macronutrients and, consequently, how well it can support plant functions, particularly photosynthesis. Thus, higher NBI supports higher yield. This is similar to the study conducted by Simón and coworkers [42], whose findings indicated that foliar fungal infections may significantly reduce wheat yield and quality. These biotic stresses could have various effects on crop development rates, altering grain carbohydrate buildup and nitrogen (N) dynamics. Another notable measurement made by the Dualex leaf sensor is the flavonoid concentration, which showed a significant difference between treated and untreated plants at the two study locations (for Elorz and Ejea, $p<0.01$ and $p<0.5$, respectively). The greater levels of flavonoids seen in the bread wheat that has not been treated in our study were likely related to stress signaling and are an indication that key photochemical processes are being compromised. Fungicides may be able to mitigate these effects by limiting fungal infection. Our research is in line with Surovy et al.'s findings [43], which claim that wheat infected by the blast fungus *Magnapoorpthe oryza*e pathotype Triticum reacts at the beginning of the attack by an increase in flavonoid concentration, followed later by a decrease in flavonoids as this pigment is involved in the plant reaction against fungal attacks and the access of the pathogen to the cell.

The analysis of the carbon and nitrogen stable isotope composition of two sites from the different Limagrain trials showed significant differences between the two sites measured ($p<0.001$). Stable carbon and nitrogen isotopes as well as the ratio of carbon and nitrogen in biomass are general indicators for plant water conditions and nutritional status. While stable carbon isotope ratios $\delta^{13}C$ (‰) immediately reflect the plant's water state, stable nitrogen isotope ratios $\delta^{15}N$ are more instructive of nutritional status and specific nutrient consumption [40]. Nitrogen composition $\delta^{15}N$ (‰) can be used to measure this reduction in N availability and utilization as water supply declines. For instance, a more negative result for $\delta^{13}C$ indicates that the plant is growing under better water conditions. The fact that Elorz had less negative value in $\delta^{13}C$ ($p<0.001$) and higher value of $\delta^{15}N$ ($p<0.001$), which significantly exceeded that of Ejea de los Caballeros, indicated that wheat in Ejea benefited from better water status, but the yield in Elorz benefited from a better uptake of nitrogen from the soil. Consequently, yield in Elorz was higher than Ejea de los Caballeros, Rezzouk

et al. [44] concluded for durum wheat that a greater $\delta^{15}N$ resulted in more nitrogen uptake and, thus, more effective photosynthesis and final production. This can be explained by the heavy precipitation in Ejea de los Caballeros during the month of April (75 mm) contrary to Elorz, which received only 50 mm and can affect the speed and the intensity of the disease invasion. In addition, Ejea de los Caballeros received 3 irrigations by inundation, each one about 40-50 mm. In the same sense a more negative $\delta^{13}C$ value, especially in mature grains, implies that the crop has received more water, and therefore produced more grain yield [45].

The experimental site distribution map reveals that the trials were spread apart from one another, creating a variety of climatic conditions between them, which is further accentuated by the topography of the region. Because the field season runs from sowing October or November with heading and maturity from the months of March to June, these characteristics have the potential to influence growth patterns, senescence, or fungal developments. We observed that some locations, such as Briviesca, were characterized by regular precipitation and high temperatures, whereas other locations were characterized by inconsistent precipitation and high temperatures. For RGB vegetation indexes assessed from the ground, we noted that bread wheat in Briviesca registered better performance than Ejea de los Caballeros, which was characterized by a greater precipitation during the month of April, which, given the mild temperature, may be the best moment for the spread of the disease in the wheat crop. Differences between the sites were observed at different times following seasonal site differences. RGB vegetation indexes, such as TGIveg and GA were higher at Ejea de los Caballeros and Sos del Rey Católico in March early in the season, whereas the same chlorophyll and vigor related indexes were higher in Tordómar and Briviesca during the visits in May and June. This may indicate that the environment has negatively influenced crop status at Ejea de los Caballeros, with an earlier onset of crop infection during April, when the crop experienced the highest precipitation out of all of the sites, combined with moderate temperatures. Considering the higher heat at Sos del Rey Católico and Ejea de los Caballeros, earlier onset of senescence was also expected, but differences between treated and untreated were also observed in June.

In this context, Mielniczuk and coworkers [46] found that cereals in the flowering and post-flowering stages were the most vulnerable to fungal infection, especially in warm, humid weather, and during this time of year there was a lot of persistent rainfall at Ejea de los Caballeros, more so that other sites. It is seen from the metrological data that Ejea de los Caballeros especially, received heavy precipitation during the month of April. In addition, this site was provided supplement irrigation by flooding which would increase the humidity

of the canopy favoring the development and spread of the disease. Relative humidity can affect the rate of plant disease spread as spore germination and infection in-creases with sufficient moisture (RH≥60%) [47]. Additionally, rainfall has been identified as a key requirement for the development of STB (Septoria leaf blotch), as it allows for the swelling of the fungal pycnidia and subsequently aids in the dispersal of spores across the upper leaves of wheat [48].

Indexes measured at both visits in April and May were close to the GA saturation limit, suggesting that the experimental plots achieved their maximum vegetation cover at Ejea de los Caballeros earlier in the season. On the other hand, the climatic circumstances at the locations at Tordómar, Briviesca and Elorz were more favorable for both crop and fungus growth in general later on in the season; that is in May. However, despite the possibility of greater yields under rainfed conditions but also more potential for late-season fungal infection compared to Sos del Rey Católico and Ejea de los Caballeros. However, Ejea de los Caballeros exhibited one of the greatest differences between treated and untreated for the two visits during the month of May (see GA and CSI in Figures 6 and 7), possibly related to the heavy rains that it experienced in late April (Figure 2e), which may have done more to intensify the fungal infection for the remainder of the season. Thus, we suggest that the severity of fungal attack on wheat crops was determined by the combination of the environment, timing of the infection with the wheat cycle, and geographic location [49].

Comparing the metrological data between the different sites, we note a difference in the month that recorded the highest precipitation. The majority of the sites were characterized by heavy precipitation early in the season (November), which presents a short time after the sowing dates. In contrast, Ejea de los Caballeros received the highest amount of precipitation in the month of April (at anthesis). This can help explain the effect of the precipitation date on the severity of the disease. Whereas the four sites (Tordómar, Elorz, Briviesca and Sos del Rey Católico) were less affected by the disease impacts and the risk of disease spread later in the season but more so during the early phases of emergence. While the risk of wheat fungal disease infection in Ejea de los Caballeros was higher at the anthesis stage due the facility of pathogen spread from the precipitation. These conditions create a humid microclimate with moderate temperature favorable to fungal invasion of wheat. A moderate temperature with humidity has been found to facilitate the penetration of *Fusarium pseudograminearum* and the infection of the wheat in Australia around 15°C and reduces the wheat resistance to the disease [50]. The same was demonstrated in other

studies, where they also indicated that the most pathogenic conditions for cereals were in warm temperatures and under high humidity [49, 51].

4.2. Are RGB and NDVI vegetation indexes able to detect the treatments and fungal tolerance?

RGB and NDVI vegetation indexes and their changes over the growing season can be used as tools to learn more about the state of a plant and, in this case, whether the fungicide treatment was beneficial towards the crop status for different varieties. Almost all of the different vegetation indexes differentiated fungicide treated plants compared to un-treated ones for at least one site or visit time, but TGIveg, GA and CSI were the most consistent from the ground level. This can be explained by the vegetation index sensitivity at different plant growth stages (some indexes may lose sensitivity at higher biomass stages). Wheat goes through senescence more quickly at hotter sites, resulting in less chlorophyll and vigor, which lowers NDVI and NGRDI values later in the season. Additionally, fun-gal attacks act as a form of stress on plants by causing a drop in chlorophyll content and crop vigor. According to Dammer et al. [49], NGRDI can be a useful index for identifying plant stress in general. This index has a strong correlation with grain yield, which de-creases under stressful conditions. Combining various vegetative indexes, such as the NDVI and NGRDI, can help to estimate the amount of wheat that will be lost due to fungal infection. The findings were in line with the study done by Vergara-Diaz et al. [20], which found that indexes retrieved from RGB images are extremely helpful for estimating wheat losses due to fungal (yellow rust) assault.

For aerial RGB indexes, particularly for GA, the differences were evident, showing that the value of treated wheat is generally higher than that of untreated wheat at most sites. This conclusion was also supported by research by Vergara-Diaz and coworkers [20], who discovered that GA had a strong correlation with grain yield at the anthesis stage, allowing for the detection of the yellow rust effect on durum wheat losses. Although keeping in mind that NDVI at the aerial level has also been proven effective as a technique to identify the impact of fungal attack on the crop of bread wheat later in the wheat cycle. Vergara-Diaz et al. [20] also demonstrated a strong correlation between ground-level NDVI and grain yield during the tillering and jointing stages, allowing for the quantification of the direct impact of the yellow rust on the durum wheat production and quality. In the same context, CSI extracted from aerial images also aligned with the results from the ground, where we note that untreated wheat exhibited higher and earlier senescence. Senescence is the natural final

phase of the plant season and may be induced by a number of different factors, from heat and drought to other stressors like fungal infection. The results showed that there were significant differences between treatments in leaf and canopy senescence parameters associated to stay green expression, which as a varietal trait can lead to increased yields. Additionally, it should be noted that, in the majority of sites, a significant difference between treated and untreated plants was observed in the CSI index near the end of the season, suggesting that fungal pressure played an important role in our trials. In the same context, we note that CSI derived from RGB aerial images were similar to CSI values from ground, where the untreated wheat had higher values than treated, which means that untreated wheat suffered more from the fungal aggression. CSI detection early in the season where the infection affects the absorption of the incident light by the chlorophyll further indicates fungal pressure. The same conclusion was found by Heidarian Dehkordi et al. [15] where these authors indicated that the winter wheat infected by leaf rust showed an early decrease in the absorption of incident light by the plant with the slope flattened from the green to the red spectral bands.

The difference between the values of the various indexes measured by the various sensors demonstrates the ability of these sensors to detect wheat cultivar susceptibility to fungal attack under untreated conditions as well as the benefits reaped from the fungicide treatments, with some notable differences at the different locations. The reaction of the wheat varieties varied between treated and untreated, and the majority of the indexes favored a greater performance for the treated wheat, indicating the wheat that has not been treated with fungicide was more affected by the fungal impacts. According to another study, indexes such as the Normalized Difference Index (NDI), Green Index (GI), Green Leaf Index (GLI), and ground NDVI in winter wheat infected by leaf rust can be an effective tool to assess fungal foliar disease in wheat, where the indexes correlated well with the coefficient infection that measured the severity of infection in the crop [52]. Meanwhile, others used different spectral vegetation indexes, including NDVI, such as NBNDVI, PRI, GI, and RVSI to quantify the severity of rust disease on the wheat crop developed using more advanced hyperspectral imaging sensors [22].

4.3. When is the best phenological time to assess vegetation indexes in order to screen for fungal resistance?

The correct sequence of images obtained during the field season as well as the period of image processing can be confirmed by comparing vegetation indexes at the aerial and

ground levels. Knowledge about plant status can be gleaned through the examination of indexes taken from ground images. Otherwise, depending on the hue shifts shown by the mosaic image, aerial pictures can give an overall view of the area and an estimate of its condition. The variations in vegetation indexes during the last stage (maturity) can serve to comprehend the phenological state of the plant. Thus, the decline in the values of the vegetation indexes at that time indicated senescence onset but could also have occurred earlier as a consequence of the fungal biotic stress. Additionally, these vegetation indexes can provide us with information regarding the state of the plants at the many experiment sites, as shown previously, where each site is characterized by a particular climate condition that may help to prevent or lessen the development and spread of a fungal infection.

The vegetation indexes performed well at detecting differences between treatments during April (booting-heading), which aligned with some prior studies have demonstrated that the RGB indexes as GA and GGA were to detect the effect of yellow rust on the losses of the durum wheat early during the anthesis stage [20]. Post anthesis/early grain filling is the optimum stage to assess the vegetation indexes because this stage has been usually considered optimal for inferring the potential yield achievable by the crop; this is in spite of the fact many vegetation indexes may exhibit saturation patterns and the consequent loss of precision when evaluated between heading to anthesis. Moreover, depending on the kind of fungal disease, the pathogen can move through exposed florets and extruded anthers on wheat spikes during that time [53]. By providing the nutrients required for germination and penetration, extruded anthers can also trap fungus and aid in their growth. The low weight and deformed kernels, together with a decrease in kernel quality of diseased plants are the consequence of disease impact on grain filling. Early detection of fungus attacks helps shield plants from the fungus damaging impacts. Whereas some research claims that anthesis is the crop’s most susceptible stage for Fusarium head blight, early detection of the disease can minimize losses to wheat crops [53]. Yet, according to one study, it was possible to detect Fusarium head blight early in the grain's development and ripening stage by employing technologies like multispectral imaging [54], to some extent comparable to the approximations of the Dualex and AgroCam NDVI sensors in our study.

4.4. Can proximal imaging or UAVs be used accurately to select cultivars with a greater fungal resistance?

While NDVI assessed at ground level correlated quite efficiently with grain yield, the NDVI aerial measurements showed overall poor association. Which leads us to favor the Trimble

GreenSeeker over the AgroCam for the NDVI measurements, the first being a more controlled and consistent active field sensor even if more time consuming in use. These results disagree with these of Moazzam et al. [55], who used images obtained from an AgroCam camera to distinguish the sesame crop from weeds in order to maintain a precise application of herbicide in the field. When we compared the aerial and ground RGB photos, we can see that the findings obtained from both are similar in terms of the way that the treatments are separated and how grain yield is correlated; the capacity of RGB indexes to distinguish between the two treatments may be employed to forecast of the disease's impact on grain yield. For example, we demonstrated that the NGRDI index showed a greater association between ground and aerial levels of observation (r=0.810). This suggests using the UAVs may offer benefits as aerial photographs can provide improved efficiency in information collection due to their ability to swiftly cover a large region. Therefore, when favorable conditions for flying as well as imaging are available, UAV platforms carrying RGB sensors or the AgroCam should have the advantage of allowing fast measurements of large crop trials [56].

The relatively comparable efficiency of ground versus aerial-assessed RGB vegetation indexes to evaluate genotypic susceptibility to fungal disease may be based in two facts. First, the high resolution of RGB images makes them less prone to loss efficiency when the indexes are formulated from aerial platforms instead than from the ground. The second factor is the size of the canopy sampled. While the aerial images gather information about the whole plot, images acquired from the ground only cover a fraction (ca ^{1} m^{2}) of the entire plot. By contrast, the NDVI camera used from the drone had a lower resolution than the RGB cameras, while the assessment of NDVI from the ground implies covering the entire plot by foot in a more time-consuming manner.

The study of indexes generated from aerial and ground images can be useful when there is a high degree of correlation between the two levels of data collection. Nevertheless, we can now foresee any alterations to the plant or dangers to its development. Using RGB and multispectral imagery taken by a UAV, Mateen and Zhu [57] showed in their research that it is feasible to find weed patches in wheat. In contrast to other studies, which focus on a specific topic, Vergara et al. [20] conducted a study, which served as the foundation for our research, tackled the estimation of grain yield losses in yellow-rusted durum wheat using digital and conventional tools. In the same sense, Francesconi et al [58] carried out studies that demonstrated the utility of integrating thermal data and RGB indexes to detect the Fusarium head blight more effectively in durum wheat. The combination of RGB images

and temperature data at this level allowed for differentiation between the biotic stress induced by Fusarium and abiotic stress caused by dry weather, which they also mentioned as possibly a decrease in stomatal conductance in response to Fusarium infection. Moreover, it may also be worth to further explore a wider range of vegetation indexes. Thus, the normalized difference red edge (NDRE) and green normalized vegetation index (GNDVI), and NDVI extracted from 5 bands of a multispectral image are the most significant factors influencing grain yield and worked well in studies of wheat phenotyping and gave better results than RGB images in some cases, where they worked well early on the growth stage [59].

The strength of the correlations across genotypes between the ratios of treated versus untreated vegetation indexes (R VI) against the corresponding ratio for grain yield (RGY) provides an insightful perspective for selecting top performing wheat phenotypes. By plotting such relationships (e.g.; Figure 11), it can be easier to observe which specific genotypes performed best in terms of tolerance to fungicides and their implication in terms of grain yield. Thus, having the grain yield ratio in the horizontal axis and considering a grain yield ratio of 1 as a threshold, all the genotypes placed on the left side would be amenable for selection based on yield. From these genotypes and considering the vertical axis depicting the ratio of treated untreated vegetation indexes, all the genotypes placed below 1 should be further selected based on their vegetation index performance.

Some practical applications can be used to reduce the severity of the fungal disease, such as the date of sowing. If the sowing date is such that flowering coincides with spore release, then more frequent and severe attacks are likely. So, the choice of an early sowing date can make early-maturing wheat cultivars tend to be less impacted via an avoidance strategy [60]. In addition, the density of the canopy can be an important factor affecting the invasion, so the high density can increase the humidity of the canopy favoring spore germination and decreasing the efficacy of the fungicide treatment. A reasonable density should be applied at the time of sowing [61]. Also, besides precipitation, the timing of irrigation of a field can influence its microclimate and may encourage the development of the pathogen. Regardless of whether the climate conditions are favorable for the disease in a given year, irrigation timing and application techniques can increase the frequency and the severity of the disease [62]. Irrigation should be limited to supplement irrigation in dry weather. The effects of crop rotation have been studied in detail [63]. They depend on the preceding crop, whether that crop is a potential host for the pathogens responsible for fungal disease, and the frequency of the crop concerned in the rotation. The shorter the rotation, the higher the

frequency of disease. A large period of rotation reduces the risk of infestation by the same pathogen [63]. The optimal fungicide application timing has also been found to be crucial for the protection of the wheat against the fungal attack [64].

5. Conclusions

Combining the information from different growing sites, remote sensing approaches (NDVI versus RGB indexes), sensor placement (ground versus aerial) and times during crop cycle, together with the effect of fungicide (Prosaro) applications have allowed concluding some general recommendations in terms of phenotyping, the likelihood of aggressiveness from fungus impacts, and the need for early fungal treatments. The difference between the several sites was apparent from the various indexes in our research, emphasizing the susceptibility of the wheat to fungal assault in different environmental conditions. The location's environment, such as that of Ejea de los Caballeros was characterized by heavy precipitations and warm temperatures during the month of April, both of which were critical for the infection, and had a significant impact on the fungus spreading. The observed conditions may help to establish a strong fungal presence early in the season and require rapid treatment.

Additionally, HTPP sensor assessments early in the wheat cycle can help to protect the wheat crop from a serious fungus attack and ultimately enhance production in terms of quantity and quality. Leaf pigment measurements proved the importance of fungicide treatment in order to protect wheat crops in terms of quantity and quality. Exploring the genetic variability of fungal resistance as the first line of defense against fungal attack needs to be explored further and can be supported with the use of HTPP technology, as fungicide applications may have additional side effects to the crop, besides the added costs associated. In summary, for now, it is clear that the application of fungicide can make a significant difference in how the wheat crop is protected from fungal disease. However, the environmental and health implication of spraying fungicides and the concern of customers makes it more urgent to push forward field crop breeding strategies with HTPPs.

For NDVI, our results suggest greater reliability from the use of the field sensor GreenSeeker NDVI as a tool due to its better overall performance in comparison to the UAV AgroCam, NDVI, which is a RGB camera modified to measure NIR, Green and Blue light to provide NDVI-Blue, a modification of the original NDVI formulation. For the rest of the RGB indexes our results indicate benefits from the UAV, which worked well, adapted well to weather conditions and were quicker to capture. However, this decision

must be supported by early threat detection capacity in order to intervene with fungicide treatment that shields the wheat from attack and encourages the plant to grow in its preferred environment without experiencing any kind of stress. The combination of vegetation indexes (TGIveg, GA, CSI or NGRDI from RGB images or NDVI) and production (grain yield and protein) data provides a useful approach to selecting the variety with highest yield potential and more resistant to the fungal disease.

The generation of new wheat varieties using HTPPS may also provide a more cost-effective approach [14]. In the current study site, in spite the fact treated plants performed far better than untreated ones, there were also cases when lack of effect of fungicide or even a negative effect was evidenced; for example, when plotting the ratios for GY and the vegetation indexes between the treated and untreated across the set of advanced lines. When using fungicides to prevent fungus penetration in wheat plants, their application should be timed for efficacy and to minimize residue buildup. Applying fungicides quickly after a pathogen has been detected by a sensor can also be effective in preventing pathogen penetration inside plants, therefore ensuring greater production with improved grain quality. The benefits provided by the various sensors and their capacity to distinguish between treatments applied at various locations, each of which is defined by a unique climatic state, will make them effective tools for identifying pathogen-resistant varieties.

References

1. Busby, J. W.; & Busby, J Climate change and national security: an agenda for action. Council on Foreign Relations Press: New York, USA. **2007**.

2. Duller, R. A.; Armitage, J. J.; Manners, H. R.; Grimes, S.; & Jones, T. D. Delayed sedimentary response to abrupt climate change at the Paleocene-Eocene boundary, northern Spain. *Geology*. **2019**, *47*.159-162.

3. Wolf, J. Effects of climate change on wheat production potential in the European Community. *Eur. J. Agron*. **1993**, *2*. 281-292.

4. Iglesias, A.; Rosenzweig, C.; & Pereira, D. Agricultural impacts of climate change in Spain: developing tools for a spatial analysis. *Glob Environ Change J*. **2000**, *10*, 69-80.

5. Porras, R.; Luque, A. P.; & Rojas, C. D. M. Behavior of Spanish durum wheat genotypes against *Zymoseptoria tritici:* resistance and susceptibility. *SJAR*. **2021**, *19*, 1.

6. Martínez-Moreno, F.; & Solís, I. Wheat rust evolution in Spain: an historical review. *Phytopathol*. **2019**, *58*,1.

7. Martínez-Moreno, F.; Giraldo, P.; Nieto, C.; & Ruiz, M. Resistance to leaf and yellow rust in a collection of Spanish bread wheat landraces and association with ecogeographical variables. *Agron*. **2022**, *12*, 187. 8.

8. Bravo, C.; Moshou, D.; West, J.; McCartney, A.; & Ramon, H. Early disease detection in wheat fields using spectral reflectance. *Biosystems Engineering*. **2003**,*84*, 137-145

9. Suffert, F.; Ravigné, V.; & Sache, I. Seasonal changes drive short-term selection for fitness traits in the wheat pathogen *Zymoseptoria tritici*. *Appl. Environ*. **2015**, *81*, 6367-6379.

10. Porras, R.; Miguel-Rojas, C.; Pérez-de-Luque, A.; & Sillero, J. C. Macro and Microscopic Characterization of Components of Resistance against *Puccinia striiformis f. sp. tritici* in a Collection of Spanish Bread Wheat Cultivars. *Agron*. **2022** *12*, 1239.

11. Shakoor, N.; Lee, S.; & Mockler, T. C. High throughput phenotyping to accelerate crop breeding and monitoring of diseases in the field. *Plant biol*. **2017**, *38*, 184-192.

12. Araus, J. L.; & Kefauver, S. C. Breeding to adapt agriculture to climate change: affordable phenotyping solutions. *Plant biol*. **2017**, *45*, 237-247.

13. Mujeeb-Kazi, A.; Kazi, A. G.; Dundas, I.; Rasheed, A.; Ogbonnaya, F.; Kishii, M.; … & Farrakh, S. Genetic diversity for wheat improvement as a conduit to food security. *Agron*. **2013**, *122*, 179-257.

14. Reynolds, D.; Baret, F.; Welcker, C.; Bostrom, A.; Ball, J.; Cellini, F.; ... & Tardieu, F What is cost-efficient phenotyping? Optimizing costs for different scenarios. *Plant Sci. J*. **2019**, *282*, 14-22.

15. Heidarian Dehkordi, R.; El Jarroudi, M.; Kouadio, L.; Meersmans, J.; & Beyer, M. Monitoring wheat leaf rust and stripe rust in winter wheat using high-resolution UAV-based red-green-blue imagery. *Remote Sens*. **2020**, *12*, 3696.

16. Moshou, D.; Bravo, C.; West, J.; Wahlen, S.; McCartney, A.; Ramon, H. Automatic detection of 'yellow rust' in wheat using reflectance measurements and neural networks. *Comp. Electron. Agric*. **2004**, *44*, 173–188.

17. Boulent, J.; Foucher, S.; Théau, J.; St-Charles, P.-L. Convolutional Neural Networks for the automatic identification of plant diseases. *Front. Plant Sci*. **2019**, 10, 941.

18. Zhang, C.; Kovacs, J.M. The application of small unmanned aerial systems for precision agriculture: A review. *Precision Agric*. **2012**, *13*, 693–712.

19. Araus, J. L.; Kefauver, S. C.; Zaman-Allah, M.; Olsen, M. S.; & Cairns, J. E. Translating high-throughput phenotyping into genetic gain. *Trends in plant sci*. **2018**, *23*, 451-466.

20. Vergara-Diaz, O.; Kefauver, S. C.; Elazab, A.; Nieto-Taladriz, M. T.; & Araus, J. L. Grain yield losses in yellow-rusted durum wheat estimated using digital and conventional parameters under field conditions. *Crop J*. **2015**, *3*, 200-210.

21. Arora, A.; Sharma, R. K.; Saharan, M. S.; Venkatesh, K.; Dilbaghi, N.; Sharma, I.; & Tiwari, R. Quantifying stripe rust reactions in wheat using a handheld NDVI remote sensor. *Gates Open Res*. **2019**, *3*, 955.

22. Ashourloo, D.; Mobasheri, M. R.; & Huete, A. Evaluating the effect of different wheat rust disease symptoms on vegetation indices using hyperspectral measurements. *Remote Sens*. **2014**, *6*, 5107-5123.

23. Jing, X.; Du, K.; Duan, W.; Zou, Q.; Zhao, T.; Li, B.; ... & Yan, L. Quantifying the effects of stripe rust disease on wheat canopy spectrum based on eliminating non-physiological stresses. *Crop J*. **2022**, *10*, 1284-1291.

24. Zhou, B.; Elazab, A.; Bort, J.; Vergara, O.; Serret, M. D.; & Araus, J. L. Low-cost assessment of wheat resistance to yellow rust through conventional RGB images. *Comput. Electron. Agric*. **2015**, *116*, 20-29.

25. Gracia-Romero, A.; Kefauver, S. C.; Fernández-Gallego, J. A.; Vergara-Díaz, O.; Nieto-Taladriz, M. T.; & Araus, J. L. UAV and ground image-based phenotyping: a proof of concept with Durum wheat. *Remote Sens*. **2019**, *11*, 1244.

26. Cerovic, Z.G.; Masdoumier, G.; Ghozlen, N.B.; Latouche, G. A new optical leaf-clip meter for simultaneous non-destructive assessment of leaf chlorophyll and epidermal flavonoids. *Physiol. Plant*. **2012**, *146*, 251–260.

27. Cerovic, Z.G.; Ghozlen, N.B.; Milhade, C.; Obert, M.; Debuisson, S.; Le Moigne, M. Non-destructive Diagnostic Test for Nitrogen Nutrition of Grapevine (*Vitis vinifera L*.) Based on Dualex Leaf-Clip Measurements in the. Field. *J. Agric. Food Chem*. **2015**, *63*, 3669–3680.

28. Cerovic, Z.G.; Ounis, A., Cartelat, A.; Latouche, G.; Goulas, Y.; Meyer, S.; Moya, I. Chlorophyll fluorescence excitation spectra can be used for the non-destructive in

situ assessment of UV-absorbing compounds in leaves. *Plant Cell Environ*. **2001**, *25*, 1663–1676.

29. Goulas, Y.; Cerovic, Z. G.; Cartelat, A.; & Moya, I. Dualex: a new instrument for field measurements of epidermal ultraviolet absorbance by chlorophyll fluorescence. *Appl. Opt.* **2004**, *43*, 4488-4496.

30. Tremblay, N.; Wang, Z.; & Belec, C. Performance of Dualex in spring wheat for crop nitrogen status assessment, yield prediction and estimation of soil nitrate content. *J. Plant Nutr*. **2009**, *33*, 57-70.

31. Kefauver, S. 2018. Available online:https://gitlab.com/sckefauver/MosaicTool, University of Barcelona, Barcelona, Spain. (acessed: 25 September 2021).

32. Zaman-Allah, M.;Vergara, O.; Araus, J.L.; Tarekegne, A.; Magorokosho, C.; Zarco-Tejada, P.J.; Hornero, A.; Albà, A.H.; Das, B.; Craufurd, P. Unmanned aerial platform-based multi-spectral imaging for field phenotyping of maize. *Plant Methods*. **2015**, *11*, 35.

33. Hunt, E. R.; Cavigelli, M.; Daughtry, C. S.; Mcmurtrey, J. E.; & Walthall, C. L. (2005). Evaluation of digital photography from model aircraft for remote sensing of crop biomass and nitrogen status. *Precis. Agric.* **2005**, *6*, 359-378.

34. Hunt, E.R.; Dorais wamy, P.C.; M cmurtrey, J.E.; Daughtry, C.S.T.; Perry, E.M.; Akhmedov, B. A visible band index for remote sensing leaf chlorophyll content at the canopy scale. *Int. J. Appl. Earth Obser. Geoinf.* **2013**, *21*, 103–112.

35. Casadesus, J.; Kaya, Y.; Bort, J.; Nachit, M.M.; Araus, J.L.; Amor, S.; Ferrazzano, G.; Maalouf, F. Using vegetation indexes derived from conventional digital cameras as selection criteria for wheat breeding in water-limited environments. *Ann. Appl. Biol*. **2007**, *150*, 227–236.

36. Vergara-Díaz, O.; Zaman-Allah, M. A.; Masuka, B.; Hornero, A.; Zarco-Tejada, P.; Prasanna, B. M.; ... & Araus, J. L. A novel remote sensing approach for prediction of

maize yield under different conditions of nitrogen fertilization. *Front. Plant Sci*. **2016**, *7*, 666

37. Stern, A.; Doraiswamy, P. C.; & Hunt Jr, E. R. Changes in crop rotation in Iowa determined from the United States Department of Agriculture, National Agricultural Statistics Service cropland data layer product. *J. Appl. Remote Sens.* **2012**, *6*, 063590-063590.

38. Hunt, E.R.; Daughtry, C.S.T.; Eitel, J.U.; Long, D.S. Remote sensing leaf chlorophyll content using a visible band index. *Agron. J*. **201**1, *103*, 1090–1099.

39. Kefauver, S.; Kerfal, S.; Fernandez Gallego, J.A.; El-Haddad, G. CerealScanner Gitlab. Available online: https://gitlab.com/ sckfauver/cerealscanner (accessed on 12 November 2021).

40. Flohr, P.; Müldner, G.; & Jenkins, E. Carbon stable isotope analysis of cereal remains as a way to reconstruct water availability: preliminary results. *Water History*. 2**011**, *3*, 121-144.

41. Porep, J. U.; Kammerer, D. R.; & Carle, R. On-line application of near infrared (NIR) spectroscopy in food production. *Trends Food Sci. Technol*. **2015**, *46*, 211-230.

42. Simón, M. R.; Fleitas, M. C.; Castro, A. C.; & Schierenbeck, M. How foliar fungal diseases affect nitrogen dynamics, milling, and end-use quality of wheat. *Front. Plant Sci*. **2020**, *11*, 569401.

43. Surovy, M. Z.; Mahmud, N. U.; Bhattacharjee, P.; Hossain, M. S.; Mehebub, M. S.; Rahman, M.; ... & Islam, T. Modulation of nutritional and biochemical properties of wheat grains infected by blast fungus *Magnaporthe oryzae Triticum* pathotype. *Front. Microbiol.* **2020**, *11*, 1174.

44. Rezzouk, F. Z.; Gracia-Romero, A.; Kefauver, S. C.; Gutiérrez, N. A.; Aranjuelo, I.; Serret, M. D.; & Araus, J. L. Remote sensing techniques and stable isotopes as phenotyping tools to assess wheat yield performance: Effects of growing temperature and vernalization. *Plant Sci*. **2020**, *295*, 110281.

45. Araus, J. L.; Villegas, D.; Aparicio, N.; Del Moral, L. G.; El Hani, S.; Rharrabti, Y.; ... & Royo, C. Environmental factors determining carbon isotope discrimination and yield in durum wheat under Mediterranean conditions. *Crop sci*. **200**3, *43*, 170-180.

46. Mielniczuk, E.; & Skwaryło-Bednarz, B. Fusarium head blight, mycotoxins and strategies for their reduction. *Agron*. **2020**, *10*, 509.

47. Suffert, F.; Sache, I.; & Lannou, C. Early stages of septoria tritici blotch epidemics of winter wheat: build-up, over seasoning, and release of primary inoculum. *Plant Pathol*. **2011**. *60*, 166-177.

48. El Jarroudi, M.; Kouadio, L.; El Jarroudi, M.; Junk, J.; Bock, C.; Diouf, A. A.; & Delfosse, P. Improving fungal disease forecasts in winter wheat: A critical role of intra-day variations of meteorological conditions in the development of Septoria leaf blotch. *Field Crops Res.* **2017**, *213*, 12-20.

49. Dammer, K. H.; Garz, A.; Hobart, M.; & Schirrmann, M. Combined UAV and tractor-based stripe rust monitoring in winter wheat under field conditions. *Agron J*. **2022**, 114651-661.

50. Sabburg, R.; Obanor, F.; Aitken, E.; & Chakraborty, S. Changing fitness of a necrotrophic plant pathogen under increasing temperature. *Glob Chang Biol*. **2015**, *21*, 3126-3137.

51. Doohan, F. M.; Brennan, J.; & Cooke, B. M. Influence of climatic factors on Fusarium species pathogenic to cereals. Epidemiology of Mycotoxin Producing Fungi: Under the aegis of COST Action 835 'Agriculturally Important Toxigenic Fungi 1998–2003', EU project (QLK 1-CT-1998–01380)**;** Springer: Berlin/Heidelberg, Germany, **2003**; pp; 755–768.

52. Bhandari, M.; Ibrahim, A. M.; Xue, Q.; Jung, J.; Chang, A.; Rudd, J. C.; ... & Landivar, J. (2020). Assessing winter wheat foliage disease severity using aerial imagery acquired from small Unmanned Aerial Vehicle (UAV). *Comput Electron Agric*. **2020**, *176*, 105665.

53. Siou D.; Gélisse S.; Laval V.; Repinçay C.; Canalès R.; Suffert F.; Lannou C. Effect of wheat spike infection timing on Fusarium head blight development and mycotoxin accumulation. *Plant. Pathol*. **2014**, *63*,390–399.

54. Zhang, D.; Wang, Q.; Lin, F.; Yin, X.; Gu, C.; & Qiao, H. Development and evaluation of a new spectral disease index to detect wheat fusarium head blight using hyperspectral imaging. *Sensors*. **2020**, *20*, 2260.

55. Moazzam, S. I.; Khan, U. S.; Nawaz, T.; & Qureshi, W. S. Crop and Weeds Classification in Aerial Imagery of Sesame Crop Fields Using a Patch-Based Deep Learning Model-Ensembling Method. In 2022: 2nd International Conference on Digital Futures and Transformative Technologies (ICoDT2). Rawalpindi, Pakistan, 24–26 May 2022; pp. 1–7

56. McMullen M.; Bergstrom G.; De Wolf E.; Dill-Macky R.; Hershman D.; Shaner G.; Van Sanford D. Fusarium head blight disease cycle, symptoms, and impact on grain yield and quality frequency and magnitude of epidemics since 1997. *Plant. Dis*. **2012**, *96*,1712–1728.

57. Mateen, A.; & Zhu, Q. Weed detection in wheat crop using UAV for precision agriculture. *Pak. J. Agric. Sci*. **2019**, *56*, 809-817.

58. Francesconi, S.; Harfouche, A.; Maesano, M.; & Balestra, G. M. UAV-based thermal, RGB imaging and gene expression analysis allowed detection of Fusarium head blight and gave new insights into the physiological responses to the disease in durum wheat. *Front. Plant Sci*. **2021**, *12*, 628575.

59. Li, J.; Veeranampalayam-Sivakumar, A. N.; Bhatta, M.; Garst, N. D.; Stoll, H.; Stephen Baenziger, P.; ... & Shi, Y. Principal variable selection to explain grain yield variation in winter wheat from features extracted from UAV imagery. *Plant Methods*. **2019**, *15*, 1-13.

60. Bajwa, A. A.; Walsh, M.; & Chauhan, B. S. Weed management using crop competition in Australia. *Crop Prot*. **2017**, *95*, 8-13.

61. Champeil, A.; Doré, T.; & Fourbet, J. F. Fusarium head blight: epidemiological origin of the effects of cultural practices on head blight attacks and the production of mycotoxins by Fusarium in wheat grains. *Plant sci*. **2004**, *166*, 1389-1415.

62. Yuen, G. Y.; & Schoneweis, S. D. Strategies for managing Fusarium head blight and deoxynivalenol accumulation in wheat. *Int. J. Food Microbiol*. **2007**, *119*, 126-130.

63. Lucas, J. A. Advances in plant disease and pest management. *J. Agric. Sci*. **2011**, *149*, 91-114.

64. Jarroudi, M. E.; Kouadio, L.; Beyer, M.; Junk, J.; Hoffmann, L.; Tychon, B.; ... & Delfosse, P. Economics of a decision support system for managing the main fungal diseases of winter wheat in the Grand-Duchy of Luxembourg. *Field Crops Res*. **2015**, *172*, 32-41.

Supplementary Materials:

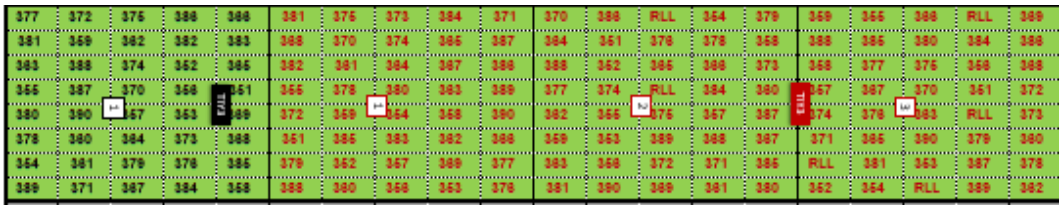

a) Tordomar

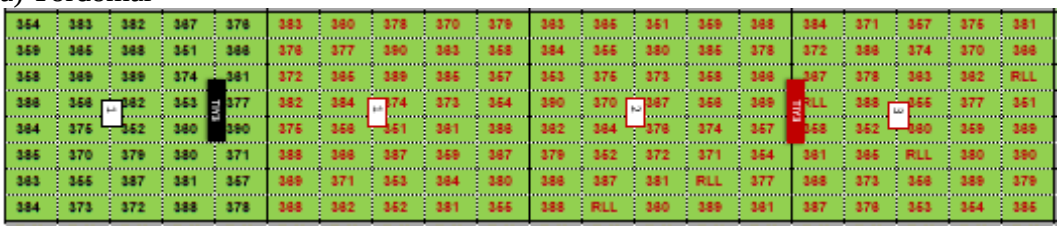

b) Briviesca

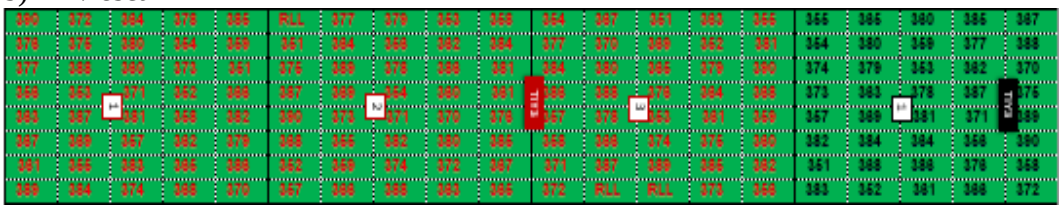

c) Elorz

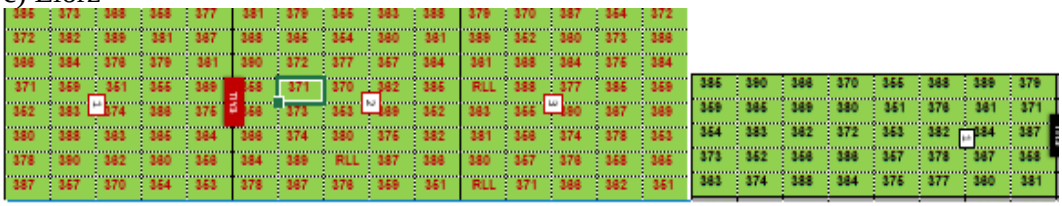

d) Sos del Rey Católico

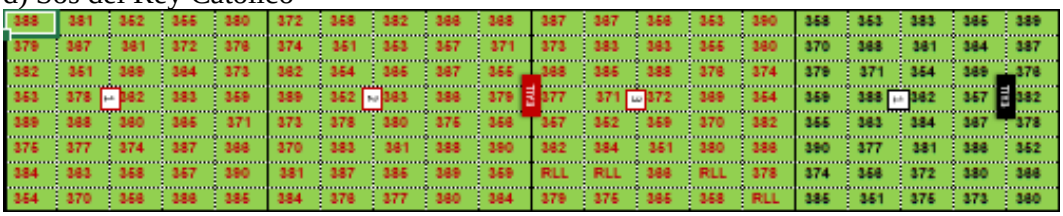

e) Ejea de los Caballeros

Supplemental Figure 1. Trial design of generation F8 around the different experimental sites: a) Tordómar b) Briviesca, c) Elorz, d) Sos del Rey Catolico, e) Ejea de los Caballeros.

Supplemental Table S1. Climate conditions in the different experimental locations: Tordómar, Briviesca, Elorz, Sos del Rey Catolico, Ejea de los Caballeros.

Site	Tordómar	Briviesca	Elorz	Sos Del Rey Católico	Ejea De Los Caballeros
Precipitation (mm)	437	768	714	532	350
Lowest precipitation (mm)	2	6	7	2	1
Maximum temperature (°C)	14-35	17-39	17-42	15-40	19-44
Minimum temperature (°C)	6-29	8-26	8-30	7-30	9-36
Mean of temperature	2-20	5-19	5-22	4-22	4-28

Supplemental Table S2. Determination coefficient (R^2), level of significance (p-value), and linear equation of the relationship between the ratio of treated versus untreated ground acquired NDVI (R NDVI ground=treated/untreated NDVI index values from the GreenSeeker) against the Ratio of Grain Yield of treated versus untreated plants (RGY=GY treated/GY untreated).

SITE	DATE	R^2	P-VALUE	LINEAR EQUATION
Tordómar	9 March	0.450	0.000	y = 0.626x + 0.4119
Tordómar	20 April	0.220	0.002	y = 0.8436x + 0.2256
Tordómar	12 May	0.200	0.004	y = 1.6824x - 0.5938
Tordómar	10 June	0.090	0.067	y = 0.0781x + 0.9323
Briviesca	10 March	0.100	0.037	y = 0.3171x + 0.7092
Briviesca	21 April	0.110	0.040	y = 0.3264x + 0.6965
Briviesca	12 May	0.030	0.128	y = -0.3038x + 1.3342
Briviesca	8 June	0.020	0.433	y = 0.1459x + 0.8728
Elorz	11 March	0.650	0.000	y = 0.5238x + 0.5347
Elorz	22 April	0.700	0.000	y = 0.9436x + 0.1802
Elorz	13 May	0.600	0.000	y = 1.5605x - 0.4087
Elorz	27 May	0.220	0.002	y = 0.8281x + 0.2572
Elorz	8 June	0.180	0.006	y = 0.6113x + 0.4084
Sos	11 March	0.030	0.570	y = -0.003x + 1.2792
Sos	22 April	0.330	0.000	y = 1.1121x + 0.1337
Sos	13 May	0.040	0.198	y = 0.0543x + 0.9301
Sos	27 May	0.270	0.001	y = 0.6598x + 0.4403
Sos	7 June	0.220	0.002	y = 0.2529x + 0.982
Ejea	12 March	0.400	0.000	y = 0.7983x + 0.1632
Ejea	14 May	0.440	0.000	y = 1.2081x - 0.2738
Ejea	28 May	0.270	0.005	y = 0.9474x - 0.0323
Ejea	7 June	0.190	0.001	y = 0.5839x + 0.4174

Supplemental Table S3. Determination coefficient (R^2), level of significance (p-value), and linear equation of the relationship between the ration of aerial acquired NDVI treated versus untreated plots (R NDVI aerial=treated/untreated NDVI index values from aerial AgroCam NDVI images) against the ratio of the grain yield of treated versus untreated plots (RGY=GY treated/GY un-treated).

SITE	DATE	R^2	P-VALUE	LINEAR EQUATION
Tordómar	9 March	0.002	0.657	Y = -0.189x+1.214
Tordómar	20 April	0.008	0.616	Y = -0.0004x+1.091
Tordómar	12 May	0.231	0.000	Y = 2.3519x-1.245
Tordómar	10 June	0.016	0.010	Y = 0.6236x+0.434
Briviesca	10 March	0.011	0.521	Y = -0.2189x+1.264
Briviesca	21 April	0.0.4	0.0.321	Y = -0.3433x+1.416
Briviesca	12 May	0.020	0.882	Y = -0.2873x+1.356
Briviesca	8 June	0.030	0.232	Y = 0.3815x+0.642
Elorz	11 March	0.042	0.15	Y = 02158x+0.825
Elorz	22 April	0.026	0.32	Y = -0.0004x+1.096
Elorz	13 May	0.017	0.433	Y = -0.5578x+1.662
Elorz	27 May	0.007	0.93	Y = 0.361x+0.792
Elorz	8 June	0.012	0.804	Y = 0.3086x+0.757
Sos	11 March	0.016	0.477	Y = 0.4771x+0.722
Sos	22 April	0.0008	0.624	Y = -0.96x+1.297
Sos	13 May	0.001	0.361	Y = 0.075x+1.134
Sos	27 May	0.054	0.020	Y = 0.5429x+0.594
Sos	7 June	0.043	0.014	Y =-0.6938x+1.882
Ejea	12 March	0.087	0.059	Y = 1.4418x-0.338
Ejea	14 May	0.072	0.725	Y = 0.3043x+0.731
Ejea	28 May	0.012	0.904	Y = 3355x+0.696
Ejea	7 June	0.001	0.260	Y =0.1339x+0.901

Supplemental Table S4. Determination coefficient (R^2), level of significance (p-value), and linear equation of the relationship between the ratio of ground level NGRDI treated versus untreated (R NGRDI ground=treated/untreated NGRDI index values from ground R GB images) against the ratio of grain yield of treated versus untreated plots (RGY=GY treated/GY untreated).

SITE	DATE	R^2	P-VALUE	LINEAR EQUATION
Tordómar	9 March	0.647	0.003	Y = 0.0015x + 1.082
Tordómar	20 April	0.007	0.229	Y = 0.2294x + 0.807
Tordómar	12 May	0.679	0.008	Y = -0.1428x + 1.235
Tordómar	10 June	0.505	0.004	Y = 0.0028x + 1.077
Briviesca	21 April	0.029	0.158	Y = 0.1261x + 0.903
Briviesca	12 May	0.991	0.001	Y= -0.0311x + 1.065
Briviesca	8 June	0.934	0.034	Y= 0.0405x + 0.975
Elorz	11 March	0.956	0.006	Y = 0.0003x + 1.096
Elorz	22 April	0.000	0.720	Y = 0.2666x + 0.823
Elorz	13 May	0.288	0.404	Y = 0.5171x + 0.634
Elorz	27 May	0.706	0.198	Y = 0.2259x + 0.847
Elorz	8 June	0.584	0.004	Y = 0.0035x + 1.093
Sos	11 March	0.652	0.0003	Y = 0.0051x + 1.212
Sos	22 April	0.000	0.428	Y = 0.2788x + 0.911
Sos	13 May	0.527	0.006	Y = 0.0238x + 1.182
Sos	27 May	0.063	0.110	Y = 0.0054x + 1.189
Sos	7 June	0.078	0.065	Y = -0.0273x + 1.238
Ejea	12 March	0.024	0.087	Y = 1.4418x - 0.338
Ejea	14 May	0.000	0.588	Y = 0.0178x + 0.977
Ejea	28 May	0.455	0.005	Y = 0.0003x + 1.028
Ejea	7 June	0.692	0.044	Y = 0.2153x + 0.954

Supplemental Table S5. Determination coefficient (R^2), level of significance (p-value), and linear equation of the relationship between the aerial level Ratio of NGRDI treated versus untreated plots (R NGRDI aerial=treated/untreated NGRDI index values from UAV RGB images) against the grain yield of the ration of treated versus untreated plots (RGY=GY treated/GY untreated).

SITE	DATE	R^2	P-VALUE	LINEAR EQUATION
Tordómar	9 March	0.000	0.657	Y = -3.06x + 1.089
Tordómar	20 April	0.016	0.617	Y = -0.0636x + 1.157
Tordómar	12 May	0.0009	0.720	Y=0.0017x + 1.087
Tordómar	10 June	0.0009	0.101	Y=-0.0005x+1.090
Briviesca	10 March	0.522	0.012	Y = 0.0173x + 1.015
Briviesca	21 April	0.322	0.010	Y=0.0143x + 1.015
Briviesca	12 May	0.883	0.002	Y=0.0054x + 1.025
Briviesca	8 June	0.2325	0.006	Y=-0.0643x+1.096
Elorz	11 March	0.154	0.003	Y=-0.0465x+1.157
Elorz	22 April	0.329	0.034	Y=0.0176x + 1.076
Elorz	13 May	0.433	0.007	Y=0.0009x + 1.101
Elorz	27 May	0.940	0.040	Y=0.1208x + 0.935
Elorz	8 June	0.805	0.005	Y=0.0508x + 1.039
Sos	11 March	0.478	0.016	Y=-0.0614x+1.281
Sos	22 April	0.624	0.090	Y=-0.0025x+1.233
Sos	13 May	0.3612	0.0141	Y= 0.072x + 1.149
Sos	27 May	0.021	0.504	Y=-0.0139x+1.242
Sos	7 June	0.014	0.057	Y=0.0133x + 1.186
Ejea	12 March	0.094	0.078	Y=0.2586x + 0.704
Ejea	21 April	0.748	0.134	Y= 0.5978x +0.398
Ejea	14 May	0.899	0.030	Y = 0.1268x+0.852
Ejea	28 May	0.273	0.044	Y= 0.0149x+0.995
Ejea	7 June	0.893	0.003	Y=0.0065x + 1.024

General Discussion

General Discussions

The goal of using different sensors at different scales of observation in this thesis was to improve the study of biotic stress on crops for optimizing resource utilization at two different scales: from smart farm management to improving the efficiency of new variety development in high throughput field phenotyping (Araus and Kefauver., 2018). In this study, the focus was on supporting more intelligent approaches to sustainable crop management strategies for crop protection against harmful soil organisms by using nematode-resistant root grafting techniques (Sorribas et al., 2005) and developing affordable phenotypical approaches for breeding new bread wheat varieties that are more resistant to fungal infection (Vergara-Diaz et al., 2015).

Grafting is a horticultural technique consisting of growing the tip (scion) of one plant on top of the base (rootstock) of another. Grafting can be used for plants of the same species, different species or across separate component species to protect horticultural crops from diseases and organisms in the continuously cultivated diseased soil. In our first study, we highlighted the efficiency of this technique in the improvement of vegetable crop production. As an example, in 2017, grafted melons on *Cucumis metuliferus* produced 3.1 kg/plant, compared to 0.3 kg/plant for non-grafted melons ($p<0.001$). Using resistant rootstocks can lower yield losses and ensure excellent adaptation to soil characteristics. The grafted melon onto the squash hybrid 'Tetsukabuto' increases the yield (Ayala-Doñas et al., 2020). In addition, other research reports that resistant tomato cultivars 'Celebrity', roots were grafted with scions of the susceptible cultivars 'Tropimech' effectively for the management of root-knot nematodes on susceptible tomato cultivars (Owusu et al., 2016). The two studies contrast not only in the cultivation systems assessed, horticultural under greenhouse in the first and extensive under a material scheme in the second but also in the number of species (four in the first study against one in the second) and varieties (one of each species in first and more than hundred in the second) Concerning the second study, the biotic stress highlighted in our second study is caused by the (Septoria, Brown rust, and Stripe rust) which affects wheat performance, so one of the main important goals is the selection of a variety of resistance to this disease from the accessions of bread wheat which is feasible, using different tools of phenotyping. As an example, the highest Coefficient of determination between the genotype performance at NDVI index and grain yield is the example of Elorz 22 April ($R^2=0.70$, $p<0.001$). This means that variations in NDVI index were explaining most of the genotype variability in grain yield, and therefore this vegetation

index was able to predict the final production of wheat. We note the usefulness of phenotyping in the breeding program as a tool to select the best resistant varieties to the fungal attack which is emphasized in our research. The importance of the breeding program in the creation of a resistant variety to fungal attack as the leaf and stem rust in wheat was available using a new approach known as "genomic selection," which is based on extensive conventional selection and the use of molecular marker information, will aid breeding programs by offering effective biotic stress resistance, decreasing the meantime generation interval (Reynolds et al., 2009). Our phenotypic approach based on high throughput phenotyping is amenable to fully contribute to the success of genomic selection.

The results of both chapters may provide lasting benefits that require fewer chemical pesticides or fungicide applications, which are often more harmful to the environment (Mahlein et al., 2016). Some of the sensors and imaging tools used in this thesis were able to detect plant stress differences before visible symptoms appeared or can be used for the selection of top-performing varieties before harvest. When preventative measures do not work, early detection of biotic stress to crops is the key to effective treatment (Prabhaka et al., 2011). These sensor-based, proximal, and remote sensing approaches may represent improvements in efficiency and provide profit margin benefits for farmers and crop breeders towards more resilient and sustainable agricultural practices (Araus et al., 2018, Araus et al., 2022). For example, the differentiation of stable carbon isotopes may provide integral assessments of crop water status over a whole growing season, but the quantification of leaf-level pigment contents including chlorophylls, anthocyanins, and flavanols may be monitored using fast and effective scientific sensors (Cerovic et al., 2005; Goulas et al., 2004; Trembley et al., 2009) which may be relevant when assessing tolerance to pests and diseases at the single leaf level.

Destructive sampling for stable isotope analyses

Stable carbon and nitrogen isotopes, expressed in composition notation ($\delta^{13}C$, ‰ and $\delta^{15}N$, ‰), are considered highly informative though destructive traits that can be used for the detection of plant water stress, water use efficiency and to inform about nitrogen sources (Lopes and Araus, 2006). The causes of the changes in the composition of these isotopes are not just abiotic, but extend beyond environmental factors to biotic impacts, for example on root health. As others have reported in potatoes (Haverkort and Valkenburg, 1992) the effect of nematode infection caused an increase in the $\delta^{13}C$, indicating poorer water conditions as a consequence of the nematodes affecting the functioning of the roots,

therefore, slowing down the uptake of water and nutrients. However, our study consistently recorded higher $\delta^{13}C$ in the leaves of plants grafted with the resistant rootstock, indicating that besides any potential effect of nematodes on root health, grafting may also affect negatively water status. For instance, the $\delta^{13}C$ of grafted pepper ($\bar{x}$=-27.05‰) leaves was significantly higher ($p<0.01$) than that of ungrafted plant leaves ($\bar{x}$=-29.08‰) (Hamdane et al., 2022).

For the second study, the $\delta^{13}C$ and $\delta^{15}N$ stable isotope analysis was limited to two sites, Elorz and Ejea de los Caballeros. We recorded higher $\delta^{15}N$ in Elorz ($\bar{x}$=2.7‰) in comparison to Ejea de los Caballeros ($\bar{x}$=1.8‰, $p<0.001$). Since the nitrogen fertilization was similar at both sites, results suggest increased assimilation of nitrogen coming from nitrification of organic matter at Elorz, in agreement with a more fertile conditions at this site, compared with Ejea. We registered a higher ($p<0.001$) $\delta^{13}C$ ($\bar{x}$=-26.00‰) in Elorz than in Ejea ($\bar{x}$=-27.06‰), which at first would be surprising since Ejea is considered far drier (warmer and with less precipitation) site than Elorz. However, the results are coherent in the sense wheat at Ejea was submitted to support irrigation during the last part of its growing cycle, totaling 150 mm, while cultivation in Elorz is purely rainfed. Moreover, Ejea experienced during May 2021 strong rainfalls, much more than in Elorz. This result illustrates the ability of carbon stable isotopes to detect the water conditions experienced by the crop, due either to management (e.g., supplemental irrigation) or natural (precipitation) affecting the production of durum wheat (Araus et al., 2003). Other studies have mentioned the efficiency of stable isotope analysis in testing accessions of winter wheat under different water management conditions (Rezzouk et al., 2020), while our study tested a set of accessions of bread wheat in different sites and proved a difference in water conditions, at least in the two sites where stable isotopes were analyzed.

These findings demonstrate that despite their limits as time-consuming, destructive, and relatively costly approach, stable isotope analyses are powerful traits informing on crop performance that can inform about the growing conditions of the plant, including the impact of stresses which affect the water or the nitrogen status of the plants. Furthermore, we have demonstrated that $\delta^{13}C$ and $\delta^{15}N$ analyses are useful tools for both biotic stress assessments in greenhouse environments as well as for field phenotyping, especially when used in combination with other complimentary techniques, such as leaf sensors or remote sensing evaluations at plot level (Elazab et al., 2015).

Leaf level sensors for monitoring chlorophyll and other stress related pigments

Leaf-level sensors have evolved beyond chlorophyll in SPAD to new sensors, such as the Dualex Scientific that can assess leaf-level pigment contents including chlorophylls, but also anthocyanins, and flavonoids (Cerovic et al., 2005; Goulas et al., 2004; Trembley et al., 2009). In both studies of this thesis, we noted that the flavonoids measured by the Dualex were highly informative for the detection of early biotic stress symptoms. For the first study, stress flavonoids were lower in the grafted crops than in the non-grafted plots, including the case of melon in 2017 ($p<0.05$) and pepper in 2019 ($p<0.05$). The increase in flavonoids is generally a sign of a stressful environment as this pigment is a plant response to stress to slow down plant function as a means of adapting to stress and plant defense responses against microorganism attacks (Chin et al., 2018). The role of the flavonoid as stress signaling has also been considered indicative of a reduction in vital processes (Goverse et al., 2014). More severe damage to the roots can affect nitrogen uptake capacity and the reduction of plant pigments, such as chlorophyll, resulting in a reduction in photosynthesis, carbon assimilation, and crop yield, as was also observed across the five years of data analyzed in the first study.

The difference between the wheat that received the fungicide treatment (Prosaro) and the untreated one is highlighted by differences in the pigment content measured by the Dualex device. One of the pigments is the flavonoid which is considered the major indicator of plant biotic stress. The highest value of flavonoid is registered in untreated wheat. As in Elorz, the value of treated was ($\bar{x}=1.510$), while the untreated part was ($\bar{x}=1.592$, $p< 0.01$) which means a more stressful situation for untreated wheat caused by the (Septoria, Brown rust and Stripe rust) disease. The efficiency of the flavonoid suggested as a target for selection in stress-adaptive crop breeding as the case of our study in wheat, for the selection of the variety of bread wheat less affected by fungal infection. However other fungal diseases affect in a different sense the content of flavonoids. Thus, it has been reported that flavonoid content was inversely related to stripe rust (*Puccinia striiformis f. sp. tritici*) response in wheat (Emebiri et al., 2019).

The NBI from the Dualex sensor is an indicator of the balance of leaf N with other essential macro-nutrients, and thus its ability to positively contribute to plant processes, specifically photosynthesis (Silva Sanchez et al., 2019). In the second study, in Eloz the NBI value of treated wheat ($\bar{x}=35.69$). was higher than for the untreated ($\bar{x}=34.56$, $p<0.01$). This can

prove the efficiency of NBI measured by Dualex in the determination of the plant nitrogen status and can be an indirect way to inform about the wheat fungal infection and the severity of the infection. where the assimilation of the nitrogen by the root can be affected by the disease. Some authors registered a good functioning of the Dualex in the detection of the plant nitrogen status in the winter wheat (Tremblay et al., 2009). In fact, the initial purpose of the handheld chlorophyll leaf meters was to assess nitrogen status (Jiang et al., 2021). However, and differently to other studies focused on nitrogen status or even drought stress effect, we tracked fungal infection in wheat through a portable leaf pigment meter.

These results indicate the ability of leaf sensors such as SPAD or Dualex in the detection of biotic stress in the first study presented by the nematode attack and in the second part by the fungal disease, also this instrument can detect, earlier than other instruments, the impact of biotic stress in the plant through the measurement of the plant pigment indicating. Our studies were conducted in a greenhouse (first study) and in field conditions (second study) which means that the leaf sensors can work in different conditions. However, a limitation of this methodological approach is that the pigment content of the leaf may be also affected by other factors (e.g., abiotic stresses) which may the quality of the measurement as an indicator of plants' susceptibility or tolerance to abiotic stresses.

Canopy NDVI and RGB images for whole plant status assessments

Canopy measurements taken by the GreenSeeker (NDVI) or RGB cameras were assessed in the two studies. First, the GreenSeeker detected a highly significant difference ($p<0.001$) between the two treatments (grafted and non-grafted) in tomatoes in 2020 and in peppers in 2019 in the first chapter. In the second chapter, NDVI taken at ground level was well correlated with grain yield as in the case of Elorz from the 22nd of April 2023 ($R^2=0.70$, $p<0.001$). Some other studies, such as Solano-Alvarez et al. (2022) proved the usefulness of the NDVI measured by the GreenSeeker as a good indicator of plant health in tomato plants (*Solanum lycopersicum*) treated with the beneficial bacteria *Bacillus cereus-Amazcala*. Another study conducted by Vergara-Diaz et al. (2015), which tested the ability of the NDVI measured with a Greenseeker, and RGB vegetation indices in the estimation of durum wheat yield losses affected by yellow rust, found a low correlation between NDVI and the grain yield, contrary to our study applied to bread wheat, where we found a strong relation between NDVI measured by GreenSeeker and grain yield was the highest value was recorded in Elorz 22 April ($R^2=0.7$, $p<0.001$). Compared to the study by Vergara-Diaz et al., (2015) our second study of bread wheat additionally assessed the AgroCam GEO NDVI integrated on a UAV to extract the NDVI index assessed from an aerial platform.

While the result collected from this camera presented a low correlation with grain yield (where the highest value was registered in Tordómar; R^2=0.231, p<0.001), the testing of that sensor and technique can be considered novel in comparison to the previous study. The reason for the poorer performance of the NDVI assessed from the ear may be the comparative low resolution of the aerial multispectral images, while taking NDVI at ground level with the GreenSeeker, implies walking through each plot and taking a value averaged from 10-15 instantaneous measurements.

In the same context, the vegetation indexes extracted from RGB cameras as GA, TGI, and CSI proved again a good ability to separate crop treatments and crop site qualities related to biotic stress (Vergara-Diaz et al., 2015, 2016; Zaman-Allah et al., 2015). In these cases, the high resolution of RGB images may them amenable to the purpose of evaluating biotic stresses, even if images are captured from aerial platforms. For example, in our greenhouse study about nematodes, the TGI index in grafted melons was higher compared to the TGI of non-grafted melons (p<0.001). In addition, in the second chapter, we note that the GA index in treated wheat was also greater than the untreated trials in the five sites, especially in the months of May and June (p<0.001). This proves the efficiency of the RGB vegetation indexes in the detection of biotic stress and the separation between the treatment. The highest correlation between the RGB indexes and grain yield in our study was between NGRDI at ground level and grain yield in Elorz 11 March (R^2=0.956, p<0.01). This result is well aligned with a previous work using RGB derived indices o predict durum wheat losses by yellow rust (Vergara -Diaz et al., 2015).

UAV remote sensing platforms for high throughput canopy imaging in field trials

Concerning the second chapter, we found a tight correlation between RGB indices taken at ground and aerial levels mostly in two indexes TGI and NGRDI (r=0.817 and r=0.810). The same conclusion is supported by another study (Gracia-Romero et al., 2019) which found that the vegetation indexes at both ground and aerial measurements performed similarly in assessing yield in the phenotyping program of durum wheat under different regimes of water irrigation. The difference from other studies, especially in our second study is that the experiment was derived in 5 different locations. So, our study covers a large area characterized by a large difference in the climate conditions, also can test the ability and the throughput of the vegetation indices as phenotypic tools detecting biotic stress caused by the fungal (Septoria, brown rust and stripe rust) disease.

It is seen from our studies that fungicide (Prosaro) treatment is crucial for the protection of crop production and performance. As an example, the value of CSI early in March (end of tillering beginning of stem elongation), respectively in Tordomar and Elorz was higher in untreated than treated wheat ($p<0.001$). This means the process of senescence caused by fungal disease is more advanced in untreated than treated plants. This finding was supported by the research conducted by Xi et al. (2015) which concluded for wheat cultivation in Canada showed that the use of fungicides boosted yield by 15 to 23%.

Nevertheless, selecting a new variety of wheat resistant to fungal disease should be still accompanied to some extent by a fungicide (Prosaro) treatment in order to ensure a better final product (Casadesus et al., 2008). In this context, we noted that a higher correlation was registered between the ratio (treated/untreated) NGRDI and ratio(treated/untreated) grain yield Elorz 11 March ($R^2=0.956$, $p<0.01$). Where the final grain yield is determined in a large part by the genotype. This result was supported by the study of Gracia-Romero et al. (2019) who found that the vegetation indices extracted from RGB images are able to select the better genotype in the durum wheat under the different regimes of irrigation and date of planting. However, our research differs in the way that it has been conducted in 5 different sites with a panel of 40 accessions, characterized by different climate conditions which not only proves the phenotypic plasticity of bread wheat accessions in from fundal diseases but also the high throughput of the remote sensing techniques assessed, which gives a large range of choice to crop breeders.

Conclusions

Conclusions

Chapter 1

1. Stable isotope composition analyses, such as that of $\delta^{13}C$ and $\delta^{15}N$, particularly when assessed in the soluble fraction, are potent tools for assessing integral water and nutritional conditions in crops and the effect of root conditions. Even if this measurement is relatively costly, time-consuming, and destructive, it nevertheless provides a reliable and powerful method for assessing crop conditions over an entire growing season or at various crop growth phases.

2. The porometer sensor may be a useful device in explaining how biotic stress affects plant water status, no matter measurements can also be affected by diurnal temperature fluctuations and other environmental factors. A significantly decreased value of stomatal conductance was recorded in the tomato in 2020 where the grafted tomato registered better stomatal conductance than the nongrafted ones ($p< 0.05$). However, the porometer is still insufficient to explain the crop's status during each stage, and in some years the measurements did not capture any significant differences, possibly due to the time of day or environmental seasonality of the measurement.

3. The attack of the nematode *Meloidogyne incognita* can cause crop biotic stress, which can be detectable by leaf pigment sensors such as the SPAD and Dualex. The SPAD-detected chlorophyll content revealed the negative effect of nematodes on the photosynthetic capacity of horticultural crops. This was the case for the tomato in 2020. However, crop stress was more frequently detected in non-grafted plants due to increased levels of pigments as flavonoids (measured by the more advanced Dualex) compared with the grafted, with differences being significant ($p<0.05$) in melons in 2017 and in peppers in 2019. While, the Dualex is considered better for the assessment of the plant state, especially in the detection of plant stress due to the fast variation of the plant pigment in reaction to the nematode stress especially the flavonoid as a major indicator of plant stress.

4. Crop canopy sensors, including Greenseeker NDVI, infrared thermal guns, and RGB cameras, are non-destructive technologies that offer precise analyses of the state of the plant at the moment of measurement. These tools provide an assessment of the plant status at the canopy level at a certain time, though they do not explain how the plant reacts during the many stages (over time). For example, a Triangular Greenness Index (TGI), a vegetation

index extracted from RGB images, was able to distinguish ($p<0.001$) between grafted and non-grafted melons in 2016 and 2017.

5. Multiple tools can be used to identify the biotic stress brought on by *Meloidogyne incognita*. For example, GreenSeeker NDVI or RGB VIs provide useful information, but it may be difficult for a layperson to use and require some training. Dualex and SPAD, on the other hand, can capture the immediate internal stress signs in the plant, but are more expensive than RGB cameras or GreenSeeker, together with limiting the measurement at the leaf level. On the other hand, destructive analyses, such as the study of isotope composition, can be a tool to give enough information about the plant over the entire season and therefore integrates through time growing conditions.

6. Finally, grafting onto resistant-tolerant rootstocks is a viable non-chemical way to manage populations of the RKN (Root-knot nematode) like the *Melodoigyne incongnita* and reduce yield losses. Our final yield data demonstrated how crucial the grafting procedure can be for safeguarding horticultural crops. As for example, we saw that in 2017 grafted melons on *Cucumis metuliferus* produced 3.1 kg/plant, compared to 0.3 kg/plant for non-grafted melons ($p< 0.001$).

Chapter 2

7. Where the analysis of stable isotopes $\delta^{13}C$ and $\delta^{15}N$ was limited to just two sites Elorz and Ejea de los Caballeros, the results showed a better water state in Ejea de los Caballeros than in Elorz ($p< 0.001$)), which was explained by the heavy rainfall in April which together with the support irrigation in May in Ejea, compared with the rainfed conditions of the Elorz. Meanwhile, Elorz was characterized by better nitrogen status as shown by a higher ($p<0.001$) $\delta^{15}N$ than Ejea, which was explained by the better soil, richer in organic matter or the former.

8. In terms of distinguishing between the wheat plants treated versus the non-treated with the fungicide (Prosaro), the Dualex leaf sensor utilized in the five fields produced significant results already at mid-season. For example, in Elorz, flavonoid content was significantly lower ($p<0.01$) in treated ($\bar{x}=1.510$) compared with untreated ($\bar{x}=1.592$) plants. This suggests that the Dualex sensors worked well to monitor this early (i.e. Not visible by the human eye) stress as a response to don’t apply fungicide.

9. At the canopy level, the NDVI results extracted from the GreenSeeker, and the vegetation indices extracted from RGB images were both able to differentiate between the treatments. For the Green Area (GA) index, we found that in the five sites during the five visits, the treated wheat exceeded their untreated counterparts.; which indicates a greater photosynthetic capacity across all sites for the treated wheat.

10. The aerial measurement carried out with the UAV's built-in RGB camera registered data that were comparable to those of the RGB camera's ground-level and aerial measurements of the ground. The Triangular Greenness Index (TGI) and Normalized Green Red Difference Index (NGRDI), respectively, were the two indices with the strongest correlations ($r=0.810$, $r=0.817$, respectively) between aerial and ground measurements.

11. AgroCam GEO was used to extract the NDVI from the aerial level UAV flights, but it had lower performance in terms of predicting yield or separating between treated and untreated plants than the ground-assessed NDVI (GreenSeeker. The measuring distance resulted in lower resolution of the aerial measurements but there were also some differences between the wavelengths used in the two NDVI sensors (the AgroCam measures NDVI using NIR and Blue compared to NIR and Red for the Greenseeker), while the Greenseeker has an active NDVI sensor with less sensitivity to environmental conditions (besides light conditions, wind also affects the UAV images). For example, the ground NDVI compared to grain yield at Elorz on April 22 was ($R^2=0.700$, $p<0.001$), whereas the aerial the highest Coefficient of determination between the NDVI at the aerial level and the grain yield was in Tordómar 12 May ($R^2=0.231$, ($p<0.001$)).

12. RGB images were also employed to identify the biotic stress brought on by the fungal attack on the wheat crop. We noticed that the value for the Crop Senescence Index (CSI) was greater ($p<0.001$) in untreated compared with treated wheat in Elorz (on 10 March) Elorz and in Tordómar (20 April). This indicates that the impact of the fungal attack on untreated wheat has accelerated the senescence process.

13. The importance of fungicide (Prosaro) treatment in the protection of wheat crops against fungal disease (Septoria, Brown rust and Stripe rust)) was also highlighted by the higher chlorophyll concentration registered in the Ejea de los Caballeros in the treated wheat ($\bar{x}=48.0$) than their untreated ($\bar{x}=45.8$) counterpart ($p<0.001$). Also, The NBI value in treated wheat ($\bar{x}=35.69$) in Elorz was higher ($p<0.01$) than that of untreated plots ($\bar{x}=34.56$). This means the fungicide to some extent protected the photosynthetic apparatus and its

functional duration.

14. The choice of the genotype that performed the best in tolerance to the fungal disease the accessions were made possible early in the crop cycle through the high correlation between the grain yield and some vegetation indices as NGRDI (e.g., R^2=0.956 for Elorz on March 11, 2021), with the best performing genotypes exhibiting larger values.

Summary of the thesis in Spanish

Summary of the thesis in Spanish

El principal objetivo detrás de la investigación de cultivos es garantizar la seguridad alimentaria. El cambio climático, que afecta a la mayoría de los cultivos y aumenta el riesgo de enfermedades y hambrunas, se aborda en esta tesis doctoral. La Organización de las Naciones Unidas para la Agricultura y la Alimentación (FAO) y las Naciones Unidas (ONU) comparten el objetivo de brindar seguridad alimentaria a todas las personas en la Tierra y acabar con el hambre a nivel mundial. Usando estrategias como reducir las pérdidas de cultivos, mantener una producción sostenible y aumentar el área de cultivo, se puede lograr este objetivo. La producción de alimentos se ve significativamente afectada por el cambio climático, que es el responsable directo de numerosos estreses tanto abióticos como bióticos. Dentro de la primera categoría caben destacar las elevadas temperaturas, la sequía y salinización del suelo. Las plagas, las enfermedades y otros factores estresantes bióticos son ejemplos del segundo tipo de estrés. Se pueden utilizar herramientas específicas para identificar las diversas formas de estrés y brindar orientación para su tratamiento. La teledetección aparece en este escenario como una tecnología no destructiva capaz de reconocer y señalar cultivos propensos a padecer estreses.

La primera investigación que aborda esta tesis es el caso de cuatro cultivos hortícolas cultivados en suelo infestado con el nemátodo *Meloidogyne incognita* durante un período de cinco años entre 2016 y 2020. Se utilizaron dos tratamientos: plantas injertadas sobre porta injertos resistentes y plantas no injertadas. El segundo estudio involucró la evaluación de 40 accesiones (líneas avanzadas F8) de trigo harinero para detectar el impacto de enfermedades fúngicas y del efecto de la aplicación de fungicida (Prosaro). Para este segundo estudio se evaluaron este conjunto de accesiones cultivadas en cinco localidades distintas de centro/norte de España: Tordómar y Briviesca (Burgos), Elorz (Navarra) y Sos del Rey Católico y Ejea de los Caballeros (Zaragoza).

De un abordaje sencillo a otro más complejo, de lo destructivo a lo no destructivo, de la alta precisión a la baja precisión, y desde el suelo a una perspectiva aérea, las mediciones se realizaron utilizando una variedad de equipos y metodologías científicas. Para la medición destructiva revelada por el análisis de isótopos estables, como $\delta^{13}C$ y $\delta^{15}N$ en materia seca de la planta. Los análisis de los isótopos estables mostraron resultados interesantes para explicar la variación del estado hídrico y nutricional de la planta a lo largo de la temporada de crecimiento. Al igual que en el primer estudio sobre nemátodos, donde el valor de $\delta^{15}N$ en melón injertado ($\bar{x}$=4,02‰) en 2016 es superior ($p<0.05$) al del melón no injertado

($\bar{x}$=3,68 ‰, p<0,05), lo que significa que el melón injertado se comporta mejor que el no injertado y se caracterizó por una mejor asimilación de nitrógeno posiblemente debido a un nivel de estrés por ataque del nematodo inferior. En el segundo estudio, el valor de δ13C nos permite evaluar las condiciones de humedad del cultivo durante la fase de llenado del grano, con valores que variaron (p<0.001) entre Elorz ($\bar{x}$=-26,00‰) y Ejea de los Caballeros ($\bar{x}$=-27,08‰), lo que indica un menor estrés hídrico en la segunda localidad, posiblemente asociado a mayor riego, junto con fuertes lluvias durante la fase reproductora en la segunda localidad. Los sensores portátiles de pigmentos foliares de hojas Dualex y SPAD, también produjeron resultados significativos que permitieron diferenciar entre plantas con injertadas con pies tolerantes a nemátodos y plantas no injertadas (primer estudio) y entre accesiones de trigo tratadas y no tratadas con fungicida (segundo experimento). Así por ejemplo los valores de flavonoides en plantas injertadas fueron menores que en el de las no injertada, o que el segundo estudio el valor del Nitrogen Balance Index (NBI) en trigo tratado con fungicida ($\bar{x}$=35.69) fue superior (p<0.01) al de las mismas accesiones sin tratar ($\bar{x}$=34.56) en el sitio de Elorz. En los dos estudios se utilizaron instrumentos de medida de verdor del dosel vegetal, como GreenSeeker NDVI (Índice normalizado de diferencia de vegetación) y cámaras RGB para medir en plantas entera, dosel vegetal o parcela elemental entera. Estos instrumentos, que miden índices de vegetación produjeron buenos resultados que permitieron comparar los dos tratamientos experimentales diferentes en ambos estudios. Por ejemplo, el Índice de Verdor Triangular (TGI) en la planta injertada de melón ($\bar{x}$=2600) en 2016 fue superior (p<0.0001) al de la planta no injertada ($\bar{x}$=1880).

En segundo estudio también demostró que estos índices permiten diferenciar entre tratamientos, con trigo tratado con fungicida presentado un índice de área verde (GA) más alto (p<0,001) que el trigo no tratado al menos en mayo y junio en cada una de las cinco ubicaciones. Además, en el caso de los índices RGB, las mediciones aéreas se utilizando una cámara RGB estándar integrada en un vehículo aéreo no tripulado (UAV) mostraron resultados similares que en el caso de los índices RGB evaluados desde el suelo. Esta evidencia se evidencias al observar las elevadas correlaciones entre los índices RGB de vegetación nivel del suelo y desde el UAV; por ejemplo, r=0,817 en el caso del TGI. Sin embargo, los resultados de NDVI medidos desde el UAV con una cámara NDVI modificada (AgroCam GEO NDVI), produjeron unos resultados mucho peores que los obtenidos desde el suelo empleando el medidor de NDV Greenseeker. Así por ejemplo las medidas de NDVI realizadas desde el suelo 22 de abril en Elorz correlacionaron contra el rendimiento

(R^2=0.700, p<0.001) mucho mejor que el NDVI medido desde la UAV. De hecho, la mejor correlación alcanzada entre NDVI medido desde el UAV y el GY fue la medida del 12 de mayo en Tordómar (R^2=0,231, p<0,001). En este sentido, el estudio concluye que es recomendable utilizar un UAV para medir los índices de vegetación RGB y el GreenSeeker para medir el NDVI (alternativamente considerar un sensor NDVI aéreo de mejor calidad) debido a las ventajas del primero (RGB desde un UAV) de cubrir rápidamente un área más grande y los mejores resultados del segundo (medir NDVI desde el suelo).

Todas estas herramientas, que operan en varios niveles, no solo permiten identificar el estrés biótico, sino que también demuestran en el caso de los cultivos hortícolas la importancia de adoptar prácticas agrícolas más inteligentes, como métodos de injerto para proteger los cultivos hortícolas de la agresión de los nematodos y el desarrollo de nuevas variedades.

References

References

Note: All of the citations for the entire thesis are included in the final part of the bibliography.

1. Abd-Elgawad, M.M. Biological control agents in the integrated nematode management of potato in Egypt. *Egypt. J. Biol. Pest Control*. **2020**, *30*, 1–13.

2. Ahmad, U.; Alvino, A.; & Marino, S. A review of crop water stress assessment using remote sensing. *Remote Sens.* **2021**, *13*, 4155.

3. Alvarez-Vanhard, E.; Corpetti, T.; & Houet, T. UAV & satellite synergies for optical remote sensing applications: *A literature review*. *Sci of remote sens.* **2021**, 3, 100019.

4. Araus, J. L.; Kefauver, S. C.; Vergara-Díaz, O.; Gracia-Romero, A.; Rezzouk, F. Z.; Segarra, J.; ... & Bort, J. Crop phenotyping in a context of global change: What to measure and how to do it. *J. Integr. Plant Biol*. **2022**, *64*, 592-618.

5. Araus, J. L.; & Kefauver, S. C. Breeding to adapt agriculture to climate change: affordable phenotyping solutions. *Current opinion in plant biol*. **2018**, *45*, 237-247.

6. Araus, J. L.; Kefauver, S. C.; Zaman-Allah, M.; Olsen, M. S.; & Cairns, J. E. Translating high-throughput phenotyping into genetic gain. *Trends in plant sci*. **2018**, *23*, 451-466.

7. Araus, J. L.; & Kefauver, S. C. Breeding to adapt agriculture to climate change: affordable phenotyping solutions. *Plant biol*. **2017**, *45*, 237-247.

8. Araus, J. L. The combined use of vegetation indices and stable isotopes to predict durum wheat grain yield under contrasting water conditions. *Agric. Water Manag.* **2015**, *158*, 196-208.

9. Araus, J. L.; and Cairns, J. E. Field high-throughput phenotyping: the new crop breeding frontier. *Trends Plant Sci*. **2014**, *19*, 52–61.

10. Araus, J. L.; Slafer, G. A.; Royo, C.; and Serret, M. D. Breeding for yield potential

and stress adaptation in cereals. *Crit. Rev. Plant Sci*. **2008**, *27*, 377–412.

11. Araus, J. L.; Villegas, D.; Aparicio, N.; Del Moral, L. G.; El Hani, S.; Rharrabti, Y.; & Royo, C. Environmental factors determining carbon isotope discrimination and yield in durum wheat under Mediterranean conditions. *Crop sci*. **2003**, *43*, 170-180.

12. Arora, A.; Sharma, R. K.; Saharan, M. S.; Venkatesh, K.; Dilbaghi, N.; Sharma, I.; & Tiwari, R. Quantifying stripe rust reactions in wheat using a handheld NDVI remote sensor. *Gates Open Res*. **2019**, *3*, 955.

13. Ashourloo, D.; Mobasheri, M. R.; & Huete, A. Evaluating the effect of different wheat rust disease symptoms on vegetation indices using hyperspectral measurements. *Remote Sens*. **2014**, *6*, 5107-5123.

14. Atkinson, N. J.; & Urwin, P. E. The interaction of plant biotic and abiotic stresses: from genes to the field. *J. Exp. Bot*. **2012**, *63*, 3523- 3543.

15. Ayala-Doñas, A.; Cara-García, M. D.; Talavera-Rubia, M.; & Verdejo-Lucas, S. Management of soil-borne fungi and root-knot nematodes in cucurbits through breeding for resistance and grafting. *Agron*. **2020**, *10*, 1641.

16. Bajwa, A. A.; Walsh, M.; & Chauhan, B. S. Weed management using crop competition in Australia. *Crop Prot*. **2017**, *95*, 8-13.

17. Balodi, R.; Bisht, Sunaina.; Ghatak, A.; & Rao, K. H. Plant disease diagnosis: technological advancements and challenges. *Indian Phytopathol*. **2017**, *70*, 275-281.

18. Ben M'Barek, S.; Laribi, M.; Kouki, H.; Castillo, D.; Araar, C.; Nefzaoui, M.; ... & Yahyaoui, A. H. Phenotyping Mediterranean durum wheat landraces for resistance to *Zymoseptoria tritici* in Tunisia. *Genes*. **2022**, *13*, 355.

19. Ben Rejeb, I.; Pastor, V.; & Mauch-Mani, B. Plant responses to simultaneous biotic and abiotic stress: molecular mechanisms. *Plants*. **2014**, *3*, 458-475.

20. Berger, K.; Machwitz, M.; Kycko, M.; Kefauver, S. C.; Van Wittenberghe, S.;

Gerhards, M.; & Schlerf, M. Multi-sensor spectral synergies for crop stress detection and monitoring in the optical domain: *A review*. *Remote Sens Environ*. **2022**, *280*,113198.

21. Bhandari, M.; Ibrahim, A. M.; Xue, Q.; Jung, J.; Chang, A.; Rudd, J. C.; ... & Landivar, J. Assessing winter wheat foliage disease severity using aerial imagery acquired from small Unmanned Aerial Vehicle (UAV). *Comput Electron Agric*. **2020**, *176*, 105665.

22. Bletsos, F.A. Use of grafting and calcium cyanamide as alternatives to methyl bromide soil fumigation and their effects on growth, yield, quality, and fusarium wilt control in melon. *J. Phytopathol*. **2005**, *153*, 155–161.

23. Blok, V.C.; Jones, J.T.; Phillips, M.S.; Trudgill, D.L. Parasitism genes and host range disparities in biotrophic nematodes: The conundrum of polyphag versus specialisation. *Bioessays* **2008**, *30*, 249–259.

24. Bock, C. H.; Poole, G. H.; Parker, P. E.; and Gottwald, T. R. Plant disease severity is estimated visually, by digital photography and image analysis, and by hyperspectral imaging. *Crit. Rev. Plant Sci*. **2010**, *29*, 59107.

25. Boulent, J.; Foucher, S.; Théau, J.; St-Charles, P.-L. Convolutional Neural Networks for the automatic identification of plant diseases. *Front. Plant Sci*. **2019**, *10*, 941.

26. Bowman, M. S.; & Zilberman, D. Economic factors affecting diversified farming systems. *Ecol. Soc.* **2013**, 18.

27. Boyer, J. S. Plant productivity and environment. *Science*. **1982**, *218*, 443.

28. Bravo, C.; Moshou, D.; West, J.; McCartney, A.; & Ramon, H. Early disease detection in wheat fields using spectral reflectance. *Biosystems Engineering*. **2003**,*84*, 137-145.

29. Busby, J. W.; & Busby, J Climate change and national security: an agenda for action. Council on Foreign Relations Press: New York, USA. **2007**.

30. Cabrera-Bosquet, L.; Albrizio, R.; Nogues, S.; Araus, J.L. Dual Delta ^{13}C/delta

^{18}O response to water and nitrogen availability and its relationship with yield in field-grown durum wheat. *Plant Cell Environ*. **2011**, *34*, 418–433.

31. Casadesus, J.; Kaya, Y.; Bort, J.; Nachit, M.M.; Araus, J.L.; Amor, S.; Ferrazzano, G.; Maalouf, F. Using vegetation indices derived from conventional digital cameras as selection criteria for wheat breeding in water-limited environments. *Ann. Appl. Biol*. **2007**, *150*, 227–236.

32. Cerovic, Z.G.; Ghozlen, N.B.; Milhade, C.; Obert, M.; Debuisson, S.; Le Moigne, M. Non-destructive Diagnostic Test for Nitrogen Nutrition of Grapevine (Vitis vinifera L.) Based on Dualex Leaf-Clip Measurements in the. *Field. J. Agric. Food Chem*. **2015**, *63*, 3669–3680.

33. Cerovic, Z.G.; Masdoumier, G.; Ghozlen, N.B.; Latouche, G. A new optical leaf-clip meter for simultaneous non-destructive assessment of leaf chlorophyll and epidermal flavonoids. *Physiol. Plant*. **2012**, *146*, 251–260.

34. Cerovic, Z. G.; Cartelat, A.; Goulas, Y.; & Meyer, S. In-the-field assessment of wheat-leaf polyphenolics using the new optical leaf-clip Dualex. *Precis. Agric*. **2005**, *5*, 243-249.

35. Cerovic, Z.G.; Ounis, A., Cartelat, A.; Latouche, G.; Goulas, Y.; Meyer, S.; Moya, I. Chlorophyll fluorescence excitation spectra can be used for the non-destructive in situ assessment of UV-absorbing compounds in leaves. *Plant Cell Environ*. **2001**, *25*, 1663–1676.

36. Chaerle, L.; Leinonen, I.; Jones, H. G.; & Van Der Straeten, D. Monitoring and screening plant populations with combined thermal and chlorophyll fluorescence imaging. *J. Exp. Bot.* **2007**, *58*, 773-784.

37. Champeil, A.; Doré, T.; & Fourbet, J. F. Fusarium head blight: epidemiological origin of the effects of cultural practices on head blight attacks and the production of mycotoxins by Fusarium in wheat grains. *Plant sci*. **2004**, *166*, 1389-1415.

38. Chin, S.; Behm, C. A.; & Mathesius, U. Functions of flavonoids in plant nematode

interactions. *Plants*. **2018**, *7*, 85.

39. Cobb, J. N.; De Clerck, G.; Greenberg, A.; Clark, R.; & Mc Couch, S. Next-generation phenotyping: requirements and strategies for enhancing our understanding of genotype phenotype relationships and its relevance to crop improvement. *Theor. Appl. Genet*. **2013**, *126*, 867-887.

40. Cogato, A.; Meggio, F.; De Antoni Migliorati, M.; & Marinello, F. Extreme weather events in agriculture: *A systematic review*. *Sustainability*. **2019**, *11*, 2547.

41. Condon, A.G.; Richards, R.A.; Rebetzke, G.J.; Farquhar, G.D. Breeding for high water-use efficiency. *J. Exp. Bot*. **2004**, *55*, 2447–2460.

42. Cramer, G. R.; Urano, K.; Delrot, S.; Pezzotti, M.; & Shinozaki, K. Effects of abiotic stress on plants: a systems biology perspective. *BMC Plant Biol*. **2011**, *11*, 1-14.

43. Cushman, J. C.; & Bohnert, H. J. Genomic approaches to plant stress tolerance. *Current opinion in plant biol*. **2000**, *3*, 117-124.

44. Dammer, K. H.; Garz, A.; Hobart, M.; & Schirrmann, M. Combined UAV and tractor-based stripe rust monitoring in winter wheat under field conditions. *Agron J*. **2022**, 114651-661.

45. Davies, F. T.; & Bowman, J. E. Horticulture, food security, and the challenge of feeding the world. *In XXIX International Horticultural Congress on Horticulture: Sustaining Lives, Livelihoods and Landscape*. IHC. **2014**, 1128, 1-6.

46. Davila, M.; Dickson, D.W. Base temperature and heat unit requirements for development of *Meloidogyne arenaria* and *Meloidogyne javanica*. *J. Nematol*. **2004**, *36*, 314.

47. De Guiran, G. Protection des Cultures Maraîchères et Fruitières Face Aux Capacités D'adaptation des Nématodes Meloidogyne; Comptes Rendus de l'Académie d'agriculture: Paris, France, **1983**.

48. Djian Caporalino, C. Root knot nematodes (*Meloidogyne spp*.), a growing problem in French vegetable crops. *EPPO Bull*. **2012**, *42*,127–137.

49. Doohan, F. M.; Brennan, J.; & Cooke, B. M. Influence of climatic factors on Fusarium species pathogenic to cereals. Epidemiology of Mycotoxin Producing Fungi: Under the aegis of COST Action 835 'Agriculturally Important Toxigenic Fungi 1998–2003', EU project (QLK 1-CT-1998–01380).**;** Springer: Berlin/Heidelberg, Germany, 2003; pp; 755–768.

50. Dresselhaus, T.; & Hückelhoven, R. Biotic and abiotic stress responses in crop plants. *Agron.* **2018**, *8*, 267.

51. Duller, R. A.; Armitage, J. J.; Manners, H. R.; Grimes, S.; & Jones, T. D. Delayed sedimentary response to abrupt climate change at the Paleocene-Eocene boundary, northern Spain. *Geology*. **2019**, *47*.159-162.

52. Duncan, G.A.; Gates, R.; Montross, M.D. Measuring Relative Humidity in Agricultural Environments; Agricultural Engineering Extension Publications-Uknowledge: Lexington, KY, USA, **2005**.

53. Elazab, A.; Bort, J.; Zhou, B.; Serret, M. D.; Nieto-Taladriz, M. T.; & Araus, J. L. The combined use of vegetation indices and stable isotopes to predict durum wheat grain yield under contrasting water conditions. *Agric. Water Manag*. **2015**, *158*, 196-208.

54. El Jarroudi, M.; Kouadio, L.; Junk, J.; Bock, C.; Diouf, A. A.; & Delfosse, P. Improving fungal disease forecasts in winter wheat: A critical role of intra-day variations of meteorological conditions in the development of Septoria leaf blotch. *Field Crops Res.* **2017**, *213*, 12-20.

55. Emebiri, L.; Taylor, K.; & Hildebrand, S. QTL Mapping of Wheat Stripe Rust Resistance in Relation to Epidermal Flavonoids Measured Using a Leaf-Clip, Optical Sensor. *Crop Sci*. **2019**, *59*, 1916-1926.

56. Evans, L. T. Crop evolution, adaptation and yield. Cambridge university press.

1996.

57. Expósito, A.; Pujolà, M.; Achaerandio, I.; Giné, A.; Escudero, N.; Fullana, A.M.; Cunquero, M.; Loza-Alvarez, P.; Sorribas, F.J. Tomato and melon *Meloidogyne* resistant rootstocks improve crop yield but melon fruit quality is influenced by the cropping season. Front. *Plant Sci*. **2020**, 1742.

58. Expósito, A.; García, S.; Giné, A.; Escudero, N.; Sorribas, F.J. *Cucumis metuliferus* reduces *Meloidogyne incognita* virulence against the Mi1.2 resistance gene in a tomato–melon rotation sequence. *Pest Manag. Sci*. **2019**, *75*, 1902–1910.

59. Expósito, A.; Munera, M.; Giné, A.; López-Gómez, M.; Cáceres, A.; Picó, B.; Gisbert, C.; Medina, V.; Sorribas, F.J. *Cucumis metuliferus* is resistant to root-knot nematode Mi1.2 gene (a)virulent isolates and a promising melon rootstock. *Plant Pathol*. **2018**,*67*, 1161–1167.

60. Fallik, E.; & Ilic, Z. Effect of pre-storage manipulation on the reduction of chilling injury in tomatoes. *In V International Postharvest Symposium*. IPS. **2004**, 682, 1639-1644.

61. Fang, Y.; & Ramasamy, R. P. Current and prospective methods for plant disease detection. *Biosensors*. **2015**, *5*, 537-561.

62. Farooq, M.; Wahid, A.; Kobayashi, N. S. M. A.; Fujita, D. B. S. M. A.; & Basra, S. M. A. Plant drought stress: effects, mechanisms and management. *Sustain. Agric*. **2009**, 153-188.

63. Feng, X.; Zhan, Y.; Wang, Q.; Yang, X.; Yu, C.; Wang, H.; He, Y. Hyperspectral imaging combined with machine learning as a tool to obtain high-throughput plant salt-stress phenotyping. *Plant. J*. **2020**, *101*, 1448–1461.

64. Fernandez-Gallego, J.A.; Kefauver, S.C.; Gutiérrez, N.A.; Nieto-Taladriz, M.T.; Araus, J.L. Wheat ear counting in-field conditions: High throughput and low-cost approach using RGB images. *Plant Methods*. **2018**, *14*, 1–12.

65. Fiorani, F.; & Schurr, Future scenarios for plant phenotyping. *Ann rev of plant biol*.

2013, *64*, 267-291.

66. Flohr, P.; Müldner, G.; & Jenkins, E. Carbon stable isotope analysis of cereal remains as a way to reconstruct water availability: preliminary results. *Water History*. 2**011**, *3*, 121-144.

67. Food and Agriculture Organization (FAO) statistic. 2023. https://www.fao.org/faostat/

68. Food and Agriculture Organization (FAO) statistic. 2019. https://www.fao.org/faostat/

69. Francesconi, S.; Harfouche, A.; Maesano, M.; & Balestra, G. M. UAV-based thermal, RGB imaging and gene expression analysis allowed detection of Fusarium head blight and gave new insights into the physiological responses to the disease in durum wheat. *Front. Plant Sci*. **2021**, *12*, 628575.

70. Gago, J.; Estrany, J.; Estes, L.; Fernie, A. R.; Alorda, B.; Brotman, Y.; ... & Medrano, H. Nano and micro unmanned aerial vehicles (UAVs): a new grand challenge for precision agriculture. *Current protocols in plant biol*. **2020**, *5*, 20103.

71. Galieni, A.; D'Ascenzo, N.; Stagnari, F.; Pagnani, G.; Xie, Q.; & Pisante, M. Past and future of plant stress detection: an overview from remote sensing to positron emission tomography. *Front. Plant Sci*. **2021**, *11*, 609155.

72. Garrett, K. A.; Dendy, S. P.; Frank, E. E.; Rouse, M. N.; & Travers, S. E. Climate change effects on plant disease: genomes to ecosystems. *Annu. Rev. Phytopathol*. **2006**, *44*, 489-509.

73. Gassmann, A.J.; Stock, S.P.; Sisterson, M.S.; Carrière, Y.; Tabashnik, B.E. Synergism between entomopathogenic nematodes and *Bacillus thuringiensis* crops: Integrating biological control and resistance management. *J. Appl. Ecol*. **2008**, *45*, 957–966.

74. Giné, A.; González, C.; Serrano, L.; Sorribas, F.J. Population dynamics of *Meloidogyne incognita* on cucumber grafted onto the Cucurbita hybrid RS841 or non-

grafted and yield losses under protected cultivation. *Eur. J.* **2017**, *148*, 795-805

75. Goulas, Y.; Cerovic, Z. G.; Cartelat, A.; & Moya, I. Dualex: a new instrument for field measurements of epidermal ultraviolet absorbance by chlorophyll fluorescence. *Appl. Opt.* **2004**, *43*, 4488-4496.

76. Govender, M.; Govender, P. J.; Weiersbye, I. M.; Witkowski, E. T. F.; & Ahmed, F. Review of commonly used remote sensing and ground-based technologies to measure plant water stress. *Water Sa*. **2009**, 35.

77. Goverse, A.; Smant, G. The activation and suppression of plant innate immunity by parasitic nematodes. *Ann Rev Phytopath*. **2014**, *52*, 243–265.

78. Gracia-Romero, A.; Kefauver, S.C.; Fernandez-Gallego, J.A.; Vergara-Díaz, O.; Nieto-Taladriz, M.T.; Araus, J.L. UAV and ground image-based phenotyping: A proof of concept with Durum wheat. *Remote Sens.* **2019**, *11*, 1244.

79. Gregory, P. J.; Ingram, J. S.; & Brklacich, M. Climate change and food security. Philosophical Transactions of the Royal Society. *Biol. sci*. **2005**, *360*, 2139-2148.

80. Hamdane, Y.; Gracia-Romero, A.; Buchaillot, M. L.; Sanchez-Bragado, R.; Fullana, A. M.; Sorribas, F. J.; ... & Kefauver, S. C. Comparison of proximal remote sensing devices of vegetable crops to determine the role of grafting in plant resistance to *Meloidogyne incognita*. *Agron*. **2022**, *12*, 1098.

81. Haverkort, A. J.; & Valkenburg, G. W. The influence of cyst nematodes and drought on potato growth. Effects on carbon isotope fractionation. *Neth. J. Plant Pathol*. **1992**, *98*, 12-20.

82. Heidarian Dehkordi, R.; El Jarroudi, M.; Kouadio, L.; Meersmans, J.; & Beyer, M. Monitoring wheat leaf rust and stripe rust in winter wheat using high-resolution UAV-based red-green-blue imagery. *Remote Sens*. **2020**, *12*, 3696.

83. Holman, F. H.; Riche, A. B.; Michalski, A.; Castle, M.; Wooster, M. J.; & Hawkesford, M.J. High throughput field phenotyping of wheat plant height and growth rate in

field plot trials using UAV-based remote sensing. *Remote Sens*. **2016**, *8*, 1031.

84. Hunt, E.R.; Doraiswamy, P.C.; Mcmurtrey, J.E.; Daughtry, C.S.T.; Perry, E.M.; Akhmedov, B. A visible band index for remote sensing leaf chlorophyll content at the canopy scale. Int. J. Appl. *Earth Obser. Geoinf.* **2013**, *21*, 103–112.

85. Hunt, E.R.; Daughtry, C.S.T.; Eitel, J.U.; Long, D.S. Remote sensing leaf chlorophyll content using a visible band index. *Agron. J.* **2011**, *103*, 1090–1099.

86. Hunt, E.R.; Cavigelli, M.; Daughtry, C.S.; Mcmurtrey, J.E.; Walthall, C.L. Evaluation of digital photography from model aircraft for remote sensing of crop biomass and nitrogen status. *Precis. Agric*. **2005**, *6*, 359–378.

87. Iglesias, A.; Rosenzweig, C.; & Pereira, D. Agricultural impacts of climate change in Spain: developing tools for a spatial analysis. *Glob Environ Change J*. **2000**, *10*, 69-80.

88. Jaffee, S.; & Henson, S. Standards and agro-food exports from developing countries: rebalancing the debate. World Bank Publications. **2004**.

89. Jarroudi, M. E.; Kouadio, L.; Beyer, M.; Junk, J.; Hoffmann, L.; Tychon, B.; ... & Delfosse, P. Economics of a decision–support system for managing the main fungal diseases of winter wheat in the Grand-Duchy of Luxembourg. *Field Crops Res*. **2015**, *172*, 32-41.

90. Jelínek, Z.; Starý, K.; Kumhálová, J.; Lukáš, J.; & Mašek, J. Winter wheat, winter rape and poppy crop growth evaluation with the help of remote and proximal sensing measurements. **2020**.

91. Jiang, J.; Wang, C.; Wang, H.; Fu, Z.; Cao, Q.; Tian, Y.; ... & Liu, X. Evaluation of Three Portable Optical Sensors for Non-Destructive Diagnosis of Nitrogen Status in Winter Wheat. *Sensors*. **2021**, *21*, 5579.

92. Jiang, Y.; & Huang, B. Physiological responses to heat stress alone or in combination with drought: A comparison between tall fescue and perennial ryegrass. *Hort Sci*. **2001**, *36*, 682-686.

93. Jing, X.; Du, K.; Duan, W.; Zou, Q.; Zhao, T.; Li, B.; ... & Yan, L. Quantifying the effects of stripe rust disease on wheat canopy spectrum based on eliminating non-physiological stresses. *Crop J*. **2022**, *10*, 1284-1291.

94. Kashaija, I.; Kizito, F.; McIntyre, B.; Sali, H. Spatial distribution of roots, nematode populations and root necrosis in highland banana in Uganda. *Nematology*. **2004**, *6*, 7–12.

95. Kaufmann, H.; Segl, K.; Itzerott, S.; Bach, H.; Wagner, A.; Hill, J.; Müller, A. *Hyperspectral Algorithms: Report in the Frame of EnMAP Preparation Activities*; Potsdam: Darst, Germany, **2010**.

96. Kefauver, S.; Kerfal, S.; Fernandez Gallego, J.A.; El-Haddad, G. CerealScanner Gitlab. Available online: https://gitlab.com/ sckefauver/cerealscanner (accessed on 14 March 2019).

97. Kefauver,S.**2018**.Availableonline:https://gitlab.com/sckefauver/MosaicTool, University of Barcelona, Barcelona, Spain (acessed 25 September 2021).

98. Koenning, S.R.; Overstreet, C.; Noling, J.W.; Donald, P.A.; Becker, J.O.; Fortnum, B.A. Survey of crop losses in response to phytoparasitic nematodes in the United States for 1994. *J. Nematol*. **1999**, *31*, 587.

99. Konica, M.O. Chlorophyll Meter SPAD-502 Plus-A Light weight Handheld Meter for Measuring the Chlorophyll Content of Leaves without Causing Damage to Plants.**2012**.Availableonline:http://www.konikcaminolta.com/instrments/download/catalog/color/pdf/spad502plus_e1.pdf (accessed on 12 March 2019).

100. La Pena, R. D.; & Hughes, J. Improving vegetable productivity in a variable and changing climate. **200**7.

101. Liebisch, F.; Kirchgessner, N.; Schneider, D.; Walter, A.; & Hund, A. Remote, aerial phenotyping of maize traits with a mobile multi-sensor approach. *Plant methods*. **2015**, *11*, 1- 20.

102. Li, J.; Veeranampalayam-Sivakumar, A. N.; Bhatta, M.; Garst, N. D.; Stoll, H.; Stephen Baenziger, P.; ... & Shi, Y. Principal variable selection to explain grain yield variation in winter wheat from features extracted from UAV imagery. *Plant Methods*. **2019**, *15*, 1-13.

103. Lopes, M. S.; & Araus, J. L. Nitrogen source and water regime effects on durum wheat photosynthesis and stable carbon and nitrogen isotope composition. *Physiol. Plant*. **2006**, *126*, 435-445.

104. Lucas, J. A. Advances in plant disease and pest management. *J. Agric. Sci*. **2011**, *149*, 91-114.

105. Lumpkin, T.; Weinberger, K.; & Moore, S. Increasing income through fruit and vegetable production opportunities and challenges. **2005**.

106. Madec, S.; Baret, F.; De Solan, B.; Thomas, S.; Dutartre, D.; Jezequel, S.; ... & Comar, A. High-throughput phenotyping of plant height: comparing unmanned aerial vehicles and ground LiDAR estimates. *Front. Plant Sci*. **2017**, *8*, 2002.

107. Mahlein, A.-K. Plant disease detection by imaging sensors, parallels and specific demands for precision agriculture and plant phenotyping. *Plant Dis*. **2016**, *100*, 241–251.

108. Malagoli, P.; Laine, P.; Rossato, L.; Ourry, A. Dynamics of nitrogen uptake and mobilization in field-grown winter oil seed rape (*Brassicanapus*) from stem extension to harvest: I. Global N flows between vegetative and reproductive tissues in relation to leaf fall and their residual N. *Ann. Bot*. **2005**, *95*, 853–861.

109. Martínez-Moreno, F.; Giraldo, P.; Nieto, C.; & Ruiz, M. Resistance to leaf and yellow rust in a collection of Spanish bread wheat landraces and association with ecogeographical variables. *Agron*. **2022**, *12*, 187.

110. Martínez-Moreno, F.; & Solís, I. Wheat rust evolution in Spain: an historical review. *Phytopathol*. **2019**, *58*,1.

111. Mateen, A.; & Zhu, Q. Weed detection in wheat crop using UAV for precision agriculture. *Pak. J. Agric. Sci*. **2019**, *56*, 809-817.

112. McMullen M.; Bergstrom G.; De Wolf E.; Dill-Macky R.; Hershman D.; Shaner G.; Van Sanford D. Fusarium head blight disease cycle, symptoms, and impact on grain yield and quality frequency and magnitude of epidemics since 1997. *Plant. Dis*. **2012**, *96*,1712–1728.

113. Mielniczuk, E.; & Skwaryło-Bednarz, B. Fusarium head blight, mycotoxins and strategies for their reduction. *Agron*. **2020**, *10*, 509.

114. Miguel, A.; Maroto, J.V.; San Bautista, A.; Baixauli, C.; Cebolla, V.; Pascual, B.; Guardiola, J.L. The grafting of triploid watermelon is an advantageous alternative to soil fumigation by methyl bromide for control of *Fusarium wilt*. *Sci. Hortic*. **2004**, *103*, 9–17.

115. Moazzam, S. I.; Khan, U. S.; Nawaz, T.; & Qureshi, W. S. Crop and Weeds Classification in Aerial Imagery of Sesame Crop Fields Using a Patch-Based Deep Learning Model-Ensembling Method. In 2022: 2nd International Conference on Digital Futures and Transformative Technologies (ICoDT2). Rawalpindi, Pakistan, 24–26 May 2022; pp. 1–7

116. Montague, T.; Hellman, E.; Krawitzky, M. Comparison of greenhouse grown, containerized grapevine stomatal conductance measurements using two differing porometers. *In Proceedings of the 2nd Annual National Viticulture Research Conference*, Davis, CA, USA, 9–11 July. **2008**, 58–61.

117. Morales, F.; Ancín, M.; Fakhet, D.; González-Torralba, J.; Gámez, A. L.; Seminario, A.; & Aranjuelo, I. Photosynthetic metabolism under stressful growth conditions as a base for crop breeding and yield improvement. *Plants*. **2020**, *9*, 88.

118. Moshou, D.; Bravo, C.; West, J.; Wahlen, S.; McCartney, A.; Ramon, H. Automatic detection of 'yellow rust' in wheat using reflectance measurements and neural networks. *Comp. Electron. Agric*. **2004**, *44*, 173–188.

119. Mujeeb-Kazi, A.; Kazi, A. G.; Dundas, I.; Rasheed, A.; Ogbonnaya, F.; Kishii, M.;

… & Farrakh, S. Genetic diversity for wheat improvement as a conduit to food security. *Agron*. **2013**, *122*, 179-257.

120. Munné-Bosch, S.; Queval, G.; Foyer, C.H. The impact of global change factors on redox signaling underpinning stress tolerance. *Plant Physiol*. **2013**, *161*, 5–19.

121. Nicol JM, Turner SJ, Coyne DL, Nijs Ld, Hockland S, Maafi ZT. Current nematode threats to world agriculture. In: Jones J, Gheysen G, Fenoll C, eds. Genomics and molecular genetics of plant nematode interactions. Amsterdam, the Netherlands. *Springer*. **2011**, 21–43.

122. Nisha, M.S.; Sheela, M.S. Bio-Management of *Meloidogyne incognita* on Coleus, *Solenostemon rotundifolius* by Integrating Solariza tion, *Paecilomyces lilacinus*, *Bacillus macerans* and Neemcake. *Indian J. Nematol*. **2006**, *36*, 136–138.

123. Owusu, S. B.; Kwoseh, C. K.; Starr, J. L.; & Davies, F. T. Grafting for management of root-knot nematodes, *Meloidogyne incognita*, in tomato (*Solanum lycopersicum L*.). *Nematropica*. **2016**, *46*, 14-21.

124. Pandey, P.; Irulappan, V.; Bagavathiannan, M. V.; & Senthil-Kumar, M. Impact of combined abiotic and biotic stresses on plant growth and avenues for crop improvement by exploiting physio-morphological traits. *Front. Plant Sci*. **2017**, *8*, 537.

125. Paramo, L. A.; Feregrino-Pérez, A. A.; Guevara, R.; Mendoza, S.; & Esquivel, K. Nanoparticles in agroindustry: Applications, toxicity, challenges, and trends. *Nanomater.* **2020**, *10*, 1654.

126. Peteinatos, G. G.; Korsaeth, A.; Berge, T. W.; & Gerhards, R. Using optical sensors to identify water deprivation, nitrogen shortage, weed presence, and fungal infection in wheat. *Agri.* **2016,** *6*, 24.

127. Peterson, B.J.; Fry, B. Stable isotopes in ecosystem studies. *Annu. Rev. Ecol. Syst*. **1987**, *18*, 293–320.

128. Piao, S.; Ciais, P.; Huang, Y.; Shen, Z.; Peng, S.; Li, J.; & Fang, J. The impacts of

climate change on water resources and agriculture in China. *Nature*. **2010**, *467*, 43- 51.

129. Porep, J. U.; Kammerer, D. R.; & Carle, R. On-line application of near infrared (NIR) spectroscopy in food production. *Trends Food Sci. Technol*. **2015**, *46*, 211-230.

130. Porras, R.; Miguel-Rojas, C.; Pérez-de-Luque, A.; & Sillero, J. C. Macro-and Microscopic Characterization of Components of Resistance against *Puccinia striiformis f. sp. tritici* in a Collection of Spanish Bread Wheat Cultivars. *Agron*. **2022**, *12*, 1239.

131. Porras, R.; Luque, A. P.; & Rojas, C. D. M. Behavior of Spanish durum wheat genotypes against *Zymoseptoria tritici:* resistance and susceptibility. *SJAR*. **2021**, *19*, 1.

132. Prabhakar, M.; Prasad, Y. G.; & Rao, M. N. Remote sensing of biotic stress in crop plants and its applications for pest management. Crop stress and its management: Perspectives and strategies. **2011**, 517-545.

133. Ray, D. K.; Mueller, N. D.; West, P. C.; & Foley, J. A. Yield trends are insufficient to double global crop production by 2050. *Plos one*. **2013**, *8*, 66428.

134. Rembold, F.; Atzberger, C.; Savin, I.; & Rojas, O. Using low-resolution satellite imagery for yield prediction and yield anomaly detection. *Remote Sens*. **2013**, *5*, 1704-1733.

135. Reynolds, M.; Manes, Y.; Izanloo, A.; & Langridge, P. Phenotyping approaches for physiological breeding and gene discovery in wheat. *Ann. Appl. Biol*. **2009**, *155*, 309-320.

136. Rezzouk, F. Z.; Gracia-Romero, A.; Kefauver, S. C.; Gutiérrez, N. A.; Aranjuelo, I.; Serret, M. D.; & Araus, J. L. Remote sensing techniques and stable isotopes as phenotyping tools to assess wheat yield performance: Effects of growing temperature and vernalization. *Plant Sci*. **2020**, *295*, 110281.

137. Rivard, C.L.; Louws, F.J. Grafting to manage soilborne diseases in heirloom tomato production. *Hort Sci*. **2008**, *43*, 2104–2111.

138. Rossato, L. Nitrogen storage and remobilization in *Brassicanapus L*. during the growth cycle: Effects of methyl jasmonate on nitrate uptake, senescence, growth, and

VSP accumulation. *J. Exp. Bot*. **2002**, *53*, 1131–1141.

139. Rutkoski, J.; Poland, J.; Mondal, S.; Autrique, E.; Pérez, L. G.; Crossa, J.; & Singh, R. Canopy temperature and vegetation indices from high-throughput phenotyping improve the accuracy of pedigree and genomic selection for grain yield in wheat. G3: Genes, Genomes, Genetics. **2016**, *6*, 2799-2808.

140. Sabburg, R.; Obanor, F.; Aitken, E.; & Chakraborty, S. Changing fitness of a necrotrophic plant pathogen under increasing temperature. *Glob Chang Biol*. **2015**, *21*, 3126-3137.

141. Sankaran, S.; Khot, L. R.; Espinoza, C. Z.; Jarolmasjed, S.; Sathuvalli, V. R.; Vandemark, G. J.; ... & Pavek, M. J. Low-altitude, high-resolution aerial imaging systems for row and field crop phenotyping: *A review*. *Eur. J. Agron*. **2015**. *70*, 112-123.

142. Shakoor, N.; Lee, S.; & Mockler, T. C. High throughput phenotyping to accelerate crop breeding and monitoring of diseases in the field. *Plant biol*. **2017**, *38*, 184-192.

143. Sharma, S.; Kooner, R.; & Arora, R. Insect pests and crop losses. In Breeding insect resistant crops for sustainable agriculture. *Springer*. **2017**, 45-66.

144. Sigüenza, C.; Schochow, M.; Turini, T.; Ploeg, A. Use of *Cucumis metuliferus* as a rootstock for melon to manage *Meloidogyne incognita*. *J. Nematol.* **2005**, *37*, 276.

145. Silva-Sánchez, A.; Buil-Salafranca, J.; Cabral, A.C.; Uriz-Ezcaray, N.; García-Mendívil, H.A.; Sorribas, F.J.; Gracia-Romero, A. Comparison of proximal remote sensing devices for estimating physiological responses of eggplants to root-knot nematodes. *Proceedings* **2019**, *18*, 9.

146. Simko, I.; Jimenez-Berni, J. A.; & Sirault, X. R. Phenomic approaches and tools for phytopathologists. *Phytopathology*. **2016**, *107*, 6-17.

147. Simón, M. R.; Fleitas, M. C.; Castro, A. C.; & Schierenbeck, M. How foliar fungal diseases affect nitrogen dynamics, milling, and end use quality of wheat. *Front. Plant Sci*. **2020**, *11*, 569401.

148. Sinclair, T.R.; Rufty, T.W. Nitrogen and water resources commonly limit crop yield increases, not necessarily plant genetics. *Glob.Food Secur*. **2012**, *1*, 94–98.

149. Siou D.; Gélisse S.; Laval V.; Repinçay C.; Canalès R.; Suffert F.; Lannou C. Effect of wheat spike infection timing on Fusarium head blight development and mycotoxin accumulation. *Plant. Pathol*. **2014**, *63*, 390–399.

150. Solano-Alvarez, N.; Valencia-Hernández, J. A.; Vergara-Pineda, S.; Millán-Almaraz, J. R.; Torres-Pacheco, I.; & Guevara-González, R. G. Comparative Analysis of the NDVI and NGBVI as Indicators of the Protective Effect of Beneficial Bacteria in Conditions of Biotic Stress. *Plants*. **2022**, *11*, 932.

151. Sorribas, Francisco Javier, et al. Effectiveness and profitability of the Mi-resistant tomatoes to control root-knot nematodes. *Eur. J. Plant Pathol.* **2005**, *111*, 29-38.

65. Stern, A.; Doraiswamy, P.C.; Hunt Jr, E.R. Changes of crop rotation in Iowa determined from the United States Department of Agriculture, National Agricultural Statistics Service cropland data layer product. *J. Appl. Remote Sens*. **2012**, *6*, 063590-063590.

152. Suffert, F.; Ravigné, V.; & Sache, I. Seasonal changes drive short-term selection for fitness traits in the wheat pathogen *Zymoseptoria tritici*. *Appl. Environ*. **2015**, *81*, 6367-6379.

153. Suffert, F.; Sache, I.; & Lannou, C. Early stages of septoria tritici blotch epidemics of winter wheat: build-up, over seasoning, and release of primary inoculum. *Plant Pathol*. **2011**. *60*, 166-177.

154. Surovy, M. Z.; Mahmud, N. U.; Bhattacharjee, P.; Hossain, M. S.; Mehebub, M. S.; Rahman, M.; ... & Islam, T. Modulation of nutritional and biochemical properties of wheat grains infected by blast fungus *Magnaporthe oryzae Triticum* pathotype. *Front. Microbiol.* **2020**, *11*, 1174.

155. Tao, M.Q.; Jahan, M.S.; Hou, K.; Shu, S.; Wang, Y.; Sun, J.; Guo, S.-R. Bitter

Melon (*Momordica charantia L.*) Rootstock Improves the Heat Tolerance of Cucumber by Regulating Photosynthetic and Antioxidant Defense Pathways. *Plants*. **2020**, *9*, 692.

156. The State of Food and Agriculture (SOFA): Climate change, agriculture and food security. **2016**.

157. Tippmann, H. F.; Schlüter, U.; & Collinge, D. B. Common themes in biotic and abiotic stress signaling in plants. *Floriculture, ornamental and plant biotechnology*. **2006**, 52-67.

158. Tremblay, N.; Wang, Z.; & Cerovic, Z. G. Sensing crop nitrogen status with fluorescence indicators. A review. *Agronomy for sustainable development*. **2012**, *32*, 451-464

159. Tremblay, N.; Wang, Z.; & Belec, C. Performance of Dualex in spring wheat for crop nitrogen status assessment, yield prediction and estimation of soil nitrate content. *J. Plant Nutr*. **2009**, *33*, 57-70.

160. Tuberosa, R. Phenotyping for drought tolerance of crops in the genomic sera. *Front. Physiol*. **2012**, *3*, 347.

161. Tucker, Compton J. Red and photographic infrared linear combinations for monitoring vegetation. *Remote Sens Environ*. **1979**, *8*, 127-150.

162. United Nations Economic Commission for Europe (UNECE) Fresh Fruit and Vegetables-Standards. Available online: https://unece.org/trade/wp7/FFV-Standards (accessed on 20 April 2022).

163. Vergara-Diaz, O.; Kefauver, S. C.; Elazab, A.; Nieto-Taladriz, M. T.; & Araus, J. L. Grain yield losses in yellow-rusted durum wheat estimated using digital and conventional parameters under field conditions. *Crop. J*. **2015**, *3*, 200-210.

164. Vergara-Díaz, O.; Zaman-Allah, M.A.; Masuka, B.; Hornero, A.; Zarco-Tejada, P.; Prasanna, B.M.; Araus, J.L. A novel remote sensing approach for prediction of maize yield under different conditions of nitrogen fertilization. *Front. Plant Sci*. **2016**, 7, 666.

165. White, J. W.; Andrade-Sanchez, P.; Gore, M. A.; Bronson, K. F.; Coffelt, T. A.; Conley, M. M.; ... & Wang, G. Field-based phenomics for plant genetics research. *Field Crops Res*. **2012**, *133*, 101-112.

166. Wolf, J. Effects of climate change on wheat production potential in the European Community. *Eur. J. Agron*. **1993**, *2*. 281-292.

167. Workneh, T. S.; & Osthoff, G. A review on integrated agrotechnology of vegetables. *Afr. J. Biotechnol*. **2010**, *9*, 9307-9327.

168. Xi, K.; Kumar, K.; Holtz, M. D.; Turkington, T. K.; and Chapman, B. Understanding the development and management of stripe rust in central Alberta. *Can. J. Plant Pathol*. **2015**, *37*,21–39. Doi: 10.1080/07060661.2014.981215.

169. Xue, J.; & Su. Significant remote sensing vegetation indices: A review of developments and applications. *J. Sens*. **2017**. 2017.

170. Yang, M.D.; Tseng, H.H.; Hsu, Y.C.; Tsai, H.P. Semantic segmentation using deep learning with vegetation indices for rice lodging identification in multi-date UAV visible images. *Remote Sens*. **2020**, *12*, 633.

171. Yang, Q.; Balint-Kurti, P.; & Xu, M. Quantitative disease resistance: dissection and adoption in maize. *Mol Plant*. **2017**, *10*, 402-413.

172. Yousfi, Salima, et al. "Combined use of $\delta^{13}C$, $\delta^{18}O$ and $\delta^{15}N$ tracks nitrogen metabolism and genotypic adaptation of durum wheat to salinity and water deficit. *New Phytol*. **2012**, *194*, 230-244.

173. Yuen, G. Y.; & Schoneweis, S. D. Strategies for managing Fusarium head blight and deoxynivalenol accumulation in wheat. *Int. J. Food Microbiol*. **2007**, *119*, 126-130.

174. Zaman-Allah, M.; Vergara, O.; Araus, J.L.; Tarekegne, A.; Magorokosho, C.; Zarco-Tejada, P.J.; Hornero, A.; Albà, A.H.; Das, B.; Craufurd, P.; et al. Unmanned aerial platform-based multi-spectral imaging for field phenotyping of maize. *Plant Methods*. **2015**,

11, 35.

175. Zhang, D.; Wang, Q.; Lin, F.; Yin, X.; Gu, C.; & Qiao, H. Development and evaluation of a new spectral disease index to detect wheat fusarium head blight using hyperspectral imaging. *Sensors*. **2020**, *20*, 2260.

176. Zhang, J.; Liu, X.; Liang, Y.; Cao, Q.; Tian, Y.; Zhu, Y.; ... & Liu, X. Using a portable active sensor to monitor growth parameters and predict grain yield of winter wheat. *Sensors*. **2019**, *19*, 1108.

177. Zhang, C.; Kovacs, J.M. The application of small unmanned aerial systems for precision agriculture: A review. *Precision Agric*. **2012**, *13*, 693–712.

178. Zhou, B.; Elazab, A.; Bort, J.; Vergara, O.; Serret, M. D.; & Araus, J. L. Low-cost assessment of wheat resistance to yellow rust through conventional RGB images. *Comput. Electron. Agric*. **2015**, *116*, 20-29.